Quantum Measurements are Disturbing: Experiments studying the role of disturbance in postselected metrology, quantum pigeonholes, and entangled sheep

by

Noah Benjamin Lupu-Gladstein

A thesis submitted in conformity with the requirements
for the degree of Doctor of Philosophy

Department of Physics
University of Toronto

Quantum Measurements are Disturbing: Experiments studying the role of disturbance in postselected metrology, quantum pigeonholes, and entangled sheep

Noah Benjamin Lupu-Gladstein
Doctor of Philosophy

Department of Physics
University of Toronto
2024

Abstract

This thesis details two experiments and one theoretical manuscript that explore the nature of measurement disturbance in quantum mechanics. The first experiment exploits measurement disturbance to enhance measurement precision by two orders of magnitude, and in principle even more. The second experiment investigates a paradox where three quantum pigeons seem to occupy two pigeonholes without any pair belonging to the same hole. It finds that measurement disturbance accounts for some, but not all of the counter-intuitive phenomena at play in the paradox. The final manuscript develops a new theoretical framework for studying quantum measurement and disturbance from the viewpoint of quantum agents. Our framework reveals how agents endowed with quantum memories might view measurement not as a stochastic collapse, but as a continuous flow of quantum information.

Acknowledgements

If I had never made it to graduate school to pursue my love of physics, it would have been enough. If I had made it to graduate school, but never found a supervisor I connected with, it would have been enough. If Aephraim Steinberg had only been a brilliant scientist, but not a patient mentor as well, it would have been enough. If he had been patient, but unwilling to support my leave of absence when my mental health was at its worst, it would have been enough. If my family had been loving and supportive, but not interested in my research, it would have been enough. If my roommates had just been pleasant enough and not a source of friendship to return to after long nights in the lab, it would have been enough. If my partner Natalie had been unfalteringly positive, but not willing to keep me company during nights and weekends of alignment and data collection, nor so helpful with scientific graphics, it would have been enough.

If the postdocs Kent Bonsma-Fisher and Aharon Brodutch that helped me through the first few years of my PhD hadn't also continued to help long after they moved on to bigger things, it would have been enough. If the two graduate students that mentored me, Hugo Ferretti and Ediwn Tham, had helped me learn my way around the lab but hadn't also been constantly willing to humor my wild ideas, it would have been enough. If my lab mate Arthur Pang had just been brilliant in his own work, but not so willing to help with mine, it would have been enough. If the graduate students I mentored, Batuhan, Pria, and Jerry had just been eager students, but hadn't also shown such appreciation and kindness as I moved from Toronto to Ottawa, it would have been enough. If my committee members John Sipe and Amar Vutha had been helpful during my committee meetings, but hadn't also been constantly within reach for help, it would have been enough. If the physics department coordinator Krystyna Biel had just pestered me to schedule committee meetings and hadn't also helped me navigate expiring study permits, funding running out, and my leave of absence, it would have been enough. If my pet rats Phoenix, Dragon, Goblin, Robo, and Frog had just been cute furballs and hadn't also been instant anxiety relief when I needed it most, it would have been enough.

I wish to acknowledge this land on which the University of Toronto operates. For thousands of years it has been the traditional land of the Huron-Wendat, the Seneca, and most recently, the Mississaugas of the Credit River. Today, this meeting place is still the home to many Indigenous people from across Turtle Island and we are grateful to have the opportunity to work on this land.

Acknowledgement provided by Assistant Vice-President & Chief of Protocol, Office of the President, University of Toronto

Contents

List of Tables

List of Figures

Chapter 1

Introduction

Quantum mechanics has been a pillar of modern physics for over a century, enabling inventions like semi-conductors, lasers, and atomic clocks. While quantum mechanics has proven to be astonishingly adept at modeling the laws of nature, humans have proven to be woefully inept at accommodating its consequences into their classical intuition. At the heart of this issue is the measurement problem.

There are many ways to phrase the measurement problem, but perhaps the most straightforward is to appreciate the absurdity of the laws of motion in quantum mechanics. They posit that the evolution of a state is determined by the Shrödinger equation at all times *except* for any time a measurement occurs, in which case it *collapses randomly* according to the Born rule. Why is the Shrödinger equation not appropriate during a measurement? How long does a measurement last? How long does it take for a state to collapse? What even is a measurement? Does you reading this page constitute a measurement? Do the photons that hit a paper copy of this manuscript measure the atoms inside it? These are the kinds of questions that make the measurement problem so puzzling.

Rather than get lost in such philosophical questions, let us discuss *physics*. Quantum mechanics, like any theory, is a model for some collection of phenomena. What is the physical phenomenon that quantum mechanics attempts to model that makes its laws of evolution so awkward? Is it measurement? Not exactly. People were doing measurements long before anyone had even dreamed of the scientific method and modeling them was never a deep issue. The troublesome phenomena is, specifically, measurement *disturbance*. It was not until science explored the insides of atoms that we became sensitive to a certain kind of *fundamental* disturbance. No matter how crafty our double slit experiment, we could not measure which slit particles traversed without disturbing their interference pattern. We realized measurement disturbance was not just an incidental consequence of imperfect measuring devices, but an inescapable law of nature.

After a century of developing quantum mechanics, we have come to see measurement disturbance as more than an annoying quirk of nature. We have put our understanding of measurement disturbance to work in quantum computing [1], quantum communication [2], and quantum metrology [3, 4]. We have come to see disturbance as essential in protecting basic notions of causality in light of quantum teleportation [5] and even time travel [6–8].

Despite all the advances in understanding disturbance, there is still much to uncover. This thesis

picks away at the mystery of measurement disturbance from three different angles. First, it details a post-selected metrology experiment where disturbance is exploited to enhance measurement precision (Ch. 2) [9]. Second, it explains a foundational experiment that tests the role of disturbance in one of the strangest predictions of quantum mechanics to date: that three quantum pigeons can be placed among two pigeonholes in such a way that no two pigeons are ever found in the same pigeonhole (Ch. 3)[10]. Finally, it develops a framework for understanding measurement and disturbance that is free from the baggage of classical intuition. It creates a natural language for describing how a quantum agent, such as an advanced artificial intelligence running on a quantum computer, might perceive its surroundings (Ch. 4)[11].

This thesis is structured as follows. There are three chapters, each covering one of the three research projects described above. The first two begin with an introduction that explain necessary background material. Then I include the journal article presenting the findings of that project. The references for these articles are included below. Their content has been largely preserved, but small formatting changes have been made to better integrate them together into a single document. The final chapter features a longer, self-contained manuscript, so no additional introduction is provided. Following each manuscript is a retrospective "outro". There I describe my personal contributions to each project, experimental details that might be helpful to future students, and ideas for how each project might be followed up with further research.

1. Noah Lupu-Gladstein, Y. Batuhan Yilmaz, David R. M. Arvidsson-Shukur, Aharon Brodutch, Arthur O. T. Pang, Aephraim M. Steinberg, and Nicole Yunger Halpern. "Negative Quasiprobabilities Enhance Phase Estimation in Quantum-Optics Experiment". In: *Phys. Rev. Lett.* 128 (22 June 2022), p. 220504. DOI: 10.1103/PhysRevLett.128.220504. URL: https://link.aps.org/doi/10.1103/PhysRevLett.128.220504

2. Noah Lupu-Gladstein, Hugo Ferretti, Weng-Kian Tham, Arthur Ou Teen Pang, Aephraim M Steinberg, Kent Bonsma-Fisher, and Aharon Brodutch. "Quantum violations of classical counting principles via variable-strength non-local measurements". In preparation. 2024

3. Noah Lupu-Gladstein, Aharon Brodutch, Hugo Ferretti, Weng-Kian Tham, Arthur Ou Teen Pang, Kent Bonsma-Fisher, and Aephraim M Steinberg. "Do qubits dream of entangled sheep? Quantum measurement without classical output". In: *New Journal of Physics* 26.5 (May 2024), p. 053029. DOI: 10.1088/1367-2630/ad48ad. URL: https://dx.doi.org/10.1088/1367-2630/ad48ad

Chapter 2

Postelected Metrology

2.1 Introduction to postselected metrology

This chapter explores how quantum measurement disturbance can be exploited to design high-precision measurements. The study of how quantum phenomena can be used to improve measurements is called quantum metrology. Suppose we wish to measure some unknown parameter θ which has been encoded in a quantum state. What is the best measurement we can perform on the state?

To answer this question in any meaningful way, we must first establish what we mean by "best." A common way to judge potential measurements is by the variance in the estimate of θ you would get if you repeated the measurement many times. To be precise, suppose you run your experiment and obtain some data X, which is a random variable distributed according to some probabilities $P(x|\theta)$. You then analyze your data and determine an estimate $\hat{\theta}(X)$ of the true value of θ. Ideally, the expected value of this estimate equals the true value θ.

$$\mathbb{E}_X\left[\hat{\theta}(X)\right] = \theta \tag{2.1}$$

Such an estimator is called unbiased. The variance of an unbiased estimator is

$$\mathrm{Var}\left[\hat{\theta}(X)\right] = \mathbb{E}_X\left[\left(\hat{\theta}(X) - \theta\right)^2\right]. \tag{2.2}$$

Given a particular unbiased estimator, one may wonder whether there are any other unbiased estimators that have a smaller variance. The Cramér-Rao bound

$$\mathrm{Var}\left[\hat{\theta}(X)\right] \geq 1/F(\theta) \tag{2.3}$$

answers this question. The quantity $F(\theta)$ is the Fisher information.

$$F(\theta) = \mathrm{Var}\left[\partial_\theta \log P(X|\theta)\right] \tag{2.4}$$

It depends only on the probability distribution $P(x|\theta)$, not on any particular estimator. If we find that our unbiased estimator has a variance equal to one over the Fisher information, we can be confident that there is not some better estimator we should be using instead.

The definition of Fisher information may seem arbitrary and confusing at first. Why is it that to make the variance of my estimator smaller, I need to make the variance of some log-derivative larger? The idea is that the Fisher information quantifies how different the distributions $P(X|\theta)$ and $P(X|\theta + d\theta)$ are in the limit $d\theta \to 0$. We compare the distributions by subtracting the log of their probabilities (log probabilities are often easier to work with numerically and analytically) and normalizing by the shift $d\theta$.

$$\lim_{d\theta \to 0} \frac{\log P(X|\theta + d\theta) - \log P(X|\theta)}{d\theta} = \partial_\theta \log P(X|\theta) \tag{2.5}$$

This calculation gives a list of derivative values for each outcome x. To aggregate this list into a single number, we might be tempted to take its expectation value, but this would cause the derivatives for outcomes with increased probabilities to cancel with outcomes with decreased probabilities. In fact, as long as changing θ does not change the normalization of $P(X|\theta)$, then we have $\mathbb{E}\left[\partial_\theta \log P(X|\theta)\right] = \partial_\theta \sum_x P(x|\theta) = 0$. So we aggregate the derivatives by taking the weighted sum of squares. Since the expectation value of the log-derivatives is 0, the expectation of their squares is just the variance. Hence $\mathrm{Var}\left[\partial_\theta \log P(X|\theta)\right]$ is a sensible way measure the extent to which a distribution changes with respect to small variations in θ.

Fisher information uses the probability distribution $P(x|\theta)$ to determine how well we can estimate a parameter, but what determines $P(x|\theta)$? In quantum metrology, we posit that the distribution arises from measuring a quantum state $\rho(\theta)$. The most general model for obtaining a probability distribution from a quantum state is called a positive operator-valued measure (POVM). A POVM $\mathcal{M}$ is a set of positive semi-definite measurement operators M_x that together sum to identity.

$$\mathcal{M} = \{M_x\}_x, \; M_x \succeq 0, \; \sum_x M_x = \mathbb{1} \tag{2.6}$$

The Born rule tells us how to turn a state $\rho(\theta)$ and a POVM $\mathcal{M}$ into a probability distribution.

$$P(x|\theta) = \mathrm{Tr}[\rho(\theta) M_x] \tag{2.7}$$

Given a quantum state ρ_θ, and the ability to measure it using any POVM we want, how well can we estimate θ? The quantum Cramér-Rao bound answers this question[12].

$$F(\theta) \leq F_q(\theta) \tag{2.8}$$

The new quantity $F_q(\theta)$ is called the quantum Fisher information.

$$F_q(\theta) = \mathrm{Var}[\Lambda(\theta)], \; \partial_\theta \rho(\theta) = \frac{\Lambda(\theta)\rho(\theta) + \rho(\theta)\Lambda(\theta)}{2} \tag{2.9}$$

The Hermitian operator $\Lambda(\theta)$ is called the symmetric logarithmic derivative (SLD). The quantum Fisher information gives a bound that is independent of any particular way to measure $\rho(\theta)$, which goes one step further than the classical Fisher information that is independent of any estimator, but does depend on the particular measurement. The SLD tells you more than just how much variance to expect from the best measurement, it actually tells you what the best measurement is. It turns out that a measurement in the eigenbasis of the SLD is optimal.

In general, the quantum Fisher information can be tricky to work with analytically because the SLD is only given implicitly (though it can be calculated using Lyapunov Equation solvers[13]). Thankfully, if $\rho(\theta)$ is a pure state $\rho(\theta) = |\psi(\theta)\rangle \langle\psi(\theta)|$, then the SLD and quantum Fisher information simplify respectively to

$$\Lambda(\theta) = 2 |\partial_\theta \psi(\theta)\rangle \langle\psi(\theta)| + 2 |\psi(\theta)\rangle \langle\partial_\theta \psi(\theta)| \tag{2.10}$$

$$F_q(\theta) = 4 \langle\partial_\theta \psi(\theta)|\partial_\theta \psi(\theta)\rangle - 4| \langle\psi(\theta)|\partial_\theta \psi(\theta)\rangle |^2. \tag{2.11}$$

If the state evolves according to a Schrödinger-like equation

$$|\partial_\theta \psi(\theta)\rangle = -iA(\theta) |\psi(\theta)\rangle \tag{2.12}$$

for some θ-dependent generator $A(\theta)$ with the same units as θ^{-1}, then

$$\Lambda(\theta) = 2i[A(\theta), |\psi(\theta)\rangle \langle\psi(\theta)|] \tag{2.13}$$

$$F_q = 4\text{Var}[A(\theta)]. \tag{2.14}$$

For example, if we are estimating how much a particle translates along the x-axis, we would identify x with θ and $A(\theta)$ with $p/\hbar$.

For a particular generator $A(\theta)$, what is the best state $|\psi(\theta)\rangle$ we could hope for? The state must maximize the variance of $A(\theta)$. Suppose the maximum eigenvalue of $A(\theta)$ is $a_{\max}(\theta)$ with associated eigenstate $|a_{\max}(\theta)\rangle$ and its minimum eigenvalue is $a_{\min}(\theta)$ with associated eigenstate $|a_{\min}(\theta)\rangle$. Then the best state $|\psi(\theta)\rangle$ is any equal superposition of $|a_{\max}(\theta)\rangle$ and $|a_{\min}(\theta)\rangle$, such as

$$\frac{|a_{\max}(\theta)\rangle + |a_{\min}(\theta)\rangle}{\sqrt{2}} \tag{2.15}$$

and such a state achieves the maximum possible Fisher information

$$F_{\max}(\theta) = \Delta a(\theta)^2 = (a_{\max}(\theta) - a_{\min}(\theta))^2 \tag{2.16}$$

It would seem that for a given Hamiltonian, $1/\Delta a(\theta)^2$ is the best variance we could ever hope to achieve, even optimizing for all possible input states, all possible measurements, and all possible estimators.

In the experiment I present at the end of this chapter, we obtain a variance roughly 100 times smaller than the $1/\Delta a(\theta)^2$ limit. How is this possible and how does it not conflict with the arguments I just presented? The trick is that while each photon we detect in that experiment caries $\approx 100 \times \Delta a(\theta)$ information, our probability to detect a photon is only 1/100. Thus each input photon still only carries "on average" $1 \times \Delta a(\theta)$ unit of information. Nevertheless, there are still individual instances where a photon truly carries more information than it has any right to.

How exactly can overcoming the $\Delta a(\theta)^2$ limit be explained? In a technical sense, we sidestep the proof given above because the mapping in our experiment from quantum states to probabilities is not, in fact, a POVM. Whereas the probabilities generated by a POVM are linear in the state ρ the probabilities in our experiment are non-linear in ρ because they are *postselected* on successfully detecting a photon. This postselection is represented mathematically by a Kraus operator K with

$\mathbb{1} - K^\dagger K \succeq 0$ and the non-linear map

$$\rho \to \frac{K\rho K^\dagger}{\mathrm{Tr}[K\rho K^\dagger]}. \tag{2.17}$$

Practically, it amounts to empirically estimating probabilities from detector counts via a formula like

$$\frac{\text{counts from detector 1}}{\text{counts from detector 1} + \text{counts from detector 2}} \tag{2.18}$$

instead of

$$\frac{\text{counts from detector 1}}{\text{counts from detector 1} + \text{counts from detector 2} + \text{number of photons not detected}}. \tag{2.19}$$

However, there is more to the story than just postselection. There are postselections that do not increase Fisher information and there are even postselections that decrease Fisher information. A thought-provoking paper[14], proved that a postselection can only break the $\Delta a(\theta)^2$ bound if it does not commute with the generator $A(\theta)$ on the support of $\rho(\theta)$. That is,

$$\text{if } \mathrm{Tr}[\rho(\theta)[A(\theta), K^\dagger K]] = 0, \text{ then } F_q(\theta) \leq \Delta a(\theta)^2. \tag{2.20}$$

They proved this result by quantifying the extent to which the postselection and Hamiltonian fail to commute using a mathematical tool called a quasiprobability distribution.

Unlike a normal probability distribution, a quasiprobability distribution is allowed to have negative, or even complex values. The only requirement is that all the quasiprobabilities in a distribution sum to unity. In quantum mechanics, quasiprobability distributions are useful for modeling quantum states in a phase space of incompatible observables, such as position and momentum or the x, y, z components of spin projection. One such distribution often encountered in quantum optics is the Wigner distribution. However, it is not the Wigner, but the lesser-known Kirkwood-Dirac quasiprobability distribution that turns out to be the natural distribution for modeling postselected quantum metrology.

The Kirkwood-Dirac distribution $\tilde{p}_\rho(a, b, c, \ldots)$ for a sequence of measurements $A, B, C, \ldots$ can be, loosely speaking, thought of as representing the "complex likelihood" for a fixed state ρ to take on value a of measurement A, then b of B, then c of C, and so on. The formula for the Kirkwood-Dirac distribution is delightfully simple:

$$\tilde{p}_\rho(a, b, c, \ldots) = \mathrm{Tr}[\ldots M_c^C M_b^B M_a^A \rho]. \tag{2.21}$$

The notation M_z^Z denotes the positive semi-definite operator that corresponds to a value z in the measurement Z with the property that $\sum_z M_z^Z = \mathbb{1}$. This property ensures that the KD distribution always has the correct marginals. That is

$$\sum_a \tilde{p}_\rho(a, b, c, \ldots) = \tilde{p}_\rho(b, c, \ldots). \tag{2.22}$$

Naturally, there is nothing special about the index a, and a similar identity holds for every index in the distribution. The paper in the next section explores the surprising connection between this abstract mathematical tool and an empirical advantage in a polarimetry experiment.

Negative Quasiprobabilities Enhance Phase Estimation in Quantum-Optics Experiment

Noah Lupu-Gladstein,[1,*] Y. Batuhan Yilmaz,[1,†] David R. M. Arvidsson-Shukur,[2,3,‡] Aharon Brodutch,[1,§] Arthur O. T. Pang,[1,¶] Aephraim M. Steinberg,[1,**] and Nicole Yunger Halpern[4,5,6,7]

[1] *CQIQC and Department of Physics, University of Toronto, 60 Saint George St., Toronto, ON M5S 1A7, Canada*
[2] *Hitachi Cambridge Laboratory, J. J. Thomson Avenue, Cambridge CB3 0HE, United Kingdom*
[3] *Cavendish Laboratory, Department of Physics, University of Cambridge, Cambridge CB3 0HE, United Kingdom*
[4] *Joint Center for Quantum Information and Computer Science, NIST and University of Maryland, College Park, Maryland 20742, USA*
[5] *Institute for Physical Science and Technology, University of Maryland, College Park, Maryland 20742, USA*
[6] *ITAMP, Harvard-Smithsonian Center for Astrophysics, Cambridge, Massachusetts 02138, USA*
[7] *Department of Physics, Harvard University, Cambridge, Massachusetts 02138, USA*

(Dated: May 2, 2024)

Operator noncommutation, a hallmark of quantum theory, limits measurement precision, according to uncertainty principles. Wielded correctly, though, noncommutation can boost precision. A recent foundational result relates a metrological advantage with negative quasiprobabilities—quantum extensions of probabilities—engendered by noncommuting operators. We crystallize the relationship in an equation that we prove theoretically and observe experimentally. Our proof-of-principle optical experiment features a filtering technique that we term *partially postselected amplification* (PPA). Using PPA, we measure a waveplate's birefringent phase. PPA amplifies, by over two orders of magnitude, the information obtained about the phase per detected photon. In principle, PPA can boost the information obtained from the average filtered photon by an arbitrarily large factor. The filter's amplification of systematic errors, we find, bounds the theoretically unlimited advantage in practice. PPA can facilitate any phase measurement and mitigates challenges that scale with trial number, such as proportional noise and detector saturation. By quantifying PPA's metrological advantage with quasiprobabilities, we reveal deep connections between quantum foundations and precision measurement.

* nlupugla@physics.utoronto.ca. The first two coauthors contributed equally.
† ybylmaz@physics.utoronto.ca.
‡ drma2@cam.ac.uk
§ brodutch@physics.utoronto.ca
¶ arthur.pang@mail.utoronto.ca
** steinberg@physics.utoronto.ca

2.2 Introduction

Advances in quantum metrology have kindled new measurement techniques [15–19]. The paradigmatic quantum measurement is phase estimation, whose applications span polarimetry, magnetic sensing, gravitational-wave astronomy, and quantum-computer calibration [20–26]. A fundamental limit bounds how precisely one can estimate a phase from a given number of trials [27, 28]. If some trials are filtered out, the average information per retained, or *postselected*, trial can exceed this limit [14]. Filtering can never increase the information per *input* trial, so successful postselections' rarity counterbalances the extra information [29, 30]. Nevertheless, distilling information from many input trials into fewer postselected trials can alleviate challenges that scale with trial number, including detector saturation, proportional noise, low-frequency noise, limited memory, and limited computational power [31–35].

We elucidate this distillation's physical and mathematical roots using a filtering technique that we call *partially postselected amplification* (PPA). Theoretically, the information obtained per PPA trial can diverge as the fraction of postselected trials vanishes [14]. A related technique, weak-value amplification, offers a similarly diverging advantage [3, 4, 31, 33–59]. Both techniques are examples of *noncommutative filtering*. We define *noncommutative filtering* as any filtering whose effect depends on when the filter acts. During the alternative, *commutative filtering*, the per–postselected-trial precision cannot exceed the per–input-trial limit [14]. Examples include the neutral-density filter that reduces a camera's overexposure. PPA's postselected trials break the per–input-trial limit by endowing a certain quasiprobability distribution with negative elements [14].

Quasiprobabilities represent quantum states as probability densities represent states in classical statistical mechanics. Like probabilities, the quasiprobabilities in a distribution sum to one. Yet quasiprobabilities can assume negative and nonreal values, called *nonclassical values*. They can arise when the quasiprobability describes quantum-incompatible operations or observables. Well-known quasiprobability distributions include the Wigner function. A rising star is the *Kirkwood-Dirac distribution* [60, 61], which has recently found applications in quantum state tomography [62–66], chaos [67–71], postselected metrology [14, 39–41, 72–78], measurement disturbance [79–82], quantum thermodynamics [67, 83–86], and quantum foundations [47, 80, 87–98]. Negative Kirkwood-Dirac quasiprobabilities have been demonstrated, under certain conditions, to underlie operational advantages in quantum computation, work extraction, and parameter estimation [14, 69, 78, 86].

In this Letter, we demonstrate PPA's parameter-estimation enhancement in a proof-of-principle polarimetry experiment. We estimate the birefringent phase imparted to photons by a near-half–waveplate. A tunable polarization filter implements the PPA. The filter boosts the per–detected-photon precision by over two orders of magnitude. Furthermore, we measure a Kirkwood-Dirac distribution that describes the experiment. Our experiment operationally motivates a measure of the distribution's negativity. We prove theoretically and confirm experimentally that the negativity is proportional to the precision enhancement when the phase is probed optimally. We also pinpoint which systematic errors limit PPA's theoretically unbounded precision enhancement (Sec. 2.6.1). Our experiment unifies theoretical quantum foundations with practical precision measurement.

2.3 Theoretical background and equality

Consider estimating a parameter θ by measuring a quantum state $\rho(\theta)$. The *quantum Fisher information* (QFI) $\mathcal{I}(\theta)$ quantifies the information provided by $\rho(\theta)$ about θ, via the state's sensitivity to changes in θ [12] (Sec. 2.6.2). The QFI's reciprocal lower-bounds the variance of every unbiased estimator θ_e of θ, in the Cramér-Rao bound, $\mathrm{var}(\theta_e) \geq 1/\mathcal{I}(\theta)$. [27, 28]

Let A denote an observable with greatest and least eigenvalues a_+ and $a_- = a_+ - \Delta$. The eigenstates $|a_\pm\rangle$ satisfy $A|a_\pm\rangle = a_\pm |a_\pm\rangle$. Let a unitary $U(\theta) = \exp(i\theta A)$ imprint θ on an input state. The optimal inputs are even-weight superpositions of extremal A eigenstates, e.g., $|0\rangle = (|a_+\rangle + |a_-\rangle)/\sqrt{2}$ and $|1\rangle = (|a_+\rangle - |a_-\rangle)/\sqrt{2}$. The imprinted state $U(\theta)|0\rangle = |\Psi(\theta)\rangle$ carries the most QFI possible without postselection, $\mathcal{I}(\theta) = \Delta^2$.

A postselected state can provide more QFI. If the angle is small ($\theta\Delta \ll 1$), then $|\Psi(\theta)\rangle \approx |0\rangle + i\frac{\theta\Delta}{2}|1\rangle$. The $|0\rangle$ coefficient is less sensitive to θ than the $|1\rangle$ coefficient, yet $|0\rangle$ has a greater population. PPA partially postselects on $|1\rangle$ via a filter whose $|1\rangle$ transmission amplitude is unity and whose $|0\rangle$ transmission amplitude is parametrically smaller.

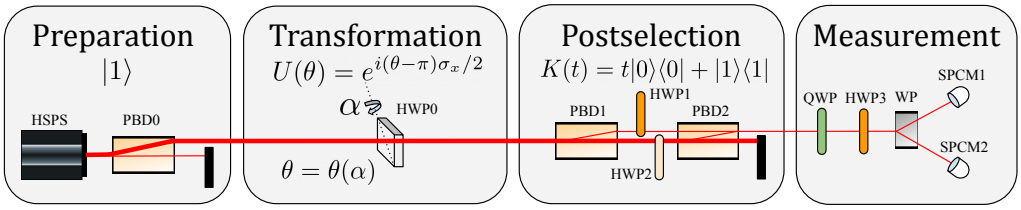

Figure 2.1: Photonic parameter-estimation experiment: Preparation: A heralded–single-photon source (HSPS) emits light that hits a polarizing–beam-displacer (PBD0) and emerges vertically polarized ($|1\rangle$). Transformation: The half-waveplate (HWP0) has an optic axis angled 45° above the horizontal. HWP0 is tilted away from normal incidence through an angle α about its optic axis. The waveplate rotates a photon's polarization through an angle $\theta(\alpha) - \pi$. A calibration curve of $\theta(\alpha) \equiv \theta$ provides a prior estimate of θ. We use this estimate to calculate the polarization projection optimal for inferring θ (Sec. 2.6.2). Postselection: A polarizing–beam-displacer interferometer, followed by a beam block in the undisplaced port, realizes a partial polarizer. The horizontal-polarization transmission amplitude, t with $|t| \in [0, 1]$, is controlled by a half-waveplate (HWP2) inside the interferometer. The filter discards all horizontally polarized photons when $|t| = 0$ and none when $|t| = 1$. Measurement: Motorized waveplates, followed by a Wollaston prism (WP) and single-photon counter modules (SPCM), project onto any desired polarization.

More precisely, let t denote the amplitude for $|0\rangle$'s survival of the filter. The filter acts as the Kraus operator [99] $K(t) = t|0\rangle\langle 0| + |1\rangle\langle 1|$, wherein $|t| \in [0, 1]$. For any $|t| < 1$, the filter does not commute with the generator A and enables noncommutative filtering. The filter lets $|\Psi(\theta)\rangle$ pass with a probability

$$p^{\mathrm{ps}}(\theta, t) = \mathrm{Tr}\big(K(t)|\Psi(\theta)\rangle\langle\Psi(\theta)|K(t)^\dagger\big) \tag{2.23}$$

$$= |t|^2 \cos^2(\Delta\theta/2) + \sin^2(\Delta\theta/2). \tag{2.24}$$

The state becomes

$$|\Psi^{\mathrm{ps}}(\theta, t)\rangle = K(t)\,|\Psi(\theta)\rangle\,/\sqrt{p^{\mathrm{ps}}(\theta, t)} \tag{2.25}$$

$$= \cos(\Delta\Theta/2)\,|0\rangle + i\,\sin(\Delta\Theta/2)\,|1\rangle\ . \tag{2.26}$$

$\tilde{p}_{\rho(\theta),t}(a,a'\|+)$	$a'=a_+$	$a'=a_-$
$a=a_+$	$\frac{1+\|t\|^2}{4p^{\rm ps}(\theta,t)}$	$e^{i\Delta\theta}\frac{-1+\|t\|^2}{4p^{\rm ps}(\theta,t)}$
$a=a_-$	$e^{-i\Delta\theta}\frac{-1+\|t\|^2}{4p^{\rm ps}(\theta,t)}$	$\frac{1+\|t\|^2}{4p^{\rm ps}(\theta,t)}$

Table 2.1: Conditional Kirkwood-Dirac distribution (2.29) for our PPA experiment and $\rho(\theta)=|\Psi(\theta)\rangle\langle\Psi(\theta)|$.

The filter effectively amplifies θ to a Θ defined through $\tan(\Delta\Theta/2)=\tan(\Delta\theta/2)/|t|$. The postselected state carries the QFI

$$\mathcal{I}(\theta)=[\Delta\ |t|/p^{\rm ps}(\theta,t)]^2\,. \tag{2.27}$$

A large angle is typically easier to observe than a smaller one. If the angle is small, $\Delta\theta\ll 1$, then Θ exceeds θ by a factor of $1/|t|$. This amplification boosts the information obtained per detected state: $\mathcal{I}(\theta)\approx(\Delta/|t|)^2$. The amplification is arbitrarily large if $\Delta\theta$ is arbitrarily small. Such extreme filtering does not significantly reduce the information obtainable per input state: $p^{\rm ps}(\theta,t)\mathcal{I}(\theta)\approx\Delta^2$, if $\tan(\Delta\theta/2)\ll|t|$.

PPA can be beneficial even if $\Delta\theta$ is large. Suppose prior knowledge indicates that $\theta\approx\theta_{\rm p}$. Performing $U(-\theta_{\rm p})$ after $U(\theta)$ shrinks the probed angle to $\Delta(\theta-\theta_{\rm p})$.

Why can a successful PPA trial offer more information than Δ^2, the most information offered by any input trial? Reference [14] identified a necessary condition. A projectively postselected trial can carry information $>\Delta^2$ only if a Kirkwood-Dirac distribution contains a negative quasiprobability. We generalize that result beyond projective postselection.

Let $\{|a\rangle\}_a$ and $\{|a'\rangle\}_{a'}$ denote copies of an A eigenbasis. Kraus operators $\{K_f\}_f$ with $\sum_f K_f^\dagger K_f=\mathbb{1}$ model the partial postselection. The information-bearing state $\rho(\theta)$ is represented by the Kirkwood-Dirac quasiprobabilities (Secp. 2.6.3)

$$\tilde{p}_{\rho(\theta)}(a,f,a'):=\mathrm{Tr}\big(|a'\rangle\langle a'|K_f^\dagger K_f|a\rangle\langle a|\rho(\theta)\big). \tag{2.28}$$

Conditioning on a postselection outcome f induces the *conditional Kirkwood-Dirac distribution*

$$\tilde{p}_{\rho(\theta)}(a,a'|f):=\tilde{p}_{\rho(\theta)}(a,f,a')/\sum_{a,a'}\tilde{p}_{\rho(\theta)}(a,f,a'). \tag{2.29}$$

These quasiprobabilities are positive if A and $K_f^\dagger K_f$ commute on the support of $\rho(\theta)$ [96].

PPA involves Kraus operators, $K_+=K(t)$ and $K_-=\sqrt{\mathbb{1}-K(t)^\dagger K(t)}$, that effect successful and unsuccessful postselection. Table 2.1 shows PPA's conditional quasiprobabilities, labeled by t, for $\rho(\theta)=|\Psi(\theta)\rangle\langle\Psi(\theta)|$. If $\Delta\,\theta<\pi$ and $|t|^2<1$, the real part of $\tilde{p}_{\rho(\theta),t}(a_\pm,a_\mp|+)$ is negative, and the postselected QFI (2.27) exceeds Δ^2. This concurrence stems from an equality that we prove.

We start by introducing a new measure of Krikwood-Dirac negativity [69, 96, 97]. Let x denote the vector of arguments for a Kirkwood-Dirac distribution $\{\tilde{p}(x)\}_x$. Define the *nonclassicality gap* as the greatest difference between quasiprobabilities' absolute squares: $\max_x\{\ |\tilde{p}(x)|^2\ \}-\min_x\{\ |\tilde{p}(x)|^2\ \}$. The gap >1 only if a quasiprobability $\notin[0,1]$. For any postselection operator

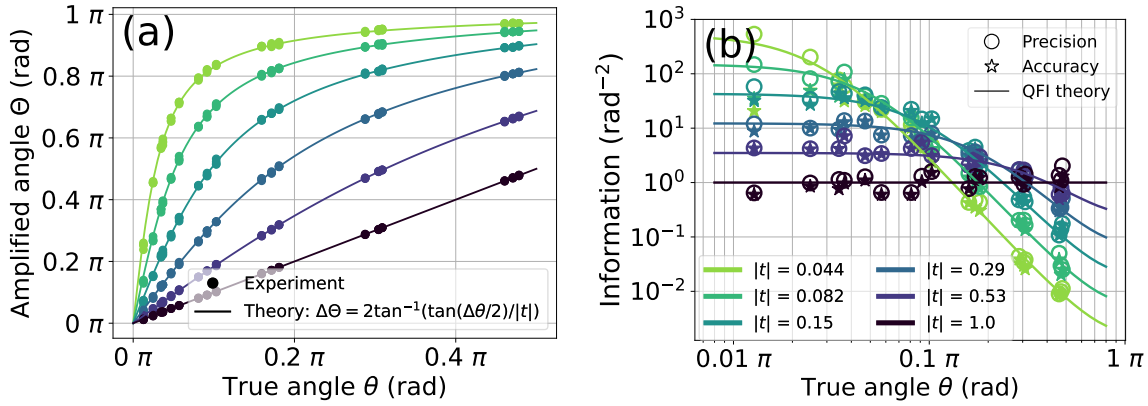

Figure 2.2: Experimental performance of PPA with different magnitudes of postselection parameter, $|t|$. (a) Amplified angle vs. true angle θ. The slope signifies sensitivity to changes in θ. When θ is small $[\tan(\Delta\theta/2) \ll |t|]$, PPA magnifies θ by a factor of $1/|t|$. Setting $|t| = \tan(\Delta\theta/2)$ amplifies θ to $\pi/2$ and optimizes the sensitivity. Decreasing $|t|$ further reduces the sensitivity, rendering prior knowledge about θ important. (b) Information per photon vs. θ. For each $(\theta, |t|)$, we make 32 independent estimates of θ and display the estimates' precision (1/variance) and accuracy (1/[mean squared error]) per mean detected photon. The per-photon precision agrees with the predicted QFI (2.27) and climbs to 540 ± 150 rad^{-2} at $(\theta, |t|) = (0.040 \text{ rad}, 0.044)$. The per-photon accuracy suffers from systematic errors at the smallest θ and $|t|$, yet still reaches 78 ± 15 rad^{-2} at $(\theta, |t|) = (0.116 \text{ rad}, 0.082)$.

K_+, the nonclassicality gap is proportional to the optimal input state's postselected QFI (Sec. 2.6.4):

$$\mathcal{I}(\theta) = 4\Delta^2 \left[\max_{a,a'} \left\{ \left| \tilde{p}_{\rho(\theta)}(a, a'|+) \right|^2 \right\} - \min_{a,a'} \left\{ \left| \tilde{p}_{\rho(\theta)}(a, a'|+) \right|^2 \right\} \right]. \tag{2.30}$$

Equation (2.30) crystallizes the relationship between postselected quantum metrology and Kirkwood-Dirac nonclassicality.

2.4 Experimental setup

We realize PPA in a proof-of-principle polarimetry experiment (Fig. 2.1). The to-be-estimated parameter θ is the excess birefringent phase, beyond π, imparted by a near-half–waveplate (HWP0). A heralded–single-photon source emits vertically polarized photons with wavelengths of 808 nm. The photons hit HWP0, whose optic axis lies 45° above the horizontal. Tilting HWP0 through an incidence angle α sets its birefringent retardance to $\theta(\alpha) - \pi$. A calibration curve of $\theta(\alpha) \equiv \theta$ provides prior knowledge about θ.

Denote horizontal polarization by $|0\rangle$; and vertical polarization, by $|1\rangle$. We filter the photons by attenuating one polarization, using an interferometer formed from polarizing beam displacers. The postselection parameter t equals the filter's ($|0\rangle$ transmission amplitude)/($|1\rangle$ transmission amplitude). We control t with a motorized waveplate (HWP2) placed in the interferometer.

HWP0 rotates the photon's polarization with the unitary $\exp(i[\theta - \pi]\sigma_x/2)$. The generator $A = \sigma_x/2$ has eigenvalues $a_\pm = \pm 1/2$ and eigenstates $|a_\pm\rangle = (|0\rangle \pm |1\rangle)/\sqrt{2}$. The filtered photons occupy the state $\rho^{\text{ps}}(\theta, t)$—ideally, the pure state (2.26). We projectively measure the state's polarization to estimate θ.

Experimental results.—First, we assess PPA's metrological performance. Then, we present the

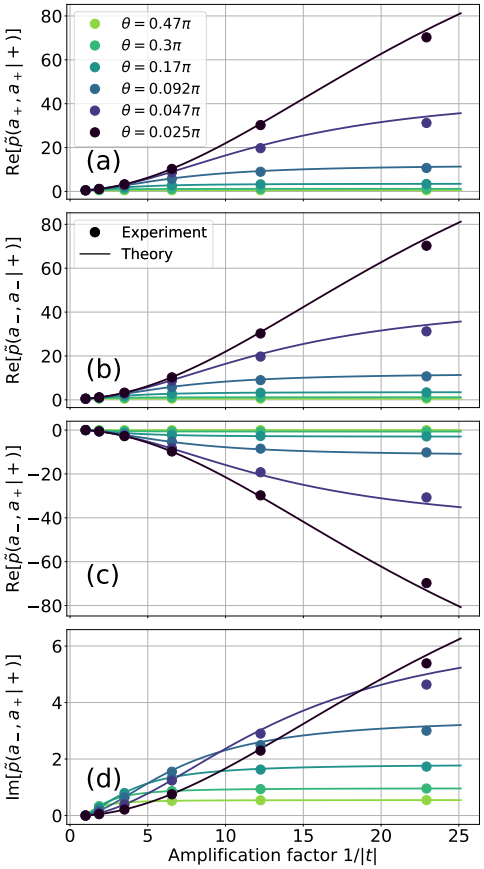

Figure 2.3: Quasiprobabilities vs. amplification factor $1/|t|$. We inferred the Kirkwood-Dirac distribution (2.28), $\tilde{p}_{\rho(\theta),t}(a, a'|+)$, from tomography of the unpostselected ($|t| = 1$) state. We present empirical results together with theoretical predictions at different θ and $|t|$ for select elements: (a) $\mathrm{Re}[\tilde{p}_{\rho(\theta),t}(a_+, a_+|+)]$, (b) $\mathrm{Re}[\tilde{p}_{\rho(\theta),t}(a_-, a_-|+)]$, (c) $\mathrm{Re}[\tilde{p}_{\rho(\theta),t}(a_-, a_+|+)]$, and (d) $\mathrm{Im}[\tilde{p}_{\rho(\theta),t}(a_-, a_+|+)]$. All other elements are redundant because (2.28) ensures $\tilde{p}_{\rho(\theta),t}(a, a'|+) = \tilde{p}_{\rho(\theta),t}(a', a|+)^*$. For each $(\theta, |t|)$, the quasiprobabilities' sum is normalized to 1. Negativity in $\mathrm{Re}[\tilde{p}_{\rho(\theta),t}(a_\pm, a_\mp|+)]$ allows the magnitude of each element to be greater than 1. The negativity increases as the amplification strengthens.

measured quasiprobabilities (2.29). Comparing the quasiprobabilities with the QFI, we support Eq. (2.30) experimentally.

Polarization tomography reveals how PPA boosts sensitivity. Figure 2.2a shows the postselected state's amplified angle, Θ, versus the true θ value. We infer the latter using state tomography without postselection ($|t| = 1$). The slope of $\Theta(\theta)$ quantifies our sensitivity to small changes in θ. When $|t| = 1$, $\Theta(\theta)$ has a unit slope. As we postselect more ($|t|$ decreases), the slope grows—by a factor of > 20 at $|t| = 0.044$.

We estimate θ by projectively measuring many copies of the amplified state identically. The measurement basis is optimized to provide the QFI according to calibrations of $\theta(\alpha)$ and t (Sec. 2.6.2).

For each (θ, t), we sample 32 independent estimates of θ. Figure 2.2b displays our estimates' precision and accuracy, normalized by the number N of detected photons. The precision per photon, $\mathrm{var}(\theta_\mathrm{e})^{-1}/N$, agrees excellently with the QFI (2.27). The accuracy per photon, $\mathrm{MSE}(\theta_\mathrm{e})^{-1}/N$, mostly agrees with the QFI but falls short at the smallest θ and $|t|$. The per-photon precision enhancement maximizes at 540 ± 150, when $\theta = 0.040$ rad, $|t| = 0.044$. The per-photon accuracy

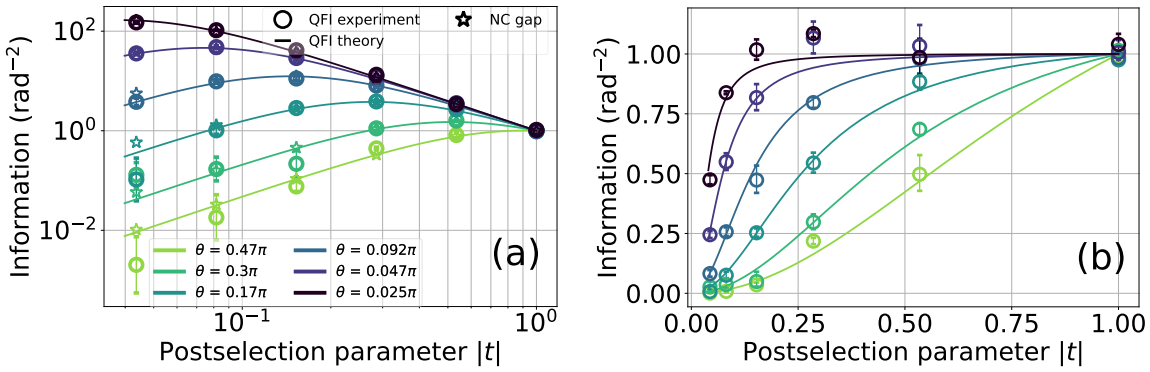

Figure 2.4: Information per detected photon (a) and per input photon (b) vs. magnitude of postselection parameter, $|t|$. Error bars denote the geometric standard error of 4 independent runs. The experimental QFI and 4 times the nonclassicality gap are within error of the theoretical QFI (2.27). Without postselection, our estimates are shot-noise–limited to the per–input-photon precision 1 rad^{-2}. As we increasingly postselect (as $|t|$ decreases), the per–detected-photon precision increases when $\theta \approx 0$ and decreases when $\tan(\theta/2) < |t|$. The smallest $|t|$ and θ provide a per–detected-photon precision > 200 rad^{-2}, despite sacrificing little per–input-photon precision.

caps at 78 ± 15, when $\theta = 0.116$ rad and $|t| = 0.082$.

The discrepancy between precision and accuracy arises because PPA amplifies systematic errors (Sec. 2.6.1). Small errors in adjusting the waveplates that set $|t|$ or A produce systematic error. These errors begin to dominate the statistical noise as the amplification increases. Remarkably, we found the amplified errors helpful for detecting and correcting errors in A that went unnoticed without PPA's amplification.

We extract the conditional quasiprobabilities (2.28) from tomography of the unpostselected ($|t| = 1$) state and present them in Fig. 2.3. At each (θ, t), the sum over the quasiprobabilities is normalized to one. When $|t| < 1$, quasiprobabilities acquire negative real parts, so other quasiprobabilities acquire real parts > 1 to ensure a unit sum. As $|t|$ decreases, elements' magnitudes increase—to > 70 at the smallest θ and $|t|$.

Figure 2.4 compares the nonclassicality gap with the QFI. We compute the gap from the quasiprobabilities shown in Fig. 2.3. The estimated gap is the arithmetic mean over four runs of tomography. We determine the QFI at $\theta = \theta_0$ empirically from estimates of $\rho^{\text{ps}}(\theta_0, t)$ and $\partial\rho^{\text{ps}}(\theta, t)/\partial\theta|_{\theta_0}$ (Sec. 2.6.2 states the formula for QFI). The derivative is the matrix slope of a linear fit through three tomographic estimates: $\rho^{\text{ps}}(\theta_0 - d\theta, t), \rho^{\text{ps}}(\theta_0, t)$, and $\rho^{\text{ps}}(\theta_0 + d\theta, t)$; $d\theta = 0.035$ radians. We repeat the procedure over four tomographic runs to obtain a distribution of QFIs at each $(\theta, |t|)$. Empirically, the distribution of the QFIs is approximately log-normal, so we estimate the QFI and its uncertainty using the geometric mean and geometric standard error.

The estimated QFI and nonclassicality gap are consistent with the theoretical QFI [Fig. 2.4(a)]. Thus, our experiment corroborates the relationship (2.30) between enhanced precision and quasiprobability negativity.

2.5 Conclusions

We have experimentally demonstrated and theoretically proved how negative Kirkwood-Dirac quasiprobabilities enhance postselected metrology. We introduced and illustrated a scheme for phase

estimation, partially postselected amplification. In our polarimetry experiment, PPA boosted our per–detected-photon precision by over two orders of magnitude. This enhancement derives from negativity of a generalized Kirkwood-Dirac quasiprobability, according to an equation that we prove and experimentally support. The negativity demonstrates that our filter provides a benefit offered by no filter that commutes with $U(\theta)$.

In theory, PPA's precision boost is unbounded. In practice, we find, the phase amplification augments systematic errors. Yet the error amplification has a silver lining, having helped us detect and correct systematic errors in our implementation of the generator A (Sec. 2.6.1).

PPA is related to weak-value amplification (WVA), a scheme for estimating couplings strengths [3, 4, 31, 33–59]. PPA and WVA concentrate information spread across many input trials into few postselected trials. Yet PPA differs from WVA in three ways: (i) PPA can amplify any phase, not just coupling strengths. (ii) PPA survives decoherence better. In WVA, an interaction couples two systems. One system is measured, the other is postselected, and both must remain coherent during the interaction. PPA only requires the measured system to maintain coherence. (iii) PPA admits of a simpler mathematical treatment: WVA requires a Hilbert-space dimensionality ≥ 4, whereas PPA works with a Hilbert-space dimensionality ≥ 2. PPA is therefore a promising tool for combating metrological challenges that scale with the number of completed trials. As a whole, our work interweaves the disparate studies of precision measurement and quantum foundations.

Acknowledgements

We thank Justin Dressel, Hugo Ferretti, Kent Fisher, Zhaokai Li, Seth Lloyd, and Edwin Tham for helpful conversations. This work was supported by the Natural Sciences and Engineering Research Council (NSERC) of Canada, the National Science Foundation under Grant No. NSF PHY-1748958, the EPSRC, CIFAR, Lars Hierta's Memorial Foundation, and Girton College. It made use of some equipment purchased through grant FQXiRFP-1819 from the Foundational Questions Institute and Fetzer Franklin Fund, a donor advised fund of Silicon Valley Community Foundation. A.M.S is a fellow of CIFAR, and N.Y.H is grateful for an NSF grant for the Institute for Theoretical Atomic, Molecular, and Optical Physics at Harvard University and the Smithsonian Astrophysical Observatory.

2.6 Postselected metrology supplementary materials

2.6.1 Postselected amplification of systematic error

Some estimates of θ (Fig. 2.5a) deviate statistically significantly from the true θ values. We now detail these deviations and explain PPA's ability to amplify certain types of systematic errors.

Figure 2.5b shows our mean estimates' residual, and residual per standard error, versus the true θ value. Deviations greater than 2 standard errors point to statistically significant systematic errors. Figure 2.5a showed rough agreement between our estimates and true values. However, Fig. 2.5b reveals that statistically significant systematic errors bedevil our estimates.

We now distinguish the systematic errors present with and without postselection. Without postselection ($|t| = 1$), our estimates of θ differ significantly from the true (tomographically extracted) values. This error is not unique to PPA and is specific to our polarimetry experiment's details. An-

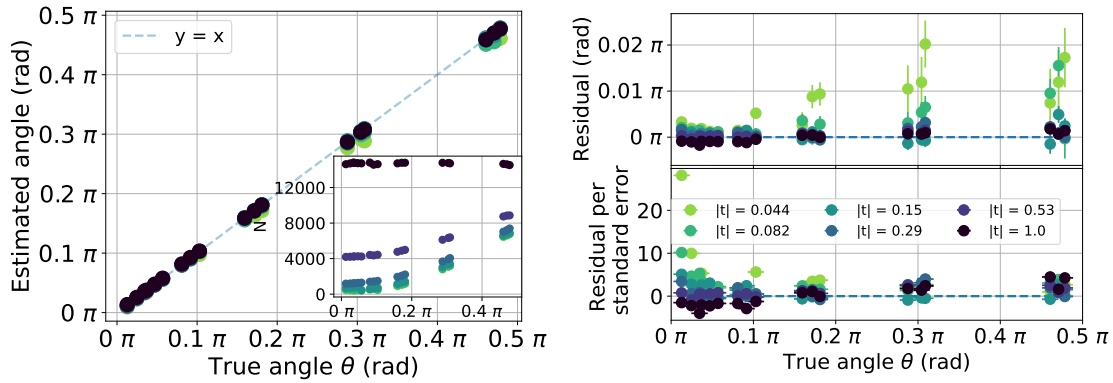

(a) **(b)**

Figure 2.5: (a) Mean estimate of θ vs. true θ value. Each mean is averaged over 32 independent estimates and agrees roughly with the true value. Inset: mean detected-photon number, N. Difference between our estimates and the true θ value. In the lower graph, the difference is normalized by standard error. Modest postselections ($|t| \geq 0.15$) do not suffer from significantly more systematic error than postselection-free measurements ($|t| = 1$). The two most severe postselections ($|t| = 0.044, 0.082$) amplify systematic errors significantly.

other type of error emerges at the two most extreme postselection levels, when $|t| \in \{0.044, 0.082\}$. The systematic errors varies strongly with θ and characterizes PPA.

While amplifying θ, PPA also amplifies small errors in the implementations of (i) the generator A and (ii) the Kraus operator K. As shown in the main text, PPA amplifies an unknown phase θ to a larger phase Θ. To obtain an estimate θ_e of θ, we first obtain an estimate Θ_e of Θ. Then, we numerically invert the amplification. Inversion requires an accurate model of the experiment, but no model is perfect. In our model, postselection amplifies the state's phase to

$$\Theta = \Theta(\theta, t) = 2 \arctan\big(\tan(\theta/2)/t\big), \tag{2.31}$$

according to Eq. (2.26). Given the amplified-angle estimate, the θ estimate is $\theta_e = \Theta^{-1}(\Theta_e, t)$.

The setting of t may suffer from a small error Δt. The estimated phase, as a function of the true phase, will become

$$\theta_e = 2 \arctan\big(\tan(\theta/2)[1 + \Delta t/t]\big). \tag{2.32}$$

The half-tangents of θ_e and θ differ by

$$\tan(\theta_e/2) - \tan(\theta/2) = [\tan(\theta/2)/t]\, \Delta t = \tan(\Theta/2)\, \Delta t. \tag{2.33}$$

This difference is proportional to the amplified half-tangent, which leads to two problems. First, amplifying θ amplifies the effects of the uncertainty in t. Second, the resulting systematic error cannot be corrected, because $\tan(\Theta/2)$ is unknown, by the phase-estimation task's nature.

Separately, errors can mar the implementation of the generator A. Ideally, $A = \sigma_x/2$. However, A is effected by a waveplate whose optic axis may be rotated by a small angle ϵ from 45° to the horizontal. The generator will become $A(\epsilon) = \cos(2\epsilon)\sigma_x/2 + \sin(2\epsilon)\sigma_z/2$. Under $e^{i(\theta-\pi)A(\epsilon)}$, the

initial state $|1\rangle$ evolves to

$$|\psi(\epsilon)\rangle = \cos(\theta/2)[\cos(2\epsilon)\,|0\rangle - \sin(2\epsilon)\,|1\rangle] + i\sin(\theta/2)\,|1\rangle\,. \tag{2.34}$$

This state's polar half-angle has a tangent

$$\frac{|\,\langle 1|\psi(\epsilon)\rangle\,|}{|\,\langle 0|\psi(\epsilon)\rangle\,|} = \sqrt{\frac{\sin^2(2\epsilon) + \tan^2(\theta/2)}{\cos^2(2\epsilon)}}\,. \tag{2.35}$$

When $\sin^2(2\epsilon) \ll \tan^2(\theta/2)$, ϵ affects the polar angle negligibly. However, if $\sin^2(2\epsilon) > \tan^2(\theta/2)$, the polar angle depends on ϵ considerably. Amplifying the polar angle with PPA amplifies also the error in the A implementation.

One can compensate, or correct, for the error amplification. Moreover, we exploited it to improve our A implementation while aligning our equipment. However, calibration and correction errors propagate to θ eventually. Thus, the precision of one's $K(t)$ and A implementations limits how much one can filter and postselect usefully. This phenomenon extends beyond our polarimetery experiment to every PPA implementation.

2.6.2 Optimal measurement

We estimated θ with an optimal polarization measurement. By *optimal measurement*, we mean a measurement whose information yield, averaged over many trials, equals the QFI. Let Λ denote the symmetric logarithmic derivative of ρ, defined implicitly through the Sylvester equation,

$$\frac{\partial\rho}{\partial\theta} = \frac{\Lambda\rho + \rho\Lambda}{2}. \tag{2.36}$$

Projectively measuring an eigenbasis of Λ is optimal [12]. Moreover, the variance of such a measurement equals the QFI.

$$\mathcal{I}(\theta) = \mathrm{Tr}\left(\rho(\theta)\Lambda^2\right) \tag{2.37}$$

Therefore, we aim to solve Eq. (2.36) for Λ.

We obtain a solution as follows. Let $\mathrm{vec}(Y)$ denote the vectorized form of a matrix Y in row-major order. For matrices X, Y, and Z with appropriate dimensions, $\mathrm{vec}(XYZ) = (X \otimes Z^T)\mathrm{vec}(Y)$. Let Y^+ denote the Moore-Penrose inverse of a matrix Y. Solving for Λ, we vectorize it:

$$\mathrm{vec}(\Lambda) = \left(\frac{\rho \otimes \mathbb{1} + \mathbb{1} \otimes \rho^T}{2}\right)^+ \mathrm{vec}\left(\frac{\partial\rho}{\partial\theta}\right). \tag{2.38}$$

In our experiment, the photon polarization is nearly, but not exactly, pure: The initial polarization is $\rho_0 = v|0\rangle\langle 0| + (1-v)\mathbb{1}/2$. The visibility v is close, but not equal, to unity. The postselected state is

$$\rho^{\mathrm{ps}}(\theta, t) = K(t)U(\theta)\rho_0 U(\theta)^\dagger K(t)^\dagger / p^{\mathrm{ps}}(\theta, t), \tag{2.39}$$

and the postselection probability is

$$p^{\mathrm{ps}}(\theta, t) = \mathrm{Tr}\big(K(t)U(\theta)\rho_0 U(\theta)^\dagger K(t)^\dagger\big). \tag{2.40}$$

Λ assumes the form

$$\Lambda = v\, p^{\rm ps}(\theta, t) \left[\frac{1-|t|^2}{2} \sin(\theta) \mathbb{1} + \cos(\theta)(\mathrm{Re}[t]\sigma_x + \mathrm{Im}[t]\sigma_y) + \frac{1+|t|^2}{2} \sin(\theta)\sigma_z \right]. \tag{2.41}$$

An optimal measurement is thus a polarization projection onto the Bloch vector whose polar angle $\theta_{\rm opt}$ and azimuthal angle $\phi_{\rm opt}$ are defined through

$$\cot(\theta_{\rm opt}) = \frac{1+|t|^2}{2|t|} \tan(\theta), \qquad \tan(\phi_{\rm opt}) = \mathrm{Im}[t]/\mathrm{Re}[t]. \tag{2.42}$$

$\theta_{\rm opt}$ turns out to be independent of v but not of θ. We use prior knowledge about θ, derived from our calibration curve $\theta(\alpha)$, to estimate $\theta_{\rm opt}$ and approximate an optimal measurement.

2.6.3 Generalized Kirkwood-Dirac distribution

We called the quasiprobabilities (2.28) "Kirkwood-Dirac quasiprobabilities." This appendix justifies that terminology. Kirkwood and Dirac independently defined a quasiprobability dependent on a pure state $|\psi\rangle$ and on two projectors, $|a\rangle\langle a|$ and $|f\rangle\langle f|$ [60, 61]: $\mathrm{Tr}(|f\rangle\langle f|a\rangle\langle a|\psi\rangle\langle\psi|)$. Wiseman generalized the pure state to an arbitrary quantum state ρ [100]: $\mathrm{Tr}(|f\rangle\langle f|a\rangle\langle a|\rho)$. Yunger Halpern and collaborators generalized to arbitrarily many projectors $\Pi_{m_j}^{M_j}$, which can project onto multi-dimensional subspaces [67, 68]: $\mathrm{Tr}\left(\Pi_{m_k}^{(k)} \Pi_{m_{k-1}}^{(k-1)} \dots \Pi_{m_1}^{(1)} \rho\right)$. They called this quantity an *extended Kirkwood-Dirac quasiprobability*.

We generalize the projectors to elements of POVMs $\left\{ M_{m_1}^{(1)} \right\}_{m_1}, \left\{ M_{m_2}^{(2)} \right\}_{m_2}, \dots, \left\{ M_{m_k}^{(k)} \right\}_{m_k}$:

$$\tilde{p}_\rho(m_1, m_2, \dots, m_k) := \mathrm{Tr}\left(M_{m_k}^{(k)} M_{m_{k-1}}^{(k-1)} \dots M_{m_1}^{(1)} \rho \right). \tag{2.43}$$

By definition, the $\ell^{\rm th}$ POVM's elements are positive-semidefinite operators that resolve unity: $M_{m_\ell}^{(\ell)} \geq 0$, and $\sum_{m_\ell} M_{m_\ell} = \mathbb{1}$. We could call our quasiprobability (2.43) a "generalized extended Kirkwood-Dirac quasiprobability"; but the name, itself, would be too extended. Following Wiseman's lead, we avoid new names; we christen our construction, and rechristen the extended Kirkwood-Dirac quasiprobability, a "Kirkwood-Dirac quasiprobability."

To merit the name, our quasiprobability distribution should exhibit two recursive properties:

1. A Kirkwood-Dirac distribution with one argument is a probability distribution.

2. Marginalizing over any argument of a Kirkwood-Dirac distribution with $k > 1$ arguments yields a Kirkwood-Dirac distribution with $k-1$ arguments.

Consequently, marginalizing over $k-1$ arguments of a k-argument Kirkwood-Dirac distribution yields a probability distribution. We now verify that our distribution (2.43) has these properties.

Consider the one-argument distribution with elements $\tilde{p}_\rho(m_1) = \mathrm{Tr}(M_{m_1}^{(1)} \rho)$. It satisfies property 1 because (i) each $M_{m_1}^{(1)}$ is positive-semidefinite, so $\tilde{p}_\rho(m_1) \geq 0$; and (ii) $\left\{ M_{m_1}^{(1)} \right\}_{m_1}$ resolves unity, so $\sum_{m_1} \tilde{p}_\rho(m_1) = \mathrm{Tr}(\rho) = 1$. The element $\tilde{p}_\rho(m_1)$ is the probability that, upon preparing ρ and measuring $\left\{ M_{m_1}^{(1)} \right\}_{m_1}$, one obtains outcome m_1.

Now, consider the k-argument distribution (2.43). Marginalizing over the ℓ^{th} POVM yields

$$\sum_{m_\ell} \tilde{p}_\rho(m_1, m_2, \ldots, m_{\ell-1}, m_\ell, m_{\ell+1}, \ldots, m_k) = \tilde{p}_\rho(m_1, m_2, \ldots m_{\ell-1}, m_{\ell+1}, m_{\ell+2}, \ldots, m_k) \tag{2.44}$$

$$= \mathrm{Tr}\left(M^{(k)}_{m_k} M^{(k-1)}_{m_{k-1}} \ldots M^{(\ell+1)}_{m_{\ell+1}} M^{(\ell-1)}_{m_{\ell-1}} M^{(\ell-2)}_{m_{\ell-2}} \ldots M^{(1)}_{m_1} \rho\right), \tag{2.45}$$

because each POVM resolves unity. The right-hand side is a $(k-1)$-argument Kirkwood-Dirac distribution. Therefore, our construction has property 2.

2.6.4 Proof of proportionality between postselected quantum Fisher information and quasiprobability nonclassicality

Equation (2.30) interrelates the postselected quantum Fisher information and the generalized quasiprobability's nonclassicality. We prove this equation—in fact, a generalization of the equation—here.

Generalized setup: All the definitions presented here are independent of the definitions presented in the main text. For example, the A defined here is independent of the A defined in the main text. However, quantities defined in the main text are examples of quantities defined here.

During a parameter-estimation experiment, the input state ρ undergoes a unitary $U(\theta) = e^{i\theta A}$ generated by a Hermitian operator A:

$$\rho \mapsto U(\theta)\rho U(\theta)^\dagger = \rho(\theta). \tag{2.46}$$

The parameter to be estimated is θ. The system corresponds to a Hilbert space of arbitrary dimensionality. We assume that ρ is a pure state with support on only two A eigenspaces. The projectors onto these eigenspaces, we denote by $\Pi_{\min}$ and $\Pi_{\max}$. Their associates eigenvalues are $a_{\min}$ and $a_{\max} > a_{\min}$.

After undergoing the unitary, the state meets a filter. If the state survives the filter, a Kraus operator K_+ updates the state. Otherwise, $K_- = \sqrt{\mathbb{1} - K_+^\dagger K_+}$ updates the state. The state survives the filter with the postselection probability $p^{\text{ps}}(\theta) = \mathrm{Tr}\big(\rho(\theta)\, K_+^\dagger K_+\big)$. We can represent the experiment with the Kirkwood-Dirac quasiprobability

$$\tilde{p}_{\rho(\theta)}(a, f, a') = \mathrm{Tr}\big(\Pi_{a'}\, K_f^\dagger K_f\, \Pi_a\, \rho(\theta)\big), \quad \text{for } a, a' \in \{a_{\max}, a_{\min}\}. \tag{2.47}$$

Our result depends on the conditional quasiprobabilities, labeled by $f = +$, associated with a successful postselection:

$$\tilde{p}_{\rho(\theta)}(a, a'|+) = \tilde{p}_{\rho(\theta)}(a, +, a')/p^{\text{ps}}(\theta). \tag{2.48}$$

We assume that two "diagonal" quasiprobabilities, labeled by $a = a'$, equal each other:

$$\mathrm{Tr}\big(\Pi_{\max}\, \rho(\theta)\, \Pi_{\max}\, K_+^\dagger K_+\big) = \mathrm{Tr}\big(\Pi_{\min}\, \rho(\theta)\, \Pi_{\min}\, K_+^\dagger K_+\big). \tag{2.49}$$

This condition is satisfied by the main text's qubit system of interest, $A = \sigma_x/2$, and input state $(|a_+\rangle + |a_-\rangle)/2 = |0\rangle$.

Generalized equality: The postselected QFI, $\mathcal{I}(\theta)$, is proportional to the quasiprobability's nonclassicality gap:

$$\mathcal{I}(\theta) = 4\,(a_{\max} - a_{\min})^2 \left(\max_{a,a'} \left\{ \; \left| \, \tilde{p}_{\rho(\theta)}(a, a'|+) \right|^2 \right\} - \min_{a,a'} \left\{ \; \left| \, \tilde{p}_{\rho(\theta)}(a, a'|+) \right|^2 \right\} \right). \tag{2.50}$$

Proof: We calculate the postselected quantum Fisher information by substituting from Eq. (2.46) into a formula for a pure state's postselected QFI {Eq. (5) in [14]}:

$$\mathcal{I}(\theta) = \frac{4}{p^{\rm ps}(\theta)} \, {\rm Tr}\big(A\,\rho(\theta)\,A\,K_+^\dagger K_+\big) - \frac{4}{[p^{\rm ps}(\theta)]^2} \, \big|{\rm Tr}\big(A\,\rho(\theta)\,K_+^\dagger K_+\big)\big|^2 \tag{2.51}$$

$$= \frac{4}{[p^{\rm ps}(\theta)]^2} \, \Big[{\rm Tr}\big(A\,\rho(\theta)\,A\,K_+^\dagger K_+\big) \, {\rm Tr}\big(\rho(\theta)\,K_+^\dagger K_+\big) - {\rm Tr}\big(A\,\rho(\theta)\,K_+^\dagger K_+\big) \, {\rm Tr}\big(\rho(\theta)\,A\,K_+^\dagger K_+\big) \Big]. \tag{2.52}$$

We will rewrite the right-hand side, by decomposing the evolved state as

$$\rho(\theta) = (\Pi_{\max} + \Pi_{\min})\,\rho(\theta)\,(\Pi_{\max} + \Pi_{\min}) \tag{2.53}$$

$$= \Pi_{\max}\,\rho(\theta)\,\Pi_{\max} + \Pi_{\max}\,\rho(\theta)\,\Pi_{\min} + \Pi_{\min}\,\rho(\theta)\,\Pi_{\max} + \Pi_{\min}\,\rho(\theta)\,\Pi_{\min}. \tag{2.54}$$

We substitute this expression into Eq. (2.52). Then, we invoke the eigenvalue equations $A\Pi_{\max} = a_{\max}\Pi_{\max}$ and $A\Pi_{\min} = a_{\min}\Pi_{\min}$. Once we multiply out, terms cancel:

$$\mathcal{I}(\theta|\rho(\theta)) = \frac{4}{[p^{\rm ps}(\theta)]^2} \, (a_{\max} - a_{\min})^2 \big[{\rm Tr}\big(\Pi_{\max}\,\rho(\theta)\,\Pi_{\max}\,K_+^\dagger K_+\big) \, {\rm Tr}\big(\Pi_{\min}\,\rho(\theta)\,\Pi_{\min}\,K_+^\dagger K_+\big)$$
$$- {\rm Tr}\big(\Pi_{\max}\,\rho(\theta)\,\Pi_{\min}\,K_+^\dagger K_+\big) \, {\rm Tr}\big(\Pi_{\min}\,\rho(\theta)\,\Pi_{\max}\,K_+^\dagger K_+\big) \big]. \tag{2.55}$$

The final term equals $|{\rm Tr}\big(\Pi_{\max}\,\rho(\theta)\,\Pi_{\min}\,K_+^\dagger K_+\big)|^2$, so

$$\mathcal{I}(\theta) = 4\,(a_{\max} - a_{\min})^2 \left[\tilde{p}_{\rho(\theta)}(a_{\max}, a_{\max}|+) \, \tilde{p}_{\rho(\theta)}(a_{\min}, a_{\min}|+) - |\tilde{p}_{\rho(\theta)}(a_{\max}, a_{\min}|+)|^2 \right]. \tag{2.56}$$

Since $\mathcal{I}(\theta)$ and $(a_{\max} - a_{\min})^2 \geq 0$, Eq. (2.56) implies

$$\tilde{p}_{\rho(\theta)}(a_{\max}, a_{\max}|+) \, \tilde{p}_{\rho(\theta)}(a_{\min}, a_{\min}|+) \geq |\tilde{p}_{\rho(\theta)}(a_{\max}, a_{\min}|+)|^2. \tag{2.57}$$

The left-hand side equals $\left[\tilde{p}_{\rho(\theta)}(a_{\max}, a_{\max}|+) \right]^2$, by Eq. (2.49). Since each side of Eq. (2.49) is overtly a probability, $\tilde{p}_{\rho(\theta)}(a_{\max}, a_{\max}|+)$ is real. The square therefore equals the square modulus. Substituting into Ineq. (2.57) yields $|\tilde{p}_{\rho(\theta)}(a_{\max}, a_{\max}|+)|^2 \geq |\tilde{p}_{\rho(\theta)}(a_{\max}, a_{\min}|+)|^2$. This inequality contains the square moduli of all the quasiprobabilities for which $f = +$. Hence the inequality's left-hand side equals the greatest square probability, $\max_{a,a'} \left\{ \, [\tilde{p}_{\rho(\theta)}(a, a' \, | \, +)]^2 \, \right\}$, while the right-hand side equals the least square modulus, $\min_{a,a'} \left\{ \, [\tilde{p}_{\rho(\theta)}(a, a' \, | \, +)]^2 \, \right\}$. Substituting the max and min into Eq. (2.56) yields Eq. (2.50). □

2.7 Postselected metrology outro

2.7.1 Contributions

Nicole Yunger Halpern and David Arvidsson-Shukur (along with Seth Lloyd initially) are responsible for proposing to Aephraim's group an experiment connecting postselected metrology and and non-classicality. I took the bait and organized conversations between our groups. I came up with the idea for the optical experiment and the quantitative equation relating Fisher information with Kirkwood-Dirac negativity. Nicole wrote the rigorous proof of the equality while Nicole and David helped with various theory calculations along the way. I designed the apparatus, except for the single-photon source built and designed by Edwin Tham. Batuhan Yilmaz built the apparatus and collected most of the preliminary data. I analyzed almost all the data throughout the project. Batuhan and I collected the final data together. I wrote most of the paper, with Batuhan responsible for polishing the figures and final rounds of edits. Arthur Pang helped in various ways as a lab mate while he, Aharon Brodutch, and Aephraim Steinberg contributed to the project via regular lab meetings.

2.7.2 Single photon source

We generated heralded single photons for our metrology experiment from the Sagnac source, which Edwin Tham built and described in detail in his thesis [101]. The source was designed to create polarization-entangled photon pairs, but in this experiment, we just used it as a bright (around 50k coincidences per second) source of heralded single photons. I will discuss this source in more detail in the next chapter (Sec. 3.3.2), where its entanglement properties were relevant. The description of the source in that chapter is accurate for the source as it was used in the metrology experiment, except that the source was pumped with a 160 MHz linewidth Ondax diode laser during the metrology experiment instead of the Cobalt 08-17 from Hübner Photonics it was eventually replaced by. In this section, I will answer the question of why we bothered to use a single photon source for our experiment at all. Theoretically, all the postselected amplification that ocurred in our single-photon experiment would have also ocurred with a coherent state. Despite that, there are two primary reasons we chose to use single photons.

Using a coherent state would have weakened our claims of experimentally achieving a non-classical metrological advantage. The classical bound we compared against was based on the minimum and maximum eigenvalues of the phase generator. In the paper, we modeled this generator A as a qubit operator: $A = \sigma_x/2$. Strictly speaking, the operator $\sigma_x/2$ only describes the generator's action on the single-photon subspace. The full generator is actually an infinite-dimensional operator of the form $(a^\dagger a - b^\dagger b)/2$, where $a^\dagger$ creates a diagonally polarized photon and $b^\dagger$ creates an anti-diagonally poalrized photon. The minimum and maximum eigenvalues of this operator are negative and positive infinity, which do not give a useful classical bound to compare against. If we had used a coherent state as our probe, which contains a superposition of photon numbers going all the way up to infinity, the large eigenvalues of the generator would have played a role in the evolution. By using a single-photon state, we ensure that only the single-photon subspace of the generator is relevant. Consequently, $A = \sigma_x/2$ is indeed a faithful model of our phase generator and its finite eigenvalues add an extra level of theoretical rigor to our claims of a non-classical advantage.

The other reason we used a single-photon state over a classical laser was to achieve the shot-noise limit. We wanted our experiment to show that we could amplify the information per detection beyond the limit on information per input. The most straightforward way to achieve this is by ensuring that without postselection, we were already at the per-input information limit. Heralded single photon sources are great for taking shot-noise limited data because a) the large statistical noise of a single-photon source can mask technical noise and b) heralding with a short coincidence window practically eliminates dark counts.

2.7.3 Polarization optics

There were several key polarization components in our experiment. First, there was the generator which implemented the polarization rotation we aimed to measure. We considered several options for implementing this generator, including a liquid crystal waveplate, a rotating waveplate, and the titled waveplate we ultimately chose. The essential requirements were that the polarization transformation be stable over time, repeatable, and easy to precisely characterize. Furthermore, we wanted the axis of the generator to be independent of the phase parameter θ because the theory work on postselected metrology we based our experiment on made the same assumption. This assumption led to us ruling out using a rotating waveplate as the generator, which would have been an operator proportional to $\cos(\theta/2)\sigma_z + \sin(\theta/2)\sigma_x$. In retrospect, we might have used the fact that two half waveplates in a row impart a phase shift between left-circular and right-circular polarization. However, this approach would probably not have been better than our titled waveplate approach as if either of those half waveplates had not had a retardance of exactly π, the axis of the generator would have varied as they were turned. Our other consideration was a liquid crystal waveplate, an optic whose birefringence can be controlled by an applied voltage. Ostensibly, the orientation of the birefringence is independent of voltage, but we have found notable variations in practice. Their relationship between voltage and birefringence is not linear and requires careful calibration. Furthermore, liquid crystal waveplates tend to be very thick and thus depend much more on temperature, wavelength, and incidence angle than typical passive waveplates.

The tilted waveplate approach worked well in the end, but did create its own set of challenges. First, the relationship between the tilt of the waveplate and birefringent phase shift it imparted was not as easy to characterize as we initially expected. This might have been because the waveplate we used was a pseudo zero-order waveplate, not a true zero-order waveplate. Our initial plan was to create a calibration curve relating tilt and retardance by fitting to equations derived from the basic physics and geometry of uniaxial crystals. We found these fits to be inadequate, and eventually resorted to spline interpolation to fill in our calibration curves. Second, setting up the waveplate so that its optical axis was parallel to the tilt axis of its mount and 45° from the horizontal axis proved more challenging than expected. We had to mount and remount the waveplate several times until these angles were all aligned to within less than a degree in order for our data with large amplification factors to agree with our predictions.

The last important decision for the experiment was the design of the partial polarizer. The partial polarizer needed to attenuate one polarization by a factor t more than the orthogonal polarization, which would ideally suffer no attenuation. Moreover, the attenuated polarization needed to be coherent with the orthogonal polarization so that the resulting polarization state was pure, not mixed. We considered three approaches: the polarizing beam displacer interferometer we settled

on, a polarizing beam splitter based displaced Sagnac interferometer, and a single polarizing beam splitter cube at variable incidence angle.

The idea behind the single polarizing beam splitter was that the reflection ports of most polarizing beam splitters have a notoriously poor extinction. Polarizing beam splitter cubes tend to have an extinction ratio of 1000 : 1 or better in their transmitted port, but only 100 : 1 in their reflected port. Moreover, the reflected port extinction is sensitive to the incidence angle of the light. While these aspects of the reflection port are typically seen as bugs, we might have turned them into features by tuning the incidence angle of a polarizing beam splitter cube to alter the extinction ratio and achieve a particular t value. The simplicity of this design is very appealing and perhaps worth exploring further in the future. One reason we decided against this design was that it would have provided a very limited range of t values. While changing the incidence angle does change the extinction ratio slightly, it cannot turn polarization splitting off completely. That is, it cannot achieve $t = 1$, which is essential in our experiment for comparing to the standard measurement that does not involve postselection. Another point against this design is that changing the incidence angle of the beam splitter changes the angle of the reflected beam and necessitates a realignment of the collection optics. Finally, it is dubious to use a device for a purpose for which it was not designed. It is unclear how coherent the leakage in the reflection port would be. While we never took the time to study this carefully, I guessed that the light leaking into the reflection port would not be very coherent with the non-leaked light.

The polarizing beam splitter based displaced Sagnac is a tried and true design for implementing arbitrary polarization operations in quantum foundations experiments, but it would not have provided the level of purity and stability required for our metrology experiment. The Sagnac design involves using both the reflected and transmitted ports of a beam splitter. As discussed above, the reflected port of a polarizing beam splitter tends to only get extinction ratios on the order of 100 : 1, thus limiting how low we can make t. Additionally, the alignment and phase of a displaced Sagnac interferometers tends to be less stable than a polarizing beam displacer interferometer because a beam displacer interferometer can be very compact and does not require any mirrors.

The polarizing beam displacer interferometer we made worked well for our metrology experiment. We bought a matched pair of anti-reflection coated α-BBO polarizing beam displacers from Newlight Photonics with 3 mm displacement. These polarizers have an extinction ratio greater than $10^5 : 1$. The alignment of our interferometer was stable over weeks at a time. For fixed values of t, the phase was stable for hours, but we found that changing t, (accomplished by rotating a waveplate within the interferometer) added a Berry phase. Although this phase shift was repeatable, it still added an extra layer of complication. In retrospect, using a variable neutral density filter in place of a waveplate to control t may have avoided this problem.

2.7.4 Follow up

The postselected metrology experiment detailed in the previous section offers several opportunities for further study. Our proof-of-principle centered around the toy problem of measuring the retardance of a half waveplate. However, our partially postselected amplification technique is applicable to any phase-estimation experiment. One interesting direction would be to apply our amplification technique to a physically interesting problem where we might be able to push the state of the art. Another direction involves relaxing the assumption that we have a good prior estimate of

the phase we wish to measure. Presumably, a good adaptive algorithm could iteratively improve our estimate of the phase (assuming the phase varies slowly over the iteration time) and feed back into progressively greater postselected amplification. Finally, we could study postselected amplification in the context of multi-parameter estimation. In one experiment, we could amplify sensitivity to a few parameters that correspond to quantum mechanically incompatible observables, such as rotations about all three Cartesian axes. Another approach would be to amplify sensitivity to a massive number of compatible parameters, such as the relative phase of each pixel in a hologram.

Chapter 3

Disturbing Quantum Pigeons

3.1 Introduction to variable-strength measurements

This chapter explores the role of measurement disturbance, or lack thereof, in some of the counter-intuitive conclusions one arrives at when attempting to infer properties of a quantum state between two measurements. Perhaps the most notorious such conclusion is that the spin of a spin-1/2 particle can be 100 in some sense [36]. To understand the properties of a state between two measurements, we must understand the dynamics of these measurements.

The canonical description of a quantum measurement is called the von Neumann model [102]. It provides a quantitative description of the physics behind a device that measures some property of a system represented by an observable $A_{\mathcal{S}}$. The input of the device is a system in an unknown state $|\psi_i\rangle_{\mathcal{S}}$ along with a meter in some pre-calibrated and well-known initial state $|\mu\rangle_{\mathcal{O}}$ that will observe the system. For now, we will imagine the meter is a single particle whose position $X_{\mathcal{O}}$ is localized within a Fourier transform-limited wavepackect. The device facilitates an interaction Hamiltonian

$$H_{\mathcal{SO}} = gA_{\mathcal{S}}P_{\mathcal{O}} \tag{3.1}$$

between the system and the meter for the duration of the measurement. $P_{\mathcal{O}}$ is the momentum of the meter and generates shifts in the meter position $X_{\mathcal{O}}$. $g = g(t)$ is an envelope function sharply peaked around the time t the measurement occurs. It is narrow compared to the free-evolution time scales of both the system and the meter. The unitary the interaction Hamiltonian generates over this short time window τ is

$$U_{\mathcal{SO}} = e^{-i\kappa A_{\mathcal{S}}P_{\mathcal{O}}}, \tag{3.2}$$

where $\kappa = g\tau/\hbar$ is a coupling coefficient.

When the device measures a system prepared in an eigenstate $|a\rangle_{\mathcal{S}}$ of $A_{\mathcal{S}}$ with eigenvalue a, it shifts the meter to the state $|\mu_a\rangle_{\mathcal{O}} = e^{-i\kappa aP_{\mathcal{O}}}|\mu\rangle$. On an arbitrary input $|\psi_i\rangle_{\mathcal{S}}$, the system and meter evolve into the state

$$U_{\mathcal{SO}}|\psi_i\rangle_{\mathcal{S}}|\mu\rangle_{\mathcal{O}} = \sum_a \Pi_{a,\mathcal{S}}|\psi_i\rangle_{\mathcal{S}}|\mu_a\rangle_{\mathcal{O}}, \tag{3.3}$$

where $\Pi_{a,\mathcal{S}}$ is the projector onto the eigenspace of $A_{\mathcal{S}}$ with eigenvalue a. The state of the meter

now allows us to infer what value of $A_{\mathcal{S}}$ the system had prior to the measurement. We represent this inference by an observable $A_{\mathcal{O}}$ which is calibrated to have an expectation value of a whenever the meter is in the state $|\mu_a\rangle_{\mathcal{O}}$. That is

$$\langle\mu_a|_{\mathcal{O}} A_{\mathcal{O}} |\mu_a\rangle_{\mathcal{O}} = a \tag{3.4}$$

for all a we might expect to measure. Using the canonical commutation relation $[X_{\mathcal{O}}, P_{\mathcal{O}}] = i\hbar$, we can see that the operator

$$A_{\mathcal{O}} = \frac{X_{\mathcal{O}} - \langle\mu|_{\mathcal{O}} X_{\mathcal{O}} |\mu\rangle_{\mathcal{O}}}{\kappa\hbar} \tag{3.5}$$

satisfies this property. It follows that the expectation value of $A_{\mathcal{O}}$ after the measurement correctly infers the expectation value of $A_{\mathcal{S}}$ on any system before the measurement.

$$\langle\psi_i|_{\mathcal{S}} A_{\mathcal{S}} |\psi_i\rangle_{\mathcal{S}} = \langle\psi_i|_{\mathcal{S}} \langle\mu|_{\mathcal{O}} U^\dagger_{\mathcal{SO}} A_{\mathcal{O}} U_{\mathcal{SO}} |\psi_i\rangle_{\mathcal{S}} |\mu\rangle_{\mathcal{O}} . \tag{3.6}$$

Suppose the system is later measured and found to be in the state $|\psi_f\rangle_{\mathcal{S}}$. With this information in hand, we can use a conditional expectation value to make an even better inference.

$$\mathbb{E}\left[A_{\mathcal{O}} || \psi_f\rangle\langle\psi_f|_{\mathcal{S}}\right] = \frac{\mathbb{E}\left[|\psi_f\rangle\langle\psi_f|_{\mathcal{S}} A_{\mathcal{O}}\right]}{\mathbb{E}\left[|\psi_f\rangle\langle\psi_f|_{\mathcal{S}}\right]} = \frac{\langle\psi_i|_{\mathcal{S}} \langle\mu|_{\mathcal{O}} U^\dagger_{\mathcal{SO}} \left(|\psi_f\rangle\langle\psi_f|_{\mathcal{S}} A_{\mathcal{O}}\right) U_{\mathcal{SO}} |\psi_i\rangle_{\mathcal{S}} |\mu\rangle_{\mathcal{O}}}{\langle\psi_i|_{\mathcal{S}} \langle\mu|_{\mathcal{O}} U^\dagger_{\mathcal{SO}} |\psi_f\rangle\langle\psi_f|_{\mathcal{S}} U_{\mathcal{SO}} |\psi_i\rangle_{\mathcal{S}} |\mu\rangle_{\mathcal{O}}} \tag{3.7}$$

If each of the various meter states $|\mu_a\rangle_{\mathcal{O}}$ are well-separated in the sense that $\langle\mu_a|\mu_{a'}\rangle \approx 0$ for all $a \neq a'$, then the probability for the meter to be in state $|\mu_a\rangle_{\mathcal{O}}$ is approximately the probability that the system had the eigenvalue a. The conditional expectation becomes

$$\lim_{\langle\mu_a|\mu_{a'}\rangle \to \delta_{a,a'}} \mathbb{E}\left[A_{\mathcal{O}} || \psi_f\rangle\langle\psi_f|_{\mathcal{S}}\right] = \frac{\sum_a a |\langle\psi_f|_{\mathcal{S}} \Pi_{a,\mathcal{S}} |\psi_i\rangle_{\mathcal{S}}|^2}{\sum_a |\langle\psi_f|_{\mathcal{S}} \Pi_{a,\mathcal{S}} |\psi_i\rangle_{\mathcal{S}}|^2}. \tag{3.8}$$

This expression is known in the literature as the ABL rule[103] after its authors Aharanov, Bergmann, and Lebowitz. In this limit, the device generates strong correlations between the system and the meter, but these correlations do not come for free. Any relative phase there might have been between different a eigenspaces has been completely washed out. This measurement is called "strong" because it creates strong correlations, but also strong disturbance.

At first glance, the formula might seem innocuous, but it exhibits some rather strange properties. First, the formula is non-linear in the observable $A_{\mathcal{S}}$, unlike the usual formula for a quantum expectation value. As a result, the ABL formula can lead us to infer that the conditionally expected valued value for a sum of observables $A_{\mathcal{S}} + B_{\mathcal{S}}$ is not the same as the sum of the conditional expectations for $A_{\mathcal{S}}$ and $B_{\mathcal{S}}$. Furthermore, the formula is sensitive to how exactly we measure observables. For example, suppose we want to check whether a spin-1 particle is spinning up or not. The corresponding observable would be $|1\rangle\langle 1|_{\mathcal{S}}$. One way to measure the observable would be to measure the spin projection of the particle using an interaction Hamiltonian $H_{\mathcal{SO}} = g S_{z,\mathcal{S}} P_{\mathcal{O}}$ and assign a value of 0 whenever the spin was 0 or $-\hbar$ and 1 otherwise. The conditional expectation would be

$$\frac{|\langle\psi_f||1\rangle\langle 1||\psi_i\rangle|^2}{|\langle\psi_f||-1\rangle\langle -1||\psi_i\rangle|^2 + |\langle\psi_f||0\rangle\langle 0||\psi_i\rangle|^2 + |\langle\psi_f||1\rangle\langle 1||\psi_i\rangle|^2}. \tag{3.9}$$

Another way would be to couple directly to the observable $|1\rangle\langle 1|_{\mathcal{S}}$ with an interaction Hamiltonian

$H_{\mathcal{SO}} = g|1\rangle\langle 1|_{\mathcal{S}} P_{\mathcal{O}}$. The conditional expectation with this approach would be

$$\frac{|\langle\psi_f||1\rangle\langle 1||\psi_i\rangle|^2}{|\langle\psi_f(||-1\rangle\langle -1| + |0\rangle\langle 0|)|\psi_i\rangle|^2 + |\langle\psi_f||1\rangle\langle 1||\psi_i\rangle|^2}. \tag{3.10}$$

These two expressions for the conditional expectation of whether or not the particle is spinning up are manifestly different, despite the fact that they both seem like perfectly legitimate ways to measure that observable. The difference comes down to the fact that the two measurement methods impart two different strong back-actions.

Strong measurements are not the only useful kind of measurement. The opposite limit is a "weak" measurement in which the meter only shifts by a tiny amount. The meter's state becomes only weakly correlated with the state of the system, so finding the meter in state $|\mu_a\rangle_{\mathcal{O}}$ does not let us immediately infer that the state had eigenvalue a. However, if we are blessed with many independent and identical copies of an unknown state $|\psi_i\rangle_{\mathcal{S}}$, we can still infer something meaningful in a statistical sense. While the state of the meter after any given trial might not be very informative, the expectation value of the meter observable $A_{\mathcal{O}}$ still lets us infer properties of the system ensemble.

We express a weak measurement mathematically by expanding the interaction unitary $U_{\mathcal{SO}}$ to first order in the coupling κ.

$$U_{\mathcal{SO}} = \mathbb{1} - i\kappa A_{\mathcal{S}} P_{\mathcal{O}} + O(\kappa^2) \tag{3.11}$$

$$\begin{aligned}
\mathbb{E}\left[|\psi_f\rangle\langle\psi_f|_{\mathcal{S}}\right] &= \langle\psi_i|_{\mathcal{S}} \langle\mu|_{\mathcal{O}} U^\dagger_{\mathcal{SO}} |\psi_f\rangle\langle\psi_f|_{\mathcal{S}} U_{\mathcal{SO}} |\psi_i\rangle_{\mathcal{S}} |\mu\rangle_{\mathcal{O}} && (3.12)\\
&= |\langle\psi_f|\psi_i\rangle|^2 + O(\kappa^2) && (3.13)
\end{aligned}$$

$$\begin{aligned}
\mathbb{E}\left[A_{\mathcal{O}}||\psi_f\rangle\langle\psi_f|_{\mathcal{S}}\right] &= \langle\psi_i|_{\mathcal{S}} \langle\mu|_{\mathcal{O}} U^\dagger_{\mathcal{SO}} |\psi_f\rangle\langle\psi_f|_{\mathcal{S}} A_{\mathcal{O}} U_{\mathcal{SO}} |\psi_i\rangle_{\mathcal{S}} |\mu\rangle_{\mathcal{O}} && (3.14)\\
&= 2\kappa \operatorname{Im}\left[\langle\psi_i|A_{\mathcal{S}}|\psi_f\rangle \langle\psi_f|\psi_i\rangle \langle\mu|P_{\mathcal{O}} A_{\mathcal{O}}|\mu\rangle\right] + O(\kappa^2) && (3.15)\\
&= 2\kappa \operatorname{Re}\left[\langle\psi_i|A_{\mathcal{S}}|\psi_f\rangle \langle\psi_f|\psi_i\rangle\right] \operatorname{Im}\left[\langle\mu|P_{\mathcal{O}} A_{\mathcal{O}}|\mu\rangle\right] && (3.16)\\
&+ 2\kappa \operatorname{Im}\left[\langle\psi_i|A_{\mathcal{S}}|\psi_f\rangle \langle\psi_f|\psi_i\rangle\right] \operatorname{Re}\left[\langle\mu|P_{\mathcal{O}} A_{\mathcal{O}}|\mu\rangle\right] + O(\kappa^2) && (3.17)
\end{aligned}$$

The conditional expectation of a weak measurement is

$$\begin{aligned}
\mathbb{E}\left[A_{\mathcal{O}}||\psi_f\rangle\langle\psi_f|_{\mathcal{S}}\right] &= 2\kappa \operatorname{Re}\left[\frac{\langle\psi_f|A_{\mathcal{S}}|\psi_i\rangle}{\langle\psi_f|\psi_i\rangle}\right] \operatorname{Im}\left[\langle\mu|P_{\mathcal{O}} A_{\mathcal{O}}|\mu\rangle\right] && (3.18)\\
&+ 2\kappa \operatorname{Im}\left[\frac{\langle\psi_f|A_{\mathcal{S}}|\psi_i\rangle}{\langle\psi_f|\psi_i\rangle}\right] \operatorname{Re}\left[\langle\mu|P_{\mathcal{O}} A_{\mathcal{O}}|\mu\rangle\right] + O(\kappa^2). && (3.19)
\end{aligned}$$

To proceed further, we must simplify the terms involving $\langle\mu|P_{\mathcal{O}} A_{\mathcal{O}}|\mu\rangle$. Using the canonical commutation relation $[X_{\mathcal{O}}, P_{\mathcal{O}}] = i\hbar$ again, we get $\operatorname{Im}\left[\langle\mu|P_{\mathcal{O}} A_{\mathcal{O}}|\mu\rangle\right] = 1/(2\kappa)$. The real part is

$$\frac{\langle\mu|\frac{1}{2}\left(P_{\mathcal{O}} X_{\mathcal{O}} + X_{\mathcal{O}} P_{\mathcal{O}}\right)|\mu\rangle - \langle\mu|P_{\mathcal{O}}|\mu\rangle \langle\mu|X_{\mathcal{O}}|\mu\rangle}{\kappa\hbar}, \tag{3.20}$$

which is proportional to the covariance between the $X_{\mathcal{O}}$ and $P_{\mathcal{O}}$ quadratures of the initial meter state. We assume the Gaussian meter state $|\mu\rangle_{\mathcal{O}}$ is aligned with the axes laid out by these quadratures so that this covariance is 0. At last, we have a simple equation for the conditional expectation in the

weak limit:

$$\mathbb{E}\left[A_{\mathcal{O}}||\psi_f\rangle\langle\psi_f|_{\mathcal{S}}\right] = \mathrm{Re}\left[\frac{\langle\psi_f|A_{\mathcal{S}}|\psi_i\rangle}{\langle\psi_f|\psi_i\rangle}\right] + O(\kappa^2). \tag{3.21}$$

The complex quantity

$$\frac{\langle\psi_f|A_{\mathcal{S}}|\psi_i\rangle}{\langle\psi_f|\psi_i\rangle} \tag{3.22}$$

is known as the "weak" value, because of its central importance in weak measurements[36].

Unlike the ABL formula, the weak value is linear in the observable $A_{\mathcal{S}}$. Moreover, it appears not to depend on how we couple to the observable like the ABL formula does. If we wanted to know whether a spin-1 particle was pointing up, we would get the same conditional expectation from a weak measurement regardless of whether the measurement device coupled to $S_{z,\mathcal{S}}$ or directly to $|1\rangle\langle 1|_{\mathcal{S}}$. However, the weak value is, at the end of the day, a property of an ensemble. It is extremely tempting to interpret it as a property of individual states as well, but such an interpretation has been the cause for decades of debate.

Famously, if we measure a spin-1/2 particle and we set $|\psi_i\rangle_{\mathcal{S}} = |1/2\rangle$, $|\psi_f\rangle_{\mathcal{S}} = (200\,|-1/2\rangle + |1/2\rangle)/\sqrt{200^2+1}$, and $A_{\mathcal{S}} = s_x$, we get

$$\frac{\langle\psi_f|A_{\mathcal{S}}|\psi_i\rangle}{\langle\psi_f|\psi_i\rangle} = 100\hbar. \tag{3.23}$$

Does this result imply that individual particles really took on a spin value of $100\hbar$ between their pre and postselection? If it does, how would we interpret situations where the spin weak value is an imaginary number like $i100\hbar$, which is the weak value we get from postselecting on $|\psi_f\rangle_{\mathcal{S}} = (i200\,|-1/2\rangle + |1/2\rangle)/\sqrt{200^2+1}$.

To understand what an imaginary weak value might mean, even as an ensemble property, we will first describe how one might actually measure this imaginary value. Previously, our conditional expectation ended up giving us the real part of the weak value because the initial meter state $|\mu\rangle_{\mathcal{O}}$ and meter observable $A_{\mathcal{O}}$ were designed so that

$$\langle\mu|P_{\mathcal{O}}A_{\mathcal{O}}|\mu\rangle = \frac{i}{2\kappa}. \tag{3.24}$$

Evidently, we can get the imaginary part of the weak value by replacing our inference from $A_{\mathcal{O}}$ to a new observable $\tilde{A}_{\mathcal{O}}$ with the properties that

$$\langle\mu|P_{\mathcal{O}}\tilde{A}_{\mathcal{O}}|\mu\rangle = \frac{1}{2\kappa} \tag{3.25}$$

and

$$\langle\mu|\tilde{A}_{\mathcal{O}}|\mu\rangle = 0. \tag{3.26}$$

These conditions are both satisfied by setting

$$\tilde{A}_{\mathcal{O}} = \frac{1}{\kappa}\frac{P_{\mathcal{O}} - \langle\mu|P_{\mathcal{O}}|\mu\rangle}{\langle\mu|P_{\mathcal{O}}^2|\mu\rangle - \langle\mu|P_{\mathcal{O}}|\mu\rangle^2}. \tag{3.27}$$

Now we have a way to measure the imaginary part of the weak value, but what does it actually tell us? The imaginary part turns out to be related to how the postselection success probability depends on the infinitesimal back-action induced by measuring $A_{\mathcal{S}}$. The probability of postselection

is

$$\mathbb{E}\left[|\psi_f\rangle\langle\psi_f|_{\mathcal{S}}\right] = \langle\psi_i|_{\mathcal{S}} \langle\mu|_{\mathcal{O}} e^{i\kappa A_{\mathcal{S}} P_{\mathcal{O}}} |\psi_f\rangle\langle\psi_f|_{\mathcal{S}} e^{-i\kappa A_{\mathcal{S}} P_{\mathcal{O}}} |\psi_i\rangle_{\mathcal{S}} |\mu\rangle_{\mathcal{O}} . \tag{3.28}$$

The right-hand side of this equation involves iterated commutators of $A_{\mathcal{S}}$ with $|\psi_f\rangle\langle\psi_f|_{\mathcal{S}}$ such as $[A_{\mathcal{S}}, |\psi_f\rangle\langle\psi_f|]$, $[A_{\mathcal{S}}, [A_{\mathcal{S}}, |\psi_f\rangle\langle\psi_f|]]$, and so on. These iterated commutators can be expressed neatly in terms of the superoperator $\mathrm{ad}_{A_{\mathcal{S}}}$ (pronounced "adjoint") which acts on an arbitrary system operator $M_{\mathcal{S}}$ as $\mathrm{ad}_{A_{\mathcal{S}}}[M_{\mathcal{S}}] = A_{\mathcal{S}} M_{\mathcal{S}} - M_{\mathcal{S}} A_{\mathcal{S}}$. Using this notation, the probability of postselection is

$$\mathbb{E}\left[|\psi_f\rangle\langle\psi_f|_{\mathcal{S}}\right] = \langle\psi_i|_{\mathcal{S}} \langle\mu|_{\mathcal{O}} e^{i\kappa\, \mathrm{ad}_{A_{\mathcal{S}}}\, P_{\mathcal{O}}} \left[|\psi_f\rangle\langle\psi_f|_{\mathcal{S}}\right] |\psi_i\rangle_{\mathcal{S}} |\mu\rangle_{\mathcal{O}} . \tag{3.29}$$

We will now assume that the meter starts with zero expected momentum $\langle\mu|P_{\mathcal{O}}|\mu\rangle = 0$ and its initial momentum uncertainty is $\sigma_p^2 = \langle\mu|P_{\mathcal{O}}^2|\mu\rangle$. To see how the postselection varies with the back-action from measuring $A_{\mathcal{S}}$, we will introduce a transformation

$$i\kappa\, \mathrm{ad}_{A_{\mathcal{S}}} \to i\kappa\, \mathrm{ad}_{A_{\mathcal{S}}} + \delta\kappa^{-1}\sigma_p^{-2}. \tag{3.30}$$

The size of the parameter δ controls the amount of back-action imparted to the meter in units of $1/A_{\mathcal{S}}$.

$$\mathbb{E}\left[|\psi_f\rangle\langle\psi_f|_{\mathcal{S}}\right](\delta) = \langle\psi_i|_{\mathcal{S}} \langle\mu|_{\mathcal{O}} e^{i\kappa\, \mathrm{ad}_{A_{\mathcal{S}}}\, P_{\mathcal{O}} + 2\delta\tilde{A}_{\mathcal{O}}} \left[|\psi_f\rangle\langle\psi_f|_{\mathcal{S}}\right] |\psi_i\rangle_{\mathcal{S}} |\mu\rangle_{\mathcal{O}} . \tag{3.31}$$

In the equation above, we used the assumption $\langle\mu|P_{\mathcal{O}}|\mu\rangle = 0$ to equate $\tilde{A}_{\mathcal{O}} = P_{\mathcal{O}}(2\kappa)^{-1}\sigma_p^{-2}$. The sensitivity of the postselection probability to δ is

$$\left.\frac{\partial \log \mathbb{E}\left[|\psi_f\rangle\langle\psi_f|_{\mathcal{S}}\right]}{\partial\delta}\right|_{\delta=0} = 2\frac{\langle\psi_i|_{\mathcal{S}} \langle\mu|_{\mathcal{O}} e^{i\kappa\, \mathrm{ad}_{A_{\mathcal{S}}}\, P_{\mathcal{O}}} \left[|\psi_f\rangle\langle\psi_f|_{\mathcal{S}} \tilde{A}_{\mathcal{O}}\right] |\psi_i\rangle_{\mathcal{S}} |\mu\rangle_{\mathcal{O}}}{\langle\psi_i|_{\mathcal{S}} \langle\mu|_{\mathcal{O}} e^{i\kappa\, \mathrm{ad}_{A_{\mathcal{S}}}\, P_{\mathcal{O}}} \left[|\psi_f\rangle\langle\psi_f|_{\mathcal{S}}\right] |\psi_i\rangle_{\mathcal{S}} |\mu\rangle_{\mathcal{O}}}. \tag{3.32}$$

The conditional expectation of the imaginary meter observable is exactly half of the above quantity. The precise relationship between the imaginary part and the sensitivity of the postselection probability is thus

$$\frac{1}{2}\left.\frac{\partial \log \mathbb{E}\left[|\psi_f\rangle\langle\psi_f|_{\mathcal{S}}\right]}{\partial\delta}\right|_{\delta=0} = \mathbb{E}\left[\tilde{A}_{\mathcal{O}} || \psi_f\rangle\langle\psi_f|_{\mathcal{S}}\right] . \tag{3.33}$$

Having gone through the archetypical von Neumann measurement model, I am ready to present the following paper.

Variable-strength non-local measurements reveal quantum violations of classical counting principles

Noah Lupu-Gladstein,[1,*] Arthur O. T. Pang,[1] Hugo Ferretti,[1] Weng-Kian Tham,[1] Aephraim M. Steinberg,[1,2] Kent Bonsma-Fisher,[1,3] and Aharon Brodutch[1]

[1] *Department of Physics and Center for Quantum Information and Quantum Control, University of Toronto, 60 St George St, Toronto, Ontario, M5S 1A7, Canada*
[2] *Canadian Institute for Advanced Research, Toronto, Ontario, M5G 1M1, Canada*
[3] *National Research Council of Canada, 100 Sussex Dr, Ottawa, Ontario, K1A 0R6, Canada*

(Dated: July 1, 2024)

We implement a variant of the quantum pigeonhole paradox thought experiment to study whether classical counting principles survive in the quantum domain. We observe strong measurements significantly violate the pigeonhole principle (that among three pigeons in two holes, at least one pair must be in the same hole) and the sum rule (that the number of pigeon pairs in the same hole is the sum of the number of pairs across each of the holes) in an ensemble that is pre and postselected into particular separable states. To investigate whether measurement disturbance is a viable explanation for these counterintuitive phenomena, we employ the first ever variable-strength measurement of a non-local observable. As we decrease the measurement strength, we find the violation of the sum rule decreases, yet the pigeonhole principle remains violated. In the weak limit, the sum rule is restored due to the cancellation between two weak values with equal and opposite imaginary parts. We observe the same kind of cancellation at higher measurement strengths, thus raising the question: do strong measurements have imaginary parts?

* nlupugla@physics.utoronto.ca.

The correspondence between quantum measurements and physical reality has been a source of intense debates since the early days of quantum theory [104–108]. One point of contention involves the connection between mathematically defined observables and our classical intuition about what these observables represent. The problem manifests starkly in *pre and postselection* (PPS) experiments where a system is first prepared in some initial state $|\psi_i\rangle$ (the preselection), then measured at some intermediate time, then projected onto some final state $|\psi_f\rangle$ (the postselection). Naively interpreting the result of the intermediate measurement as reflecting elements of physical reality can lead to paradoxes [109–121]. One resolution invokes measurement back-action, implying a disconnect between measurement results and the real state of affairs.

We present an experiment that probes the role of back-action in these paradoxes by varying the type and strength of measurement disturbance. The experiment is inspired by the so-called quantum pigeonhole paradox [120, 122]. The paradox arises from a counter-intuitive prediction that three pigeons placed among two holes can each occupy a different hole. This apparent logical contradiction has been observed indirectly at the weak limit in the correlations of a neutron interferometer [123] and directly at the the strong limit, using the Hong-Ou-Mandel effect to check if a pair of photons are in the same polarization state [124]. Our experiment is the first to investigate the pigeonhole paradox across the full spectrum of measurement strengths, and indeed, the first to measure any non-local observable of a spatially distributed system over such a range of strengths.

In our experiment, the "pigeons" are photons in displaced Sagnac interferometers and the "pigeonholes" are the two possible travel directions: clockwise $|\mathcal{C}\rangle$ and anti-clockwise $|\mathcal{A}\rangle$ (see Fig. 3.1). The corresponding, observables for a particular pigeon $k \in \{(1,2,3)\}$ are the projectors $\Pi_{\mathcal{C}}{}^k = |\mathcal{C}\rangle^k \langle\mathcal{C}|^k$ and $\Pi_{\mathcal{A}}{}^k = |\mathcal{A}\rangle^k \langle\mathcal{A}|^k$. Each photon is preselected in the state $|+\rangle^k = \left(\frac{|\mathcal{C}\rangle^k + |\mathcal{A}\rangle^k}{\sqrt{2}}\right)$ as it enters the interferometer and later postselected in the state $|+i\rangle^k = \left(\frac{|\mathcal{C}\rangle^k + i|\mathcal{A}\rangle^k}{\sqrt{2}}\right)$ as it leaves. The quantum pigeonhole paradox concerns the observables $\Pi_{\mathcal{S}}^{k,\ell} = \Pi_{\mathcal{A}}{}^k \Pi_{\mathcal{A}}{}^\ell + \Pi_{\mathcal{C}}{}^k \Pi_{\mathcal{C}}{}^\ell$, which asks whether a particular pair of photons $(k,\ell) \in \{(1,2),(1,3),(2,3)\}$ traveled the same direction. These observables seems to defy two fundamental counting principles.

1. **The pigeonhole principle**: when there are more pigeons than holes, at least one pair of pigeons must be in the same hole. Violated because $|\langle+i|^k \langle+i|^\ell \Pi_{\mathcal{S}}^{k,\ell} |+\rangle^k |+\rangle^\ell|^2 = 0$.

2. **The sum rule**: the number of pigeons among two holes is at least the number of pigeons in either hole. Violated because $|\langle+i|^k \langle+i|^\ell \Pi_{\mathcal{C}}{}^k \Pi_{\mathcal{C}}{}^\ell |+\rangle^k |+\rangle^\ell|^2 = 1/16 > 0$ and $|\langle+i|^k \langle+i|^\ell \Pi_{\mathcal{A}}{}^k \Pi_{\mathcal{A}}{}^\ell |+\rangle^k |+\rangle^\ell|^2 = 1/16 > 0$.

The quantum pigeonhole paradox

As a quantum paradox, the pigeonhole paradox exhibits several crucial features. First, the paradox involves correlations in a non-local system: each pigeon could be in a different space-like separated region of the galaxy, but quantum mechanics predicts the paradox will occur nevertheless. Second, the preselection and postselection are both separable states, making it difficult to rely on the features of quantum entanglement to explain away the paradox. Finally, these separable states are symmetric, making it irrelevant which particular pair of pigeons are observed.

This last feature is experimentally convenient, as it enables us to measure only a single pair of pigeons. While putting two pigeons in two different holes is trivial, we can still derive a bound

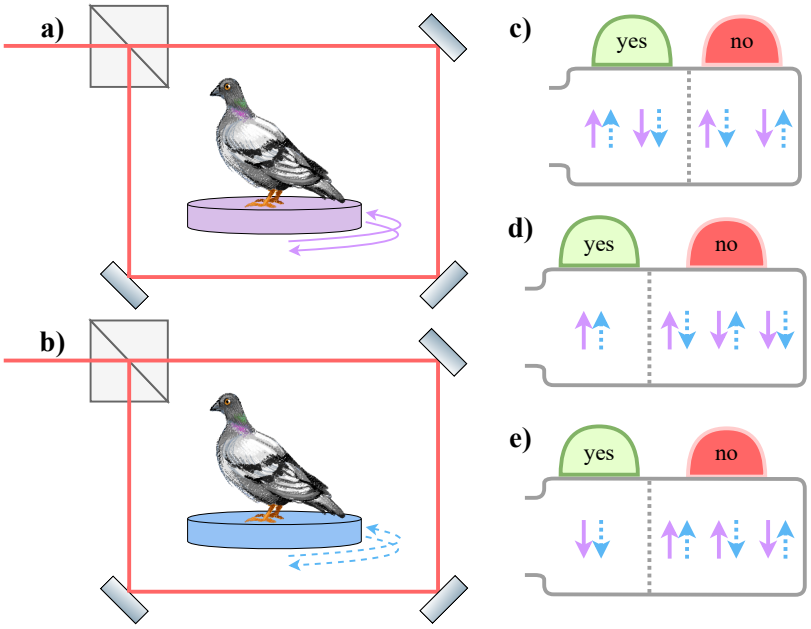

Figure 3.1: Conceptual overview. a) and b): quantum pigeons in two pigeonholes are represented as photons that can propagate clockwise or anti-clockwise through a displaced Sagnac interferometer. Beamsplitters prepare the pigeons in $|+\rangle|+\rangle$, then one of the devices c), d), or e) measures them, then we postselect them onto the state $|+i\rangle|+i\rangle$ by only detecting photons that exit the same port of the interferometer they entered. c), d), and e): different measurements used to observe the pigeons. c) asks "are both pigeons traveling the same direction?" d) asks "are both pigeons traveling clockwise?" e) asks "are both pigeons traveling anti-clockwise?".

that separates intuitive classical behavior from the phenomna arising in the pigeonhole paradox. Suppose three pigeons are placed in two holes according to an arbitrary probability distribution $P(b_1, b_2, b_3)$, where $b_i \in \{\mathcal{C}, \mathcal{A}\}$ are boolean variables indicating which of two holes the ith pigeon is placed. Uniformly at random, a pair of pigeons are examined to determine whether or not they are in the same hole. The chance to find the random pair in the same hole is

$$\begin{aligned}
&(P(\mathcal{C},\mathcal{C},\mathcal{C}) + P(\mathcal{A},\mathcal{A},\mathcal{C}) + P(\mathcal{C},\mathcal{C},\mathcal{A}) + P(\mathcal{A},\mathcal{A},\mathcal{A}) \\
&+P(\mathcal{C},\mathcal{C},\mathcal{C}) + P(\mathcal{A},\mathcal{C},\mathcal{A}) + P(\mathcal{C},\mathcal{A},\mathcal{C}) + P(\mathcal{A},\mathcal{A},\mathcal{A}) \\
&+P(\mathcal{C},\mathcal{C},\mathcal{C}) + P(\mathcal{C},\mathcal{A},\mathcal{A}) + P(\mathcal{A},\mathcal{C},\mathcal{C}) + P(\mathcal{A},\mathcal{A},\mathcal{A}))/3 \\
&= 1/3 + (P(\mathcal{C},\mathcal{C},\mathcal{C}) + P(\mathcal{A},\mathcal{A},\mathcal{A}))2/3 \\
&\geq 1/3.
\end{aligned}$$

There is no classical distribution of three pigeons across two holes in which a random pair of pigeons is found in the same hole less than $1/3$ of the time. In this sense, a measurement of $\Pi_{\mathcal{S}}^{\ell k}$ that comes out "yes" with any frequency less than $1/3$ violates the classical pigeonhole principle. For the rest of the manuscript, we will deal only with Pigeons 1 and 2 without loss of generality, so we set $\Pi_{\mathcal{S}} = \Pi_{\mathcal{S}}^{12}$, $\Pi_{\mathcal{CC}} = \Pi_{\mathcal{C}}{}^1\Pi_{\mathcal{C}}{}^2$, and $\Pi_{\mathcal{AA}} = \Pi_{\mathcal{A}}{}^1\Pi_{\mathcal{A}}{}^2$.

Our experiment hones in on the distinction between an observable and the variety of ways to measure that observable. We compare several different ways to measure $\Pi_{\mathcal{S}}$. The first has only two outcomes: {"same direction", "different direction"}. That is, the measurement reveals whether

photon 1 and 2 travelled the same direction, but not which direction they travelled. The second sums the results of {"both clockwise", "neither clockwise" } and {"both anti-clockwise", "neither anti-clockwise" }.

Every "yes" or "no" question in quantum mechanics can be represented by some projector Π. We will call a measurement of Π "direct" if it indicates whether or not the system was in a "yes" (or "no") state, but not which among potentially many "yes" (or "no") states the system was in. Mathematically, we represent such a "direct" measurement by a unitary $U_\Pi(s)$ that acts on any system state $|\psi\rangle$ and a particular meter state $|\mu\rangle$ according to

$$U_\Pi(s)\,|\psi\rangle\,|\mu\rangle = \Pi\,|\psi\rangle\,|s\rangle + (\mathbb{1}-\Pi)\,|\psi\rangle\,|-s\rangle\,, \tag{3.34}$$

where

$$s = \sqrt{1-|\,\langle s|-s\rangle\,|^2} \tag{3.35}$$

is the "strength" of the measurement. A strong measurement has $s = 1$ and sends the meter into one of two orthogonal state: $|s=1\rangle$ or $|s=-1\rangle$. A weak measurement has $s \ll 1$, meaning the meter shifts to one of two nearly indistinguishable states.

While a single weak measurement provides vanishing information about whether the system was in a "yes" or "no" state, averaging the results of weak measurements across many independent and identical systems yields the so-called "weak value" [125]. The weak value of an observable Π prepared in state $|\psi_i\rangle$ and postselected in state $|\psi_f\rangle$ is the complex number

$$\frac{\langle\psi_f|\,\Pi\,|\psi_i\rangle}{\langle\psi_f|\psi_i\rangle}. \tag{3.36}$$

The real part of the weak value is obtained by measuring the meter in the "real" basis $|\pm\,\mathrm{Re}\rangle = |s=\pm 1\rangle$. The imaginary part comes from measuring the meter in the "imaginary" basis $|\pm\,\mathrm{Im}\rangle = (|+\,\mathrm{Re}\rangle \pm i\,|-\,\mathrm{Re}\rangle)/\sqrt{2}$.

In the strong limit, measuring the meter in the real basis gives the probability for the system to have been in a "yes" state, given the postselection succeeded. This probability is predicted by the Aharonov-Bergmann-Lebowitz formula [103].

$$\frac{|\,\langle\psi_f|\,\Pi\,|\psi_i\rangle\,|^2}{|\,\langle\psi_f|\,\Pi\,|\psi_i\rangle\,|^2 + |\,\langle\psi_f|\,(\mathbb{1}-\Pi)\,|\psi_i\rangle\,|^2} \tag{3.37}$$

Curiously, the literature on PPS experiments has so far ignored the strong limit of measuring the meter in the imaginary basis. Even the recent work of De Zela, which studied the role of weak values in strong measurements, did not comment on such strong imaginary measurements[126]. Like their weak counterparts [81], they can be related to the sensitivity of the postselection probability to the measurement's back-action (see Sec. 3.2.2 for more details). The usual model of quantum measurement uses a Gaussian probe, and in fact, this model predicts the imaginary part goes to 0 in the infinitely strong limit [81]. However, the decay of the imaginary part to 0 is not a universal feature of quantum measurement. For a strong, direct measurement of a projector via a qubit probe, the quantity comes out to

$$\frac{\mathrm{Im}[\langle\psi_i|\psi_f\rangle\,\langle\psi_f|\,\Pi\,|\psi_i\rangle]}{|\,\langle\psi_f|\,\Pi\,|\psi_i\rangle\,|^2 + |\,\langle\psi_f|\,(\mathbb{1}-\Pi)\,|\psi_i\rangle\,|^2}. \tag{3.38}$$

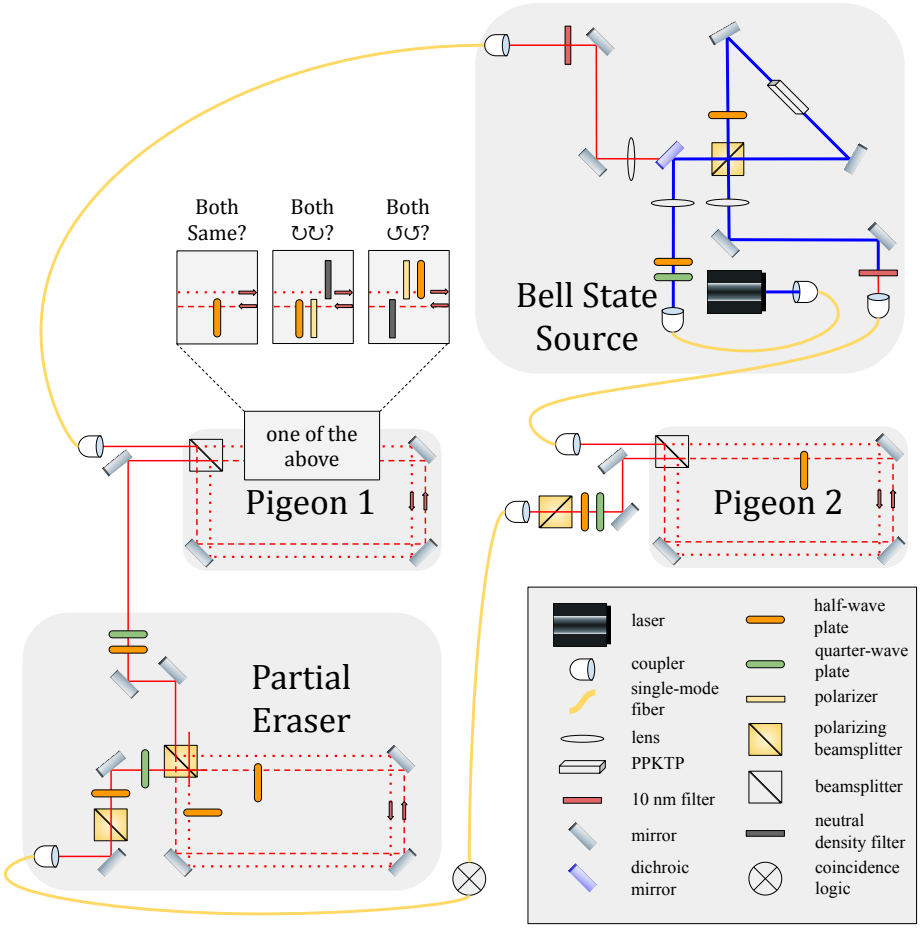

Figure 3.2: Experimental setup. A Bell-state source generates polarization-entangled photons by pumping a PPKTP crystal with a continuous-wave laser at 405 nm. Each photon enters a non-polarizing displaced Sagnac interferometer which allows the photonic pigeon to travel in a superposition of two pigeonholes. The photons are postselected by ignoring an output port of each interferometer. A half waveplate in the anti-clockwise path of the Pigeon 2 interferometer performs a strong which-path measurement. The photon is detected and the result of its which-path measurement steers Pigeon 1. One of three different sets of optics in Pigeon 1 encode a strong, direct measurement of either $\Pi_{\mathcal{S}}$, $\Pi_{\mathcal{CC}}$, or $\Pi_{\mathcal{AA}}$ onto polarization. The partial eraser, a polarizing displaced Sagnac interferometer, couples polarization to path, then erases the polarization information. The strength of the polarization-path coupling is set by the angle of two half waveplates inside the partial eraser.

This value is not always 0, which complicates criticisms of the weak value on the basis of its imaginary component [127–129]. Strong measurements, at least in some sense, have imaginary parts too.

Direct non-local measurements

Our experiment implements three direct measurements at a continuum of measurement strengths: $U_{\Pi_{\mathcal{S}}}(s)$, $U_{\Pi_{\mathcal{CC}}}(s)$, and $U_{\Pi_{\mathcal{AA}}}(s)$. These measurements are made on pairs of particles, and must be non-destructive [130]. These types of non-local measurements are currently attracting considerable attention with a number of recent theoretical proposals [114, 131–137] and experimental results at both the strong limit [138–140] and the weak limit [112, 115, 141]. The Hamiltonians that generates variable-strength, direct measurements of two-body observables such as $\Pi_{\mathcal{CC}}$ require three-body interaction terms of the form

$$M^0\Pi^1\Pi^2, \tag{3.39}$$

where M^0 is some meter observable. Physically, these terms represent a single meter interacting simultaneously with two spatially separate systems. This interaction would have to be non-local, and thus un-physical. Nevertheless, it is possible to simulate these interactions using a combination of quantum steering and quantum erasure [131].

The first step in generating these non-local interactions is to prepare our photonic pigeons with a shared and entangled polarization probe. We use the Bell state source, illustrated in Fig. 3.2 and described in detail in Sec. 3.2.3 to generate pairs of photons whose joint polarization state is $\frac{|H\rangle|H\rangle+|V\rangle|V\rangle}{\sqrt{2}}$. We use the standard notation $|H\rangle$, $|V\rangle$ for horizontal and vertical polarization respectively, $|D\rangle = (|H\rangle+|V\rangle)/\sqrt{2}$, $|A\rangle = (|H\rangle-|V\rangle)/\sqrt{2}$ for diagonal and anti-diagonal respectively, and $|R\rangle = (|H\rangle + i\,|V\rangle)/\sqrt{2}$, $|L\rangle = (|H\rangle - i\,|V\rangle)/\sqrt{2}$ for right- and left-circular polarizations, respectively. Each photon is then sent into its own displaced Sagnac interferometer, which is opened and closed with a 50/50 beamsplitter to create the initial and final states. The initial state is always $|\psi_i\rangle = |+\rangle\,|+\rangle$ and the final state, which is selected by only detecting photons that exit the interferometer through the same port they entered and optionally blocking one of the paths is $|\psi_f\rangle \in \{|+i\rangle\,|+i\rangle, |\mathcal{C}\rangle\,|\mathcal{C}\rangle, |\mathcal{C}\rangle\,|\mathcal{A}\rangle, |\mathcal{A}\rangle\,|\mathcal{C}\rangle, |\mathcal{A}\rangle\,|\mathcal{A}\rangle\}$.

Polarization optics in the Sagnc interferometers perform strong, but non-destructive which-path measurements. The Pigeon 2 interferometer has a half waveplate in its anti-clockwise path, but not its clockwise path. Projecting photon 2 onto $|D\rangle$ (which succeeds with probability 1/2) steers Photon 1's initial polarization to $|D\rangle$ if photon 2 went clockwise and $|A\rangle$ if photon 2 went anti-clockwise. At this stage, the polarization-path state (with normalization indicating success probability) is

$$\left(|D\rangle^1 \otimes {\Pi_{\mathcal{C}}}^2\,|\psi_i\rangle^{12} + |A\rangle^1 \otimes {\Pi_{\mathcal{A}}}^2\,|\psi_i\rangle^{12}\right)/\sqrt{2}. \tag{3.40}$$

One of three different strong which-path measurements (shown in Fig. 3.2), corresponding to $\Pi_{\mathcal{S}}$, $\Pi_{\mathcal{CC}}$, and $\Pi_{\mathcal{AA}}$, shifts the polarization of photon 1. To measure $\Pi_{\mathcal{S}}$, we place a half waveplate in the anti-clockwise path, but not in the clockwise path, which evolves the state to

$$\left(|D\rangle^1 \otimes \Pi_{\mathcal{S}}^{12}\,|\psi_i\rangle^{12} + |A\rangle^1 \otimes (\mathbb{1} - \Pi_{\mathcal{S}}^{12})\,|\psi_i\rangle^{12}\right)/\sqrt{2}. \tag{3.41}$$

The polarization of photon 1 at this stage strongly encodes whether both photons have traveled the

same direction, but not which direction they traveled.

To measure $\Pi_{\mathcal{CC}}$, we place a polarizer followed by a half waveplate in the anti-clockwise path that together apply the operator $-|A\rangle\langle V|$. Photon 1 only survives this operator with probability 1/2. To keep the interferometer balanced, we place a neutral density filter with transmission probability 1/2 in the clockwise path. The state at this point is

$$\left(|D\rangle^1 \otimes \Pi^{12}_{\mathcal{CC}} |\psi_i\rangle^{12} + |A\rangle^1 \otimes (\mathbb{1} - \Pi^{12}_{\mathcal{CC}}) |\psi_i\rangle^{12}\right)/\sqrt{4}. \tag{3.42}$$

The approach for $\Pi^{12}_{\mathcal{AA}}$ is similar. In the clockwise path, we place a polarizer and half waveplate to effect the operator $-|D\rangle\langle V|$ and in the other path we place a neutral density filter. The state becomes

$$\left(|D\rangle^1 \otimes (\mathbb{1} - \Pi^{12}_{\mathcal{AA}}) |\psi_i\rangle^{12} + |A\rangle^1 \otimes \Pi^{12}_{\mathcal{AA}} |\psi_i\rangle^{12}\right)/\sqrt{4}. \tag{3.43}$$

The next step for all three measurements is to project the path state onto $|\psi_f\rangle$ by closing the Pigeon 1 interferometer. A quarter and half waveplate apply a unitary U, which rotates the results of the strong measurement into either the H/V basis, for a "real" measurement or the R/L basis for an "imaginary" measurement. The state of Photon 1's polarization at this point is proportional to

$$\langle\psi_f| \Pi |\psi_i\rangle U |D\rangle + \langle\psi_f| (\mathbb{1} - \Pi) |\psi_i\rangle U |A\rangle \tag{3.44}$$

for any of the three projectors Π.

We use a quantum eraser to erase some, but not all, of the coupling created by the strong measurement. We send the photon into a partial eraser (see Fig. 3.2), which we implement as a displaced Sagnac interferometer that opens and closes with a polarizing beamsplitter. The interferometer couples polarization and path with a strength determined by the angle of two waveplates that enact equal and opposite rotations to photons traveling through either of the two interferometer paths. The strong correlations between polarization and the original pigeon observable are destroyed by projecting the polarization onto an unbiased basis, which incurs another loss factor of 1/2. The path state of the photon just before being detected is proportional to

$$\langle\psi_f| \Pi |\psi_i\rangle |s\rangle + \langle\psi_f| (\mathbb{1} - \Pi) |\psi_i\rangle |-s\rangle\,, \tag{3.45}$$

where

$$|s\rangle = \sqrt{\frac{1+s}{2}} |\text{yes}\rangle + \sqrt{\frac{1-s}{2}} |\text{no}\rangle\,. \tag{3.46}$$

In a "real" measurement, $|\text{yes}\rangle$ and $|\text{no}\rangle$ correspond the output ports of the partial eraser. The imaginary measurement rotates these states to the superpositions $(|\text{yes}\rangle \pm i\,|\text{no}\rangle)/\sqrt{2}$. All told, the variable-strength non-local measurement procedure works with probability 1/4 for $\Pi_{\mathcal{S}}$ and probability 1/8 for $\Pi_{\mathcal{CC}}$ or $\Pi_{\mathcal{AA}}$.

Results

The results of our experiment are plotted in Fig. 3.3. Our goal is to observe properties of the pigeon system, but our data come from measurements of a polarization meter. We call the probability of finding our polarization probe in its real "yes" state the "real meter value" and the

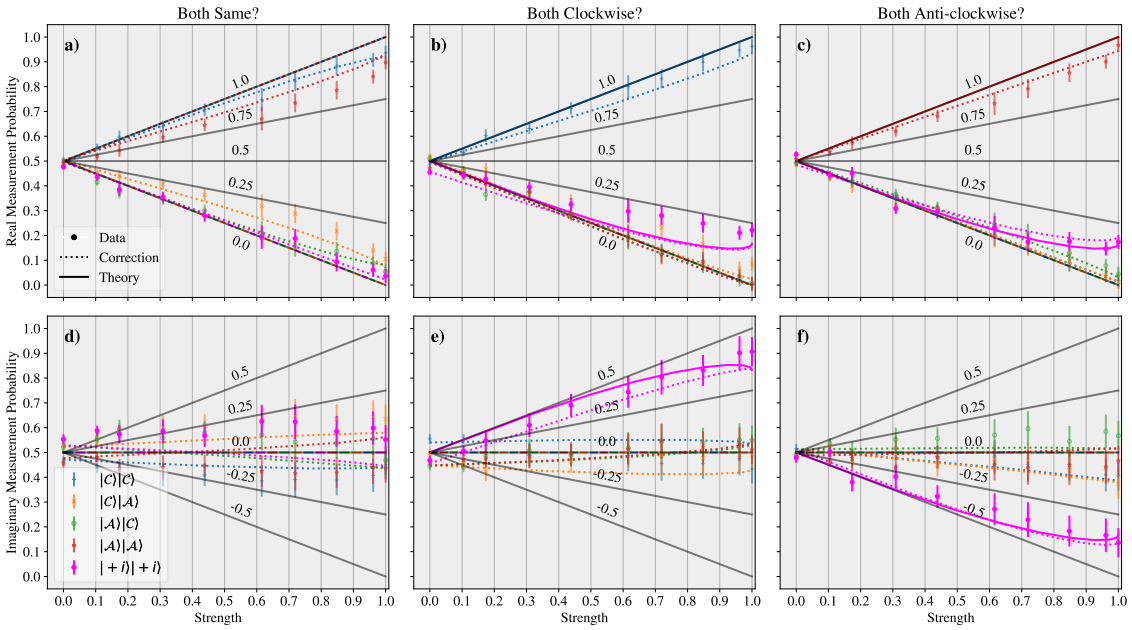

Figure 3.3: Variable-strength measurement results. In each plot, the x-axis denotes measurement strength (Eq. 3.35) such that 0 is a weak measurement and 1 is a strong measurement. a), b), and c) show the results for direct measurements of the projectors $\Pi^{12}_{\mathcal{S}}$, $\Pi^{12}_{\mathcal{CC}}$, and $\Pi^{12}_{\mathcal{AA}}$ respectively. The y-axis is the probability for the polarization meter to be in the real "yes" state. The labeled grid slopes denote the corresponding probability for the pigeons to be in the "yes" subspace of the projector, after accounting for measurement strength. At small measurement strengths, these values correspond to the real part of the weak value. Each marker and color combination represents a different path postselection. The fuchsia dots represent the paradoxical postselection $|+i\rangle\,|+i\rangle$. The other four colors are calibration data. Two different theoretical models are plotted for comparison. Solid lines are theory. Dotted lines represent a correction to this theory tomographic calibrations. d), e), and f) are organized similarly, but their y-axes show the results of measuring in the imaginary basis. At small measurement strengths, the values denoted by the labelled grid slopes correspond to the imaginary part of the weak value. The direct measurements of $\Pi^{12}_{\mathcal{S}}$ suggest that photons postselected in $|+i\rangle\,|+i\rangle$ propagate in different directions at least as often as photons which always take the $|\mathcal{C}\rangle\,|\mathcal{A}\rangle$ path or the $|\mathcal{A}\rangle\,|\mathcal{C}\rangle$ path at all strengths. The disturbance to the meter along its imaginary axis for photons postselected in $|+i\rangle\,|+i\rangle$ is somewhere between that of $|\mathcal{C}\rangle\,|\mathcal{A}\rangle$ path or the $|\mathcal{A}\rangle\,|\mathcal{C}\rangle$ for all strengths. Thus, measurement disturbance cannot explain why 3 pigeons among 2 pigeonholes can each be in a different hole. On the other hand, direct measurements of $\Pi^{12}_{\mathcal{CC}}$ and $\Pi^{12}_{\mathcal{AA}}$ show that measurement disturbance is responsible for violation of the sum rule. Strong measurements suggest photons postselected in $|+i\rangle\,|+i\rangle$ both travel clockwise/anti-clockwise a significant fraction of the time, but at weaker measurements, they fall within the "no" calibration points and agree with the direct measurement of $\Pi^{12}_{\mathcal{S}}$.

probability for the pigeon system to be in a "yes" state of our pigeon observable the "real system value". In a strong measurement, the real meter value is simply equal to the real system value. For weaker measurements, pigeons in a "yes" state of an observable only shift the meter by a small amount, leaving the meter in the real "no" state some fraction of the time. To convert meter values to system values, we divide by measurement strength.

Similarly, we call the probability of finding our polarization probe in the imaginary "yes" state the "imaginary meter value". To convert to the corresponding "imaginary system value", we subtract 1/2 (so that a probe in the real "yes" state registers as having 0 imaginary component) and then divide by measurement strength. In the weak limit, the real and imaginary system value equal the real and imaginary component of the weak value (Eq. 3.36). In the strong limit, the real system value equals the ABL probability (Eq. 3.37). The strong limit of the imaginary system value has not been described previously in the literature, but it can be related to the sensitivity of the postselection probability as described in Sec. 3.2.2.

All data in Fig. 3.3 are plotted according to their meter value. Grid slopes represent the conversion between meter values and system values. We begin with the calibration points, which were taken by blocking one path in each pigeon interferometer to postselect the state on one of $|\mathcal{C}\rangle|\mathcal{C}\rangle$, $|\mathcal{C}\rangle|\mathcal{A}\rangle$, $|\mathcal{A}\rangle|\mathcal{C}\rangle$, or $|\mathcal{A}\rangle|\mathcal{A}\rangle$. These photons should all have a real system value of either 0 or 1 and their real meter values should move towards 1/2 linearly in the measurement strength. Their imaginary meter value should be 1/2 and their imaginary system value should be 0 at all measurement strengths. These predictions (solid lines in Fig. 3.3) agree qualitatively with our data (points in Fig. 3.3).

The data postselected on $|+i\rangle|+i\rangle$ are the meat of the experiment (fuchsia dots in 3.3). The direct measurements of $\Pi_{\mathcal{S}}$ (3.3 a) reveal that the real system value for both pigeons to be in the same hole is indeed consistent with 0 at all measurement strengths. This can be seen from the fact that the real meter value of the $|+i\rangle|+i\rangle$ data is never significantly higher than the $|\mathcal{C}\rangle|\mathcal{A}\rangle$ or $|\mathcal{A}\rangle|\mathcal{C}\rangle$ calibration data. While the imaginary values of the $|+i\rangle|+i\rangle$ data do not quite match their predicted value of 0, they are no further from this prediction than the calibration data. Thus, measurement disturbance is not a viable resolution to the quantum pigeonhole paradox.

On the other hand, our data confirm that measurement disturbance does explain the violation of the sum rule. The real part of our $|+i\rangle|+i\rangle$ data is "both clockwise" or "both anti-clockwise" significantly more often than it is "both same" at high strengths, but agrees with the "both same" values at weaker strengths. For both strong and weak measurements, the imaginary part of "both same" significantly differs from the imaginary parts of "both clockwise" and "both anti-clockwise". Nevertheless, the sum rule holds because the imaginary parts of "both clockwise" and "both anti-clockwise" are equal and opposite. While the cancellation of the imaginary parts in the weak limit was predicted by the weak value formula 3.36, it is remarkable that the cancellation extends into the strong regime, even as the sum rule for the real part fails. The question of whether this kind of cancellation is a general feature of imaginary system values at all measurement strengths is a fascinating avenue for further study.

Having explained the qualitative features of our data, we turn to its quantitative agreement with theory. Most of the discrepancy between our data and theory is accounted for by the quality of our Bell state source and polarization optics. The fidelity of our actual Bell state to the desired one is 95%. Furthermore, the nominally non-polarizing beamsplitters used to open and close our pigeon

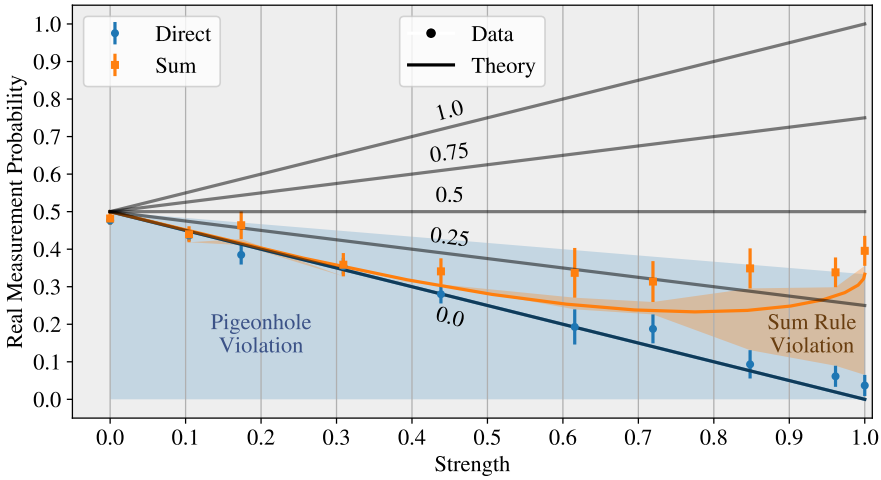

Figure 3.4: Violation of classical counting principles. The x-axis denotes measurement strength (Eq. 3.35) such that 0 is a weak measurement and 1 is a strong measurement. The y-axis is the probability for the polarization meter to be in the real "yes" state. The labeled grid slopes denote the corresponding probability for the pigeons to be in the same hole after accounting for measurement strength. Blue dots show results from direct measurements of the same hole projector Π_S. Orange squares denote an indirect measurement obtained from summing the direct measurements for Π_{CC} and Π_{AA}. Blue and orange slopes denote theoretical predictions for the respective points. The orange region highlights the difference between our two methods for measuring Π_S, indicating a violation of the sum rule. The violation shrinks as the measurement strength decreases. The blue region indicates where direct measurements of Π_S would violate the pigeonhole principle. At all strengths, our direct measurements of Π_S fall in this region.

interferometers are birefringent, complicating our polarization-based which-path measurements. We measure these effects using polarization state tomography of our Bell state source and polarization process tomography in each path of our pigeon interferometer and use them to generate refined predictions, plotted as dotted lines in Fig. 3.3. The systematic uncertainty of our data dominates its statistical uncertainty. The error bars in Fig. 3.3 and Fig. 3.4 denote the root-mean-square deviation of our calibration data from these refined predictions. They are computed separately for each measurement strength and quadrature (real or imaginary).

To conclude, we realized the first variable-strength measurement of a non-local observable to study quantum violations of two seemingly irrefutable counting laws: the pigeonhole principle and the sum rule. Our data show that the violation of the sum rule is an artifact of measurement disturbance. On the other hand, the violation of the pigeonhole principle is the same, regardless of the strength of the back-action. Our experiment shows there is a concrete, empirical, and measurement-independent sense in which three quantum pigeons really can occupy two holes without any being in the same hole. Finally, our variable-strength apparatus led us to discover that the same process that yields the imaginary part of a weak measurement can yield a non-trivial quantity in the strong limit as well. Further exploration of the quantity is a ripe opportunity for further research.

Acknowledgements

This work was supported by NSERC and the Fetzer Franklin Fund of the John E. Fetzer Memorial Trust and by grant number FQXi-RFP-1819 from 821 the Foundational Questions Institute and

Fetzer Franklin Fund, 822 a donor advised fund of Silicon Valley Community Foundation. 823 A.M.S. is a fellow of CIFAR.

3.2 Disturbing quantum pigeons supplementary materials

3.2.1 Variable-strength measurements with a qubit meter

The direct measurements of projectors $\Pi_{\mathcal{S}}$ on the pigeon system are described by the von Neumann interaction unitary

$$U_{\mathcal{SO}} = e^{-i\theta(2\Pi_{\mathcal{S}} - \mathbb{1}_{\mathcal{S}})\sigma_{y,\mathcal{O}}} \tag{3.47}$$

between the pigeon system $\mathcal{S}$ and an observer $\mathcal{O}$ with a spin-1/2 meter. The meter momentum $\sigma_{y,\mathcal{O}}$ generates rotations of the initial meter state $|+z\rangle_{\mathcal{O}}$ by $\pm\theta$ radians in Hilbert space depending on whether the initial pigeon state $|\psi_i\rangle_{\mathcal{S}}$ is in a "yes" (eigenvalue 1) or "no" (eigenvalue 0) eigenspace of $\Pi_{\mathcal{S}}$. Euler's theorem simplifies the unitary to

$$U_{\mathcal{SO}} = \Pi_{\mathcal{S}}(\cos\theta\,\mathbb{1}_{\mathcal{O}} - i\sin\theta\sigma_{y,\mathcal{O}}) + (\mathbb{1} - \Pi_{\mathcal{S}})(\cos\theta\,\mathbb{1}_{\mathcal{O}} + i\sin\theta\sigma_{y,\mathcal{O}}). \tag{3.48}$$

This unitary evolves the initial system and meter state to

$$U_{\mathcal{SO}}\,|\psi_i\rangle_{\mathcal{S}}\,|+z\rangle_{\mathcal{O}} = \Pi_{\mathcal{S}}\,|\psi_i\rangle_{\mathcal{S}}\,|s\rangle_{\mathcal{O}} + (\mathbb{1} - \Pi_{\mathcal{S}})\,|\psi_i\rangle_{\mathcal{S}}\,|-s\rangle_{\mathcal{O}}\,, \tag{3.49}$$

where

$$|s\rangle_{\mathcal{O}} = \sqrt{\frac{1+s}{2}}\,|+x\rangle_{\mathcal{O}} + \sqrt{\frac{1-s}{2}}\,|-x\rangle_{\mathcal{O}}\,, \tag{3.50}$$

and $s = \sin\theta$. The meter observable $\Pi_{\mathcal{O}}$ for the real basis is calibrated so that

$$\langle \pm s|\Pi_{\mathcal{O}}|\pm s\rangle = \frac{1 \pm 1}{2}, \tag{3.51}$$

which is satisfied when

$$\Pi_{\mathcal{O}} = \frac{\mathbb{1} + \sigma_{x,\mathcal{O}}/s}{2}. \tag{3.52}$$

The real part of the system value is the expectation of $\Pi_{\mathcal{O}}$ conditioned on successful postselection

$$\mathbb{E}\left[\Pi_{\mathcal{O}}||\psi_f\rangle\langle\psi_f|_{\mathcal{S}}\right] = \frac{\mathbb{E}\left[|\psi_f\rangle\langle\psi_f|_{\mathcal{S}}\Pi_{\mathcal{O}}\right]}{\mathbb{E}\left[|\psi_f\rangle\langle\psi_f|_{\mathcal{S}}\right]}, \tag{3.53}$$

where the expectation value is taken over the coupled state $U_{\mathcal{SO}}\,|\psi_i\rangle_{\mathcal{S}}\,|+z\rangle_{\mathcal{O}}$. The denominator is the probability that the postselection succeeds.

$$\mathbb{E}\left[|\psi_f\rangle\langle\psi_f|_{\mathcal{S}}\right] = |\,\langle\psi_f|\Pi_{\mathcal{S}}|\psi_i\rangle\,|^2 + |\,\langle\psi_f|(\mathbb{1} - \Pi_{\mathcal{S}})|\psi_i\rangle\,|^2 \tag{3.54}$$

$$+ 2\sqrt{1-s^2}\,\mathrm{Re}[\langle\psi_f|\Pi_{\mathcal{S}}|\psi_i\rangle\,\langle\psi_i|(\mathbb{1} - \Pi_{\mathcal{S}})|\psi_f\rangle]. \tag{3.55}$$

The numerator is the joint expectation

$$\mathbb{E}\left[|\psi_f\rangle\langle\psi_f|_{\mathcal{S}}\Pi_{\mathcal{O}}\right] = |\,\langle\psi_f|\Pi_{\mathcal{S}}|\psi_i\rangle\,|^2 + \sqrt{1-s^2}\times \tag{3.56}$$

$$\mathrm{Re}[\langle\psi_f|\Pi_{\mathcal{S}}|\psi_i\rangle\,\langle\psi_i|(\mathbb{1} - \Pi_{\mathcal{S}})|\psi_f\rangle]. \tag{3.57}$$

When $s = 0$, the conditional expectation simplifies to the real part of the weak value (Eq. 3.36) and when $s = 1$, it simplifies to the Aharonov-Bermann-Lebowitz formula [103] (Eq. 3.37).

3.2.2 Imaginary measurements

To measure the imaginary part of the weak value, we measure in the imaginary meter basis $\sigma_{y,\mathcal{S}}$. The imaginary meter observable $\tilde{\Pi}_{\mathcal{O}}$ is calibrated so that

$$\langle \pm s|\tilde{\Pi}_{\mathcal{O}}| \mp s\rangle = \pm i/2, \tag{3.58}$$

which is satisfied with

$$\tilde{\Pi}_{\mathcal{O}} = \frac{\sigma_{y,\mathcal{O}}}{2s}. \tag{3.59}$$

The conditional expectation of the imaginary meter observable is

$$\mathbb{E}\left[\tilde{\Pi}_{\mathcal{O}}||\psi_f\rangle\langle\psi_f|_{\mathcal{S}}\right] = \frac{\mathbb{E}\left[|\psi_f\rangle\langle\psi_f|_{\mathcal{S}}\tilde{\Pi}_{\mathcal{O}}\right]}{\mathbb{E}\left[|\psi_f\rangle\langle\psi_f|_{\mathcal{S}}\right]}. \tag{3.60}$$

The denominator is the postselection probability probability from the real case treated earlier. The numerator is

$$\mathbb{E}\left[|\psi_f\rangle\langle\psi_f|_{\mathcal{S}}\tilde{\Pi}_{\mathcal{O}}\right] = \mathrm{Im}[\langle\psi_f|\Pi_{\mathcal{S}}|\psi_i\rangle\,\langle\psi_i|(\mathbb{1}-\Pi_{\mathcal{S}})|\psi_f\rangle]. \tag{3.61}$$

When $s = 0$, the conditional expectation simplifies to the imaginary part of the weak value (Eq. 3.36). Curiously, the joint expectation $\mathbb{E}\left[|\psi_f\rangle\langle\psi_f|_{\mathcal{S}}\tilde{\Pi}_{\mathcal{O}}\right]$ does not depend on the measurement strength s at all. If the imaginary part of the weak value is non-zero, the conditional expectation of the imaginary meter observable $\tilde{\Pi_{\mathcal{O}}}$ will be non-zero at all measurement strengths. However, this result is specific to a spin-1/2 meter. If the meter was instead the position of a particle, the Euler expansion of the coupling unitary used to evaluate the evolution at all measurement strengths would not be valid.

We have shown how to calculate the conditional expectation of the imaginary meter observable, but we have so far said nothing on how to interpret it. The imaginary part of the weak value is related to the sensitivity of the postselection success probability to the back-action the meter suffers from measuring a system observable[81]. The probability P_{ps} of successfully postselecting an initial system state $|\psi_i\rangle_{\mathcal{S}}$ onto a final system state $|\psi_f\rangle_{\mathcal{S}}$ is

$$P_{\mathrm{ps}} = ||\,\langle\psi_f|_{\mathcal{S}}\, e^{-i\theta(2\Pi_{\mathcal{S}}-\mathbb{1}_{\mathcal{S}})\sigma_{y,\mathcal{O}}}\,|\psi_i\rangle_{\mathcal{S}}\,|{+z}\rangle_{\mathcal{O}}\,||^2. \tag{3.62}$$

$$= \mathbb{E}\left[e^{i2\theta\,\mathrm{ad}_{\Pi_{\mathcal{S}}}\,\sigma_{y,\mathcal{O}}}\,[|\psi_f\rangle\langle\psi_f|_{\mathcal{S}}]\right]. \tag{3.63}$$

The super operator $\mathrm{ad}_{\Pi_{\mathcal{S}}}$ represents the infinitesimal back-action due to measuring $\Pi_{\mathcal{S}}$. The action of $\mathrm{ad}_{\Pi_{\mathcal{S}}}$ on an arbitrary system operator $A_{\mathcal{S}}$ is $\mathrm{ad}_{\Pi_{\mathcal{S}}}[A_{\mathcal{S}}] = \Pi_{\mathcal{S}}A_{\mathcal{S}} - A_{\mathcal{S}}\Pi_{\mathcal{S}}$. To describe how the postselection probability changes with the strength of the back-action, we will increase the size of $\mathrm{ad}_{\Pi_{\mathcal{S}}}$ uniformly with the transformation $i\theta\,\mathrm{ad}_{\Pi_{\mathcal{S}}} \to i\theta\,\mathrm{ad}_{\Pi_{\mathcal{S}}} + \delta\mathbb{1}_{\mathcal{S}}/\sin(\theta)$. δ is an artificial parameter that lets us tune the strength of the back-action independently from the measurement strength. The postselection probability $P_{\mathrm{ps}}(\delta)$ as a function of this back-action parameter is

$$P_{\mathrm{ps}}(\delta) = \mathbb{E}\left[e^{i2\theta\,\mathrm{ad}_{\Pi_{\mathcal{S}}}\,\sigma_{y,\mathcal{O}}+2\delta\tilde{\Pi}_{\mathcal{O}}}\,[|\psi_f\rangle\langle\psi_f|_{\mathcal{S}}]\right] \tag{3.64}$$

using the fact that $\tilde{\Pi}_{\mathcal{O}} = \sigma_{y,\mathcal{O}}/(2\sin\theta)$. The sensitivity of the postselection probability to back-action is

$$\left.\frac{\partial \log P_{\text{ps}}}{\partial \delta}\right|_{\delta=0} = 2\frac{\mathbb{E}\left[e^{i2\theta\,\text{ad}_{\Pi_{\mathcal{S}}}\,\sigma_{y,\mathcal{O}}}\left[|\psi_f\rangle\langle\psi_f|_{\mathcal{S}}\tilde{\Pi}_{\mathcal{O}}\right]\right]}{\mathbb{E}\left[e^{i2\theta\,\text{ad}_{\Pi_{\mathcal{S}}}\,\sigma_{y,\mathcal{O}}}\left[|\psi_f\rangle\langle\psi_f|_{\mathcal{S}}\right]\right]}. \tag{3.65}$$

The right-hand side of this expression is exactly twice the conditional expectation of the imaginary meter observable.

$$\frac{1}{2}\left.\frac{\partial \log P_{\text{ps}}}{\partial \delta}\right|_{\delta=0} = \mathbb{E}\left[\tilde{\Pi}_{\mathcal{O}}||\psi_f\rangle\langle\psi_f|_{\mathcal{S}}\right] \tag{3.66}$$

In the weak limit, this conditional expectation equals the imaginary part of the weak value. In the strong limit, it may not manifestly be the imaginary part of a complex number, but it is still related to the sensitivity of the postselection probability in the same way.

3.2.3 Entangled photon source

We create photon pairs with a wavelength near 810 nm via type II colinear spontaneous parametric down-conversion. We pump a periodically polled potassium titanyl phosphate (PPKTP) crystal with 2 mW of 405 nm light emitted from a continuous wave laser diode. Before being coupled into a single-mode fiber, each photon passes through a 10 nm band-pass filter centered at 810 nm. The source produces 40,000 pairs per second.

The photons are entangled in polarization because the crystal sits inside a polarizing Sagnac interferometer as shown in Fig. 3.2. The polarization of the pump is set to $|D\rangle$ so that when pump light hits the two-color (405 nm and 810 nm) polarizing beamsplitter (PBS) that opens the Sagnac, it splits into an equal superposition of illuminating the crystal from the front and back. A two-color half waveplate placed just after the reflected port of the PBS rotates $|V\rangle$ to $|H\rangle$ so that the crystal is illuminated by $|H\rangle$ polarized pump light from both sides. The crystal emits photons in the state $(|HV\rangle|\mathcal{C}\rangle + |HV\rangle|\mathcal{A}\rangle)/\sqrt{2}$. The photons in the anti-clockwise path see the two-color half waveplate, rotating their state to $|VH\rangle|\mathcal{A}\rangle$. Then the clockwise and anti-clockwise paths recombine at the two-color PBS and exit the interferometer with the polarization state $(|HV\rangle + e^{i\phi_S}|VH\rangle)/\sqrt{2}$, where ϕ_S is the relative phase between the two paths in the Sagnac. We apply local polarization rotations on both photons until their state upon exiting the fibers and entering the experiment is as close to $(|HH\rangle + |VV\rangle)/\sqrt{2}$ as possible.

3.3 Disturbing quantum pigeons outro

3.3.1 Contributions

The manuscript presented in the previous section would not have been possible without the contributions of several individuals. As the lead author in the experiment, I built the experiment, collected and analyzed the data, and wrote much of the paper. However, the original idea for the experiment came from Aharon Brodutch and Hugo Ferretti. Specifically, Aharon proposed an experiment studying the pigeonhole paradox and conceived the scheme for weakly measuring non-local observables using partial erasure while Hugo designed the optical implementation. Aharon also wrote an initial draft for the paper, which I subsequently adapted. Edwin Tham designed and built the entangled photon source. Hugo, Edwin, Arthur Pang, and Kent Bonsma-Fisher provided invalu-

able advice and experimental support throughout the project. As principle investigator, Aephraim Steinberg lead numerous helpful lab meetings.

3.3.2 Sagnac source

A vital ingredient in the non-local measurements we preformed in the pigeonhole experiment was the entangled photon source. In the lab, we often refer to this source as the "Sagnac source" because it uses a Sagnac interferometer to generate polarization entanglement. Edwin Tham, the designer and builder of the source, details its specifications in his thesis [101]. Originally, the source was pumped with a 160 MHz linewidth Ondax diode laser, but it was replaced with a 1 pm linewidth Cobalt 08-17 from Hübner Photonics. Arthur Pang's thesis [142] explains the details behind this switch, which was done to improve the second-order interference between signal and idler photons.

One difficulty with using the Sagnac source is determining exactly which entangled state it generates. The photon pairs are coupled into single-mode fiber, which means they undergo some polarization rotation determined by the stresses and strains on each fiber. Thus the polarization state of the source must be characterized every time the fibers are moved and once every day during active use to account for changes in lab temperature and humidity. As a result, it is crucial that any experimental apparatus using entangled light from the Sagnac source has a setup for performing state tomography *in situ*. Here are some typical properties of the source which are independent of local polarization unitaries on the signal and idler. The entanglement of formation ranges between 0.81 and 0.87 ebits. The maximum eigenvalue ranges from 0.93 to 0.95 and the entanglement of formation of the corresponding eigenstate is always greater than 0.998 ebits. Numerically optimized over local rotations, the fidelity to the singlet state (i.e. expectation value of the singlet state projector) ranges from 0.93 to 0.96. Doing my best to physically optimize over local rotations, I typically get a fidelity between 0.91 and 0.95 with a desired maximally entangled state.

To physically optimize over local unitaries, I do not actually make iterative local adjustments while performing state tomography at each step, as this would be far too time consuming. Instead, I take one round of tomography, then numerically optimize over rotations to a pair of quarter and half waveplates placed just after the signal and idler launch from their respective fibers into my experiment. I then apply these optimized rotations (4 angles in total for 2 quarter and 2 half waveplates) and perform another round of state tomography to confirm that the new state is a better match to my desired state. This second verification round is crucial as there are many opportunities to make sign errors when calculating the optimized angles. For example, one must be sure that the rotation direction in the optimization code matches the physical rotation direction of the waveplate, which might vary for each waveplate depending on which way the mount is facing. In addition, the orientation of the simulated waveplates must match the physical waveplates modulo 180°, not just modulo 90°.

A typical coincidence rate for the source is 40k per second at 2 mW of pump power. In principle, we could use a much higher pump power and get higher rates, but I am paranoid about burning the dual-wavelength polarizing beam splitter that opens and closes the Sagnac interferometer. When the source was first built, it used a polarizing beam splitter from Bernhard Halle Nachfolger GmbH with a nominal damage threshold of only $100\text{W}/\text{cm}^2$. The beam splitter was positioned after a lens, where the beam had a waist less than 1 mm. We noticed burn spots would develop on the beam splitter after just a week or so of use at pump powers around 1 mW. I replaced that old

beam splitter with PBS0012-405/810 from Newlight Photonics, which features a nominal damage threshold of 0.6GW/cm^2. If this damage threshold is to be trusted, the beam splitter could easily handle 30 mW of pump power, the maximum output of the Cobolt pump. However, the fact that the beam splitter is coated for both 405 nm and 808 nm might skew these numbers, so I have never pumped with much more than 2 mW just to be safe.

3.3.3 Characterizations

The key novelties of the pigeonhole experiment made quantifying and, to the extent possible, correcting for systematic errors extremely experimentally challenging. The pigeonhole experiment involved weak measurements, which like the partially postselected measurements described in Ch. 2, have amplified sensitivity to systematic errors. Furthermore, we measured real and imaginary values, which meant we were sensitive to phases that we could have otherwise ignored if we had just measured only real or only imaginary values. Finally, measuring joint non-local observables between Pigeon 1 and Pigeon 2 meant that characterizing each system independently was not enough to characterize the joint system. In this section, I will detail the tomography we did to tame and quantify these systematic errors. In particular, I will describe how I arrived at the dotted lines in Fig. 3.3, which represent theoretical predictions based on our calibrations of the apparatus.

The pigeonhole apparatus consisted of several distinct modules. The first was the Sagnac source of entangled photons, which was characterized with polarization state tomography as described in the previous section. Next were the Pigeon 1 and Pigeon 2 interferometers. Both the clockwise and anti-clockwise paths through these interferometers were characterized separately via polarization process tomography. Finally, the eraser interferometer was characterized at several different measurement strengths via detector tomography. Each of these characterizations were fed into a numerical simulation of the experiment to yield the dotted lines in Fig. 3.3.

Polarization process tomography was a two-step process. The usual setup for polarization process tomography of an unknown channel is polarizer, half waveplate, quarter waveplate, channel, quarter waveplate, half waveplate, polarizer. However, the initial part of my apparatus was set up as quarter waveplate, half waveplate, polarizer so that I could perform state tomography as described above. The simplest, but least cost-effective solution would have been to add an additional set of motorized quarter and half waveplates after the tomography polarizer before each pigeon interferometer. I decided to use a more economical solution, removing the state tomography polarizers when I wanted to do process tomography. The cost of this approach was that there was no longer a polarizer to fix the initial polarization to a well-known state. To do process tomography, I would first set up the Sagnac source to generate a separable state and characterize it using the tomography polarizer. Having measured the state, I would remove the tomography polarizer, then perform process tomography. Despite the extra complication this method introduced, it seemed repeatable and accurate enough.

Detector tomography on the eraser interferometer was the simplest, and most robust of the characterizations. For each of several measurement strengths, I sent in a tomographically complete set of input states, then found the positive polarization operator that best fit the data. The results of these characterizations were nearly ideal, so the simulation used the ideal eraser interferometer for simplicity. One noteworthy exception is the phase of the eraser interferometer. Unlike most of the parameters of the eraser interferometer, its phase was configured and characterized relative to the rest

of the apparatus. In an ideal weak measurement, postselecting the system onto a state orthogonal to its initial state never succeeds. I used this fact to set the phase of the eraser interferometer. Specifically, I set the path phase of Pigeon 1 and Pigeon 2 to π to postselect the initial path state of $|+\rangle|+\rangle$ onto the orthogonal state $|-\rangle|-\rangle$. Then I set the eraser to preform a weak measurement and tuned its phase to minimize coincidence counts. Unfortunately, this procedure was not very accurate as it a) depended on how close the phase of Pigeon 1 and Pigeon 2 actually were to π and b) required minimizing coincidence counts at the very end of my apparatus, where after all the postselections inherent to the experiment, I was left with a coincidence rate of only around 50 per second. An alternative way to set the phase, though arguably less theoretically justifiable, would have been to tune the eraser phase to balance counts in the imaginary basis when one of the paths in Pigeon 1 and Pigeon 2 was blocked. This method would have amounted to ensuring that one of the path postselections, say $|\mathcal{C}\rangle|\mathcal{C}\rangle$, had an imaginary weak value of 0. Although I did not use this method to set the eraser phase, I did use it to get a more or less independent measurement of the eraser phase, which I fed into my simulation of the experiment. According to this method, my eraser phases erred by +100 mrad during the "both clockwise?" data run, −60 mrad during the "both same?" data run, and −30 mrad during the "both anti-clockwise?" data run.

The last few pages of this chapter display the results of state and process tomography for each data run. For each of the three runs, I present state tomography of the polarization entangled state, process tomography of the Pigeon 1 clockwise path, and process tomography of the Pigeon 1 anti-clockwise path. Pigeon 2 did not change over the three data runs, so I present the results of a typical tomographic reconstruction for the Pigeon 2 clockwise and anti-clockwise paths, which are fed into the simulation for all three data runs. The eraser interferometer tomography is not included as it was close to ideal and not used in my final simulation.

All of the tomographic reconstructions were computed using the maximum likelihood method. I used the MOSEK convex optimization solver via the Python package CVXPY to ensure that the reconstructions were globally optimal. The channel solutions were constrained to be completely positive, but not trace-preserving to account for preferential transmission of one polarization over another. Instead, the channels were normalized so that the Choi matrix had a trace of 4, the dimension of the process. An unphysical consequence of this normalization method is that certain Choi matrix elements come out slightly greater than 1, which implies some polarizations are amplified. This spurious amplification is negligible in the final simulation, as the largest estimated Choi matrix element is less than 1.02. The purity, entanglement of formation, and fidelity with the ideal state or process are included in the caption of each figure. Some of the reconstructions have a purity of 1 or 0.99, but these are likely overestimates. Maximum likelihood reconstructions of nearly pure states and channels have a tendency to overestimate purity. Finally, the numerical values of the state and Choi matrix elements are included up to 3 decimal points. The 3 digits of precision are included for the sake of reproducing the simulation and do not reflect my systematic or statistical uncertainty. I did not rigorously compute uncertainties on these values, but experience suggests the matrix elements are accurate to roughly 2 decimal points.

3.3.4 Follow up

Over the course of the pigeonhole experiment, two interesting ideas emerged that merit further study. First, there is the matter of imaginary parts of strong measurements. While I have given an

interpretation of the imaginary part of general strength measurements in terms of the sensitivity of the postselection probability, it is unclear to what extent the value I have been referring to as the "imaginary" part is really the imaginary part of a complex number. By which I mean, if I define a complex number z as being "real part" $+i$ "imaginary part", is there any physical significance to quantities like $|z|^2$, z^2, or e^z? There is also the question of which measurement dynamics allow for strong imaginary parts. The pigeonhole experiment demonstrates that a qubit pointer measuring a two-outcome observable can have a non-zero strong imaginary part. However, the prototypical gaussian pointer coupled via the von Neumann Hamiltonian always has a zero-valued imaginary part in the strong limit [81]. Is the same true for all purely real continuous variable pointer wavefunctions? What about a qutrit pointer that measures a three-outcome observable?

The second idea leverages the quantum pigeonhole effect to control interaction strengths. Consider a pair-wise interaction which shifts the energies of particles in similar modes as each other. Interactions of this type are ubiquitous. For example, the Coulomb potential shifts the energy of two charged particles in close proximity and certain forms of χ_2 non-linear media shift the energy of photon pairs that occupy the same mode. The interference phenomenon at the heart of the quantum pigeonhole effect allows one to perform a selective measurement that tunes the strength of these interactions by controlling how many "pigeons" are allowed to be in the same "pigeonhole." For example, consider a χ_2 non-linear medium with a hamiltonian of the form $H \propto a_1^\dagger a_1^\dagger a_1 a_1 + a_2^\dagger a_2^\dagger a_2 a_2$, where $a_1^\dagger$ and $a_2^\dagger$ create photons in distinct modes. An interferometer prepares a coherent state $|\alpha/\sqrt{2}\rangle\,|\alpha/\sqrt{2}\rangle$ and postselects on $|\alpha/\sqrt{2}\rangle\,|i\alpha/\sqrt{2}\rangle$. The resulting weak value of the interaction energy is 0, just like the weak value for a pair of pigeons to be in the same pigeonhole in the pigeonhole experiment. This effect relies on postselection, so the interaction cannot be zeroed out deterministically. In fact, to balance out the null interaction in the cases that the postselection succeeds, the interaction must be stronger in the events where the postselection fails. Thus the result of the postselective measurement can act as a kind of heralded knob for tuning the interaction strength.

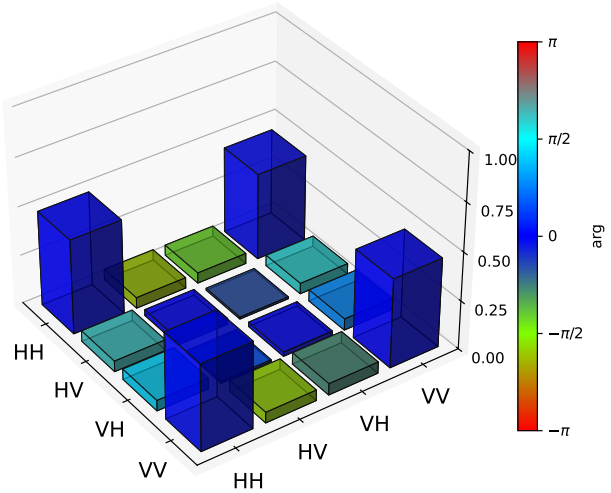

$$\begin{bmatrix} 0.488 & (-0.019-0.052j) & (0.013-0.053j) & (0.445-0.031j) \\ (-0.019+0.052j) & 0.031 & (0.009-0.005j) & (-0.014+0.053j) \\ (0.013+0.053j) & (0.009+0.005j) & 0.023 & (0.039+0.044j) \\ (0.445+0.031j) & (-0.014-0.053j) & (0.039-0.044j) & 0.459 \end{bmatrix}$$

Figure 3.5: Density matrix of the entangled polarization probe after passing through the clockwise paths of both pigeon interferometers during the "both clockwise?" data run. Purity: 0.87. Entanglement of formation: 0.83 ebits. Fidelity with ideal: 0.92.

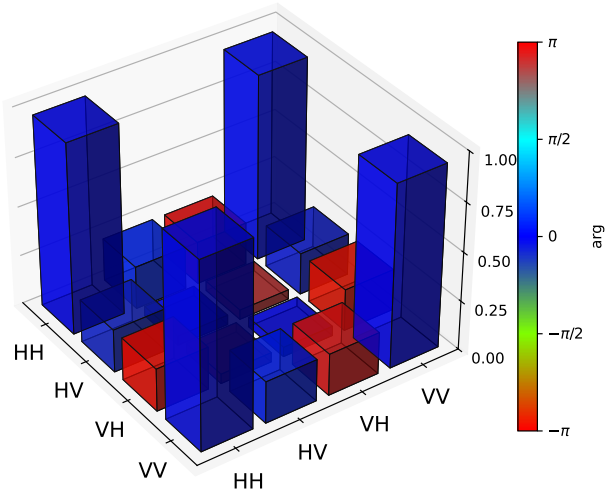

$$\begin{bmatrix} 0.986 & (0.01-0.001j) & (0.005+0.027j) & (0.917+0.248j) \\ (0.01+0.001j) & 0.014 & 0.003 & (0.014-0.014j) \\ (0.005-0.027j) & 0.003 & 0.024 & (0.008-0.017j) \\ (0.917-0.248j) & (0.014+0.014j) & (0.008+0.017j) & 0.976 \end{bmatrix}$$

Figure 3.6: The Choi matrix of the polarization process applied by the clockwise path of Pigeon 1 during the "both clockwise?" data run. Purity: 1. Entanglement of formation: 1 ebit. Fidelity with ideal: 0.95.

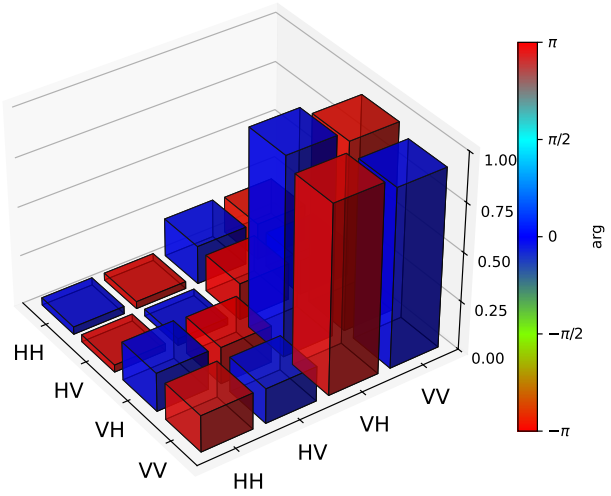

$$\begin{bmatrix} 0.038 & (-0.037-0.001j) & (0.197+0.007j) & (-0.186-0.021j) \\ (-0.037+0.001j) & 0.035 & -0.188 & (0.178+0.013j) \\ (0.197-0.007j) & -0.188 & 1.014 & (-0.959-0.073j) \\ (-0.186+0.021j) & (0.178-0.013j) & (-0.959+0.073j) & 0.913 \end{bmatrix}$$

Figure 3.7: The Choi matrix of the polarization process applied by the anti-clockwise path of Pigeon 1 during the "both clockwise?" data run. Purity: 1. Entanglement of formation: 0 ebits. Fidelity with ideal: 0.96.

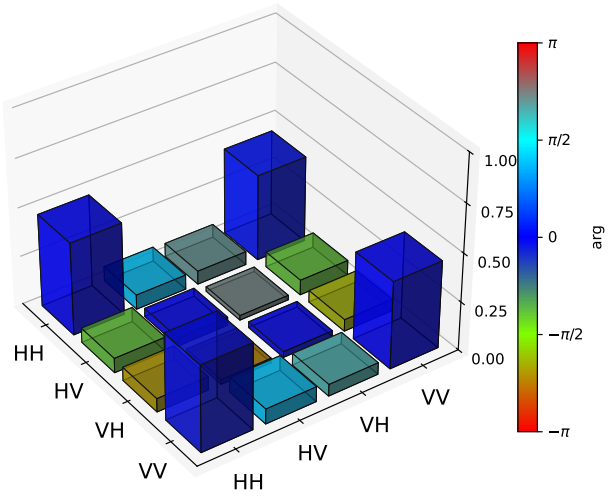

$$\begin{bmatrix} 0.477 & (0.026+0.07j) & (-0.041+0.056j) & (0.442+0.054j) \\ (0.026-0.07j) & 0.043 & (-0.016+0.018j) & (0.028-0.073j) \\ (-0.041-0.056j) & (-0.016-0.018j) & 0.03 & (-0.027-0.054j) \\ (0.442-0.054j) & (0.028+0.073j) & (-0.027+0.054j) & 0.45 \end{bmatrix}$$

Figure 3.8: The density matrix of the entangled polarization probe after passing through the clockwise paths of both pigeon interferometers during the "both same?" data run. Purity: 0.87. Entanglement of formation: 0.81 ebits. Fidelity with ideal: 0.91.

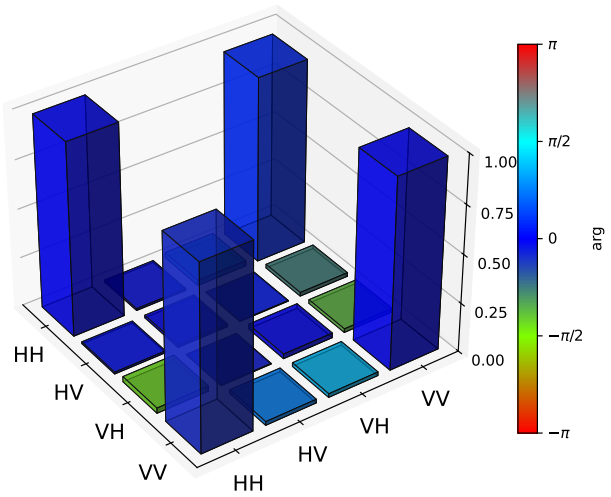

$$\begin{bmatrix} 0.986 & (0.01-0.001j) & (0.005+0.027j) & (0.917+0.248j) \\ (0.01+0.001j) & 0.014 & 0.003 & (0.014-0.014j) \\ (0.005-0.027j) & 0.003 & 0.024 & (0.008-0.017j) \\ (0.917-0.248j) & (0.014+0.014j) & (0.008+0.017j) & 0.976 \end{bmatrix}$$

Figure 3.9: The Choi matrix of the polarization process applied by the clockwise path of Pigeon 1 during the "both same?" data run. Purity: 0.93. Entanglement of formation: 0.91 ebits. Fidelity with ideal: 0.95.

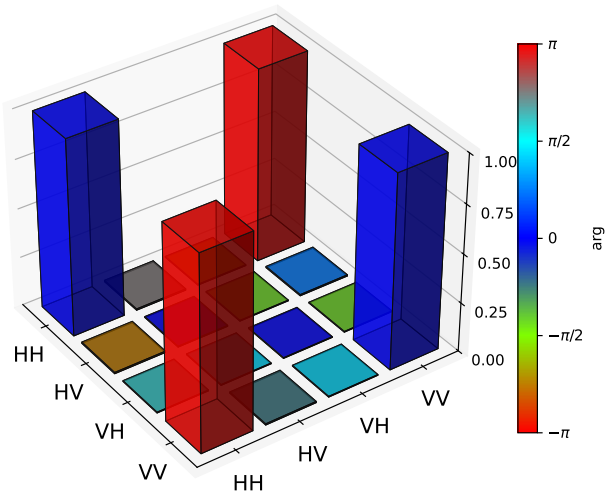

$$\begin{bmatrix} 1.0 & (-0.005+0.005j) & (-0.001-0.004j) & (-0.991+0.04j) \\ (-0.005-0.005j) & 0.005 & (0.001-0.004j) & (0.005+0.004j) \\ (-0.001+0.004j) & (0.001+0.004j) & 0.004 & (0.001-0.004j) \\ (-0.991-0.04j) & (0.005-0.004j) & (0.001+0.004j) & 0.991 \end{bmatrix}$$

Figure 3.10: The Choi matrix of the polarization process applied by the anti-clockwise path of Pigeon 1 during the "both same?" data run. Purity: 0.99. Entanglement of formation: 0.98 ebits. Fidelity with ideal: 0.99.

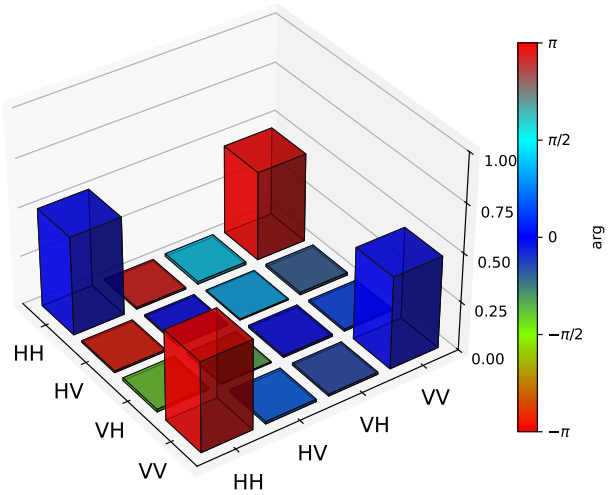

$$\begin{bmatrix} 0.507 & (-0.009+0.001j) & (0.004+0.013j) & (-0.461+0.006j) \\ (-0.009-0.001j) & 0.009 & (0.003+0.005j) & (0.01-0.007j) \\ (0.004-0.013j) & (0.003-0.005j) & 0.011 & (0.01+0.004j) \\ (-0.461-0.006j) & (0.01+0.007j) & (0.01-0.004j) & 0.473 \end{bmatrix}$$

Figure 3.11: The density matrix of the entangled polarization probe after passing through the anti-clockwise paths of both pigeon interferometers during the "both anti-clockwise?" data run. Purity: 0.91. Entanglement of formation: 0.87 ebits. Fidelity with ideal: 0.95.

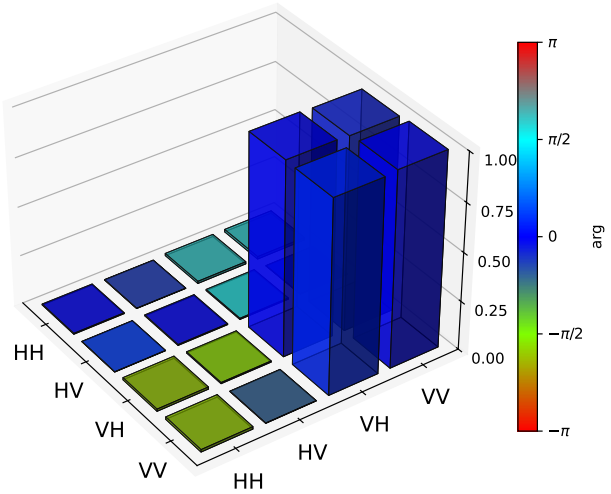

$$\begin{bmatrix} 0.005 & (0.002-0.001j) & (-0.004+0.011j) & (-0.004+0.012j) \\ (0.002+0.001j) & 0.005 & (-0.001+0.006j) & (0.002+0.001j) \\ (-0.004-0.011j) & (-0.001-0.006j) & 0.993 & (0.96-0.235j) \\ (-0.004-0.012j) & (0.002-0.001j) & (0.96+0.235j) & 0.998 \end{bmatrix}$$

Figure 3.12: The Choi matrix of the polarization process applied by the clockwise path of Pigeon 1 during the "both anti-clockwise?" data run. Purity: 0.98. Entanglement of formation: 0 ebits. Fidelity with ideal: 0.98.

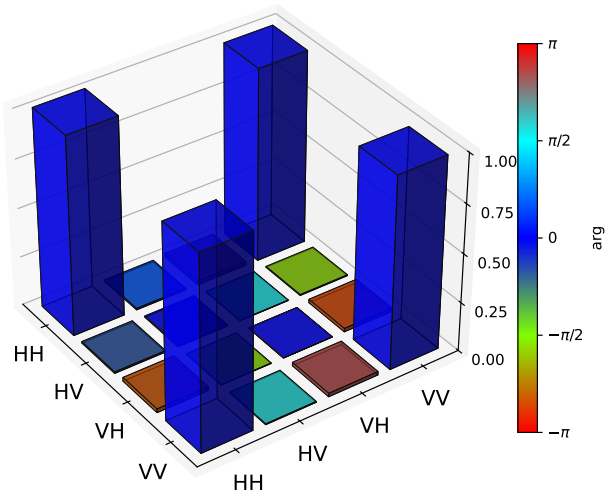

$$\begin{bmatrix} 1.014 & (0.007+0.004j) & (-0.016+0.01j) & (0.991+0.023j) \\ (0.007-0.004j) & 0.006 & (-0+0.002j) & (-0.001-0.004j) \\ (-0.016-0.01j) & (-0-0.002j) & 0.001 & (-0.016-0.008j) \\ (0.991-0.023j) & (-0.001+0.004j) & (-0.016+0.008j) & 0.979 \end{bmatrix}$$

Figure 3.13: The Choi matrix of the polarization process applied by the anti-clockwise path of Pigeon 1 during the "both anti-clockwise?" data run. Purity: 0.99. Entanglement of formation: 0.99 ebits. Fidelity with ideal: 0.99.

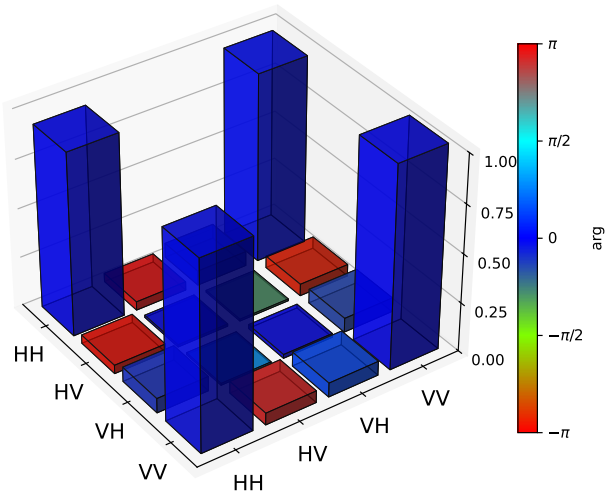

$$\begin{bmatrix} 0.005 & (0.002-0.001j) & (-0.004+0.011j) & (-0.004+0.012j) \\ (0.002+0.001j) & 0.005 & (-0.001+0.006j) & (0.002+0.001j) \\ (-0.004-0.011j) & (-0.001-0.006j) & 0.993 & (0.96-0.235j) \\ (-0.004-0.012j) & (0.002-0.001j) & (0.96+0.235j) & 0.998 \end{bmatrix}$$

Figure 3.14: The Choi matrix of the polarization process applied by the clockwise path of Pigeon 2. Purity: 0.96. Entanglement of formation: 0.95 ebits. Fidelity with ideal: 0.98.

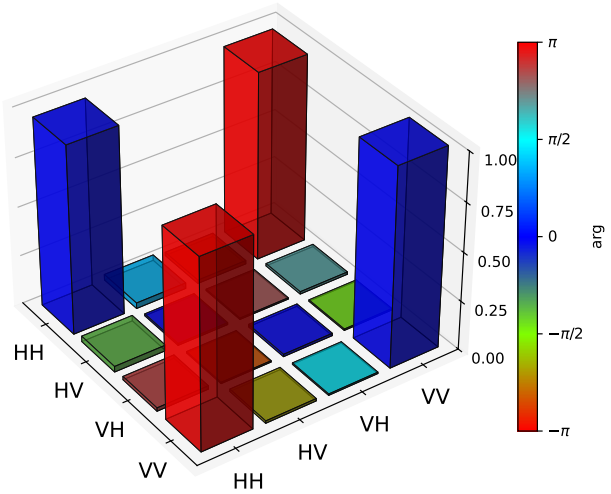

$$\begin{bmatrix} 1.014 & (0.007+0.004j) & (-0.016+0.01j) & (0.991+0.023j) \\ (0.007-0.004j) & 0.006 & (-0+0.002j) & (-0.001-0.004j) \\ (-0.016-0.01j) & (-0-0.002j) & 0.001 & (-0.016-0.008j) \\ (0.991-0.023j) & (-0.001+0.004j) & (-0.016+0.008j) & 0.979 \end{bmatrix}$$

Figure 3.15: The Choi matrix of the polarization process applied by the anti-clockwise path of Pigeon 2. Purity: 0.96. Entanglement of formation: 0.94 ebits. Fidelity with ideal: 0.98.

Chapter 4

Quantum Agents

Do qubits dream of entangled sheep?
Quantum measurement without classical output

Noah Lupu-Gladstein,[1,*] Aharon Brodutch,[1,2,†] Hugo Ferretti,[1] Weng-Kian Tham,[1]
Arthur Ou Teen Pang,[1] Kent Bonsma-Fisher,[1,3,‡] and Aephraim M. Steinberg[1,4,§]

[1]*Department of Physics and Center for Quantum Information and Quantum Control, University of Toronto, 60 St George St, Toronto, Ontario, M5S 1A7, Canada*

[2]*IonQ, Inc, College Park, MD, USA*

[3]*National Research Council of Canada, 100 Sussex Dr, Ottawa, Ontario, K1A 0R6, Canada*

[4]*Canadian Institute for Advanced Research, Toronto, Ontario, M5G 1M1, Canada*

(Dated: May 2, 2024)

Abstract

Quantum mechanics is usually formulated with an implicit assumption that agents who can observe and interact with the world are external to it and have a classical memory. However, there is no accepted way to define the quantum-classical cut and no *a priori* reason to rule out fully quantum agents with coherent quantum memories. In this work, we introduce an entirely quantum notion of measurement, called a *sensation*, to account for quantum agents that experience the world through quantum sensors. Sensations eschew probabilities and instead describe a deterministic flow of quantum information. We quantify the information gain and disturbance of a sensation using concepts from quantum information theory and find that sensations always disturb at least as much as they inform. Viewing measurements as sensations could lead to a new understanding of quantum theory in general and to new results in the context of quantum networks.

* nlupugla@physics.utoronto.ca

† brodutch@physics.utoronto.ca

‡ kent.bonsma-fisher@nrc-cnrc.gc.ca

§ steinberg@physics.utoronto.ca

4.1 Introduction

> *It is decisive to recognize that, however far the phenomena transcend the scope of classical physical explanation, the account of all evidence must be expressed in classical terms.*
>
> *Niels Bohr [143]*

Measurement has been central to quantum mechanics since its inception. Historically, measurements were formalized with the notion of observables: Hermitian operators [102, 144] that represent quantities like position, momentum, and spin. This formulation of measurement has since been generalized several times [145–148], but none of these advances have questioned the basic notion that a measurement yields a classical outcome that can be copied. To account for classical outcomes, quantum mechanical models of measurement invoke an external, classical observer.

As quantum technology improves, we draw closer to an age where quantum machines make complex decisions using quantum computations that run on quantum data gathered with quantum sensors. These systems would be quantum agents in the sense that they autonomously sense and act upon the quantum world [149, 150]. When a quantum agent measures its surroundings, is it really natural to view the results of that measurement as merely classical? Should the agent be viewed as external to the quantum world, or an active participant within it (see Fig. 4.1)?

Our aim is to model quantum measurements as a quantum agent might: free of classical outcomes and external observers. A fully quantum paradigm will facilitate the development of new experiments, measurement techniques, communication protocols, and computational algorithms that do not fit easily in a classical framework. A complete description of quantum agents would not just model their observations, but also their decisions and actions. In this work, we focus solely on observation and leave the matter of decisions and actions for further study. We assume that a quantum agent has some ability to decide when and how to observe a given system. The mechanics behind this decision process is beyond the scope of this work, seeing as modeling how a classical agent makes decisions is already a difficult problem. We take for granted that a quantum agent can distinguish between its external environment and "itself", leaving the question of how a quantum agent even develops a sense of "self" for future research. Although this work does not paint a complete picture of quantum agency, its ideas have already inspired a forthcoming experiment [151].

Agents, both classical and quantum, experience the world through sensors. We define a sensor as a system with a memory that can interact with another system and store information from that system in its memory. We compare two types of relationships between an observer and a sensor:

- **Classical** - The sensor is separate from the observer and the sensor's memory decoheres faster than the observer can process it
- **Quantum** - The sensor is a part of the observer and the sensor's memory remains coherent throughout being processed by the observer

For a given observer, we classify a sensor as classical or quantum accordingly. A quantum sensor can take in incoherent information like a classical sensor, but it can also take in and store quantum information about a quantum system.

As humans, we are naturally equipped only with classical sensors and the standard notion of measurement (see Fig. 4.2) reflects that. Traditionally, a measurement involves a system and an observable property of that system. The measurement is completed when an observer obtains a *result*, i.e. a *classical* record which can be copied and shared. Von Neumann developed a pragmatic quantum measurement model that is satisfactory for predicting our classical experience, yet invokes an observing agent external to the system [102]. There have been many attempts to adapt von Neumann's model and keep the observer inside the system (notably collapse theories and the approaches following Everett and Bohm [152–154]), but all cling to the central role of *observables*.

We adopt a radical view of measurement: a measurement is any interaction between two systems in which the final state of one system depends on the initial state of the other. To avoid confusion with the historically laden term "measurement", we call such an interaction a *sensation*. The result of a sensation is a quantum state, not a classical label. Completing a sensation does not require an external agent.

Any traditional measurement can be cast as a sensation followed by a transition to a classical value (the sensation is the so-called pre-measurement[155]), but there are sensations that transcend traditional measurements. For example, consider a sensor that swaps a state in its memory with a state in the environment. This interaction does not result in a distinct set of classical outcomes, so it cannot be associated with an observable or positive operator valued measure (POVM). It is nevertheless a sensation because the final state of the sensor depends on the initial state of the environment.

We explore how an agent that uses sensations might view the world. We do not attempt to describe the inner workings of a quantum agent, nor attempt to accommodate the way humans with classical memories observe the world through events and probabilities. Instead, our aim is to describe information flow in a deterministic theory with as few assumptions as possible. In this sense our work is also very different from approaches that put the observer at the center (e.g [156, 157]) which tend to begin with probabilities as a primitive. Our results give a consistent way of understanding information in a deterministic (collapse-free) interpretation of quantum mechanics as a complete theory in the sense that all physical objects (including observers) and all dynamical processes (including sensation) are described by the same rules.

Our work takes a world-view which is similar to the Everettian (many-worlds, relative-state) interpretation, i.e., starting from Sec. 4.3 we will consider the sensor as part of the quantum world and assume a unitary theory. However, our work is not an interpretation of quantum mechanics. It is instead the beginning of a framework for studying quantum agents.

We begin in the next section with a description of the traditional — classical sensor — approach to measurement. In Sec. 4.3 we define sensations with quantum sensors. We introduce the *result channel* as the extension of the positive operator-valued measure (POVM) into the deterministic quantum regime, and give two examples of sensations: the von Neumann sensation, and the swap sensation (Sec. 4.3.1). We then show how such swap sensations can be implemented in practice (Sec. 4.3.2). In Sec. 4.4 we develop a method to quantify information gain, and disturbance. Using these tools, we compare the von Neumann and swap sensations. Implications of quantum agency are discussed in Sec. 4.5 where we provide examples involving multiple agents sharing information, emphasising one of the limitations of the swap sensation, and mention the relation to quantum computing (Sec. 4.5.2). Our main conclusion (Sec. 4.6) is that a complete quantum treatment of

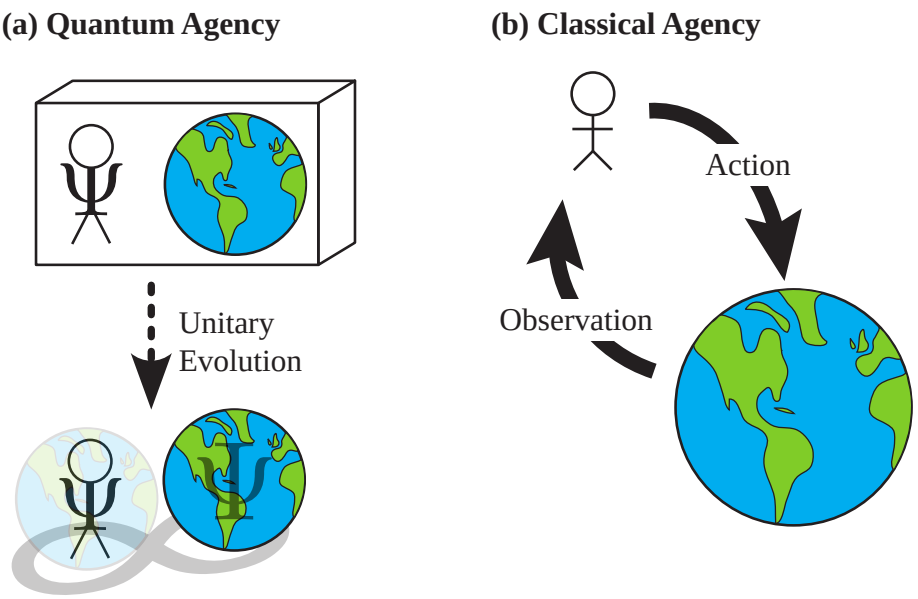

Figure 4.1: Agency with internal (*quantum*) agents compared to external (*classical*) agents. External agents can observe the world or act on it (note that these these distinct operations can be inextricably connected through back-action). Quantum agents have quantum memories which are part of the quantum world. In the quantum scenario there is no clear distinction between an observation of the world and an action on the world.

agency which is free from anthropocentric pre-conceptions can lead to new results. It is conceivable that by ignoring the possibility of quantum agents with quantum sensors we are in danger of making an oversight similar to the one made by the founders of modern computing and information theory (many of whom had in-depth knowledge of quantum mechanics) who missed or ignored the possibility of quantum information processing.

4.2 External observers: Observables and POVMs

John von Neumann first described the measurement of an observable A in terms of three separate subsystems:

1. A system to be measured with an associated Hilbert space $\mathcal{H}_\mathcal{S}$ on which the observable A is an Hermitian operator
2. A sensor with Hilbert space $\mathcal{H}_\mathcal{M}$ on which there are two canonically conjugate operators: the pointer operator $P_\mathcal{M}$ and its canonical conjugate $Q_\mathcal{M}$
3. An external agent with no mathematical representation

The measurement process according to von Neumann's scheme can be broken into two stages: interaction and readout. In the interaction stage a Hamiltonian of the type

$$H_i \propto A_\mathcal{S} \otimes Q_\mathcal{M} \tag{4.1}$$

is switched on to couple the system and sensor. The result can then be amplified (see Fig. 4.2 b). At the readout stage, an external agent records the state of the sensor. Prior to the mathematical

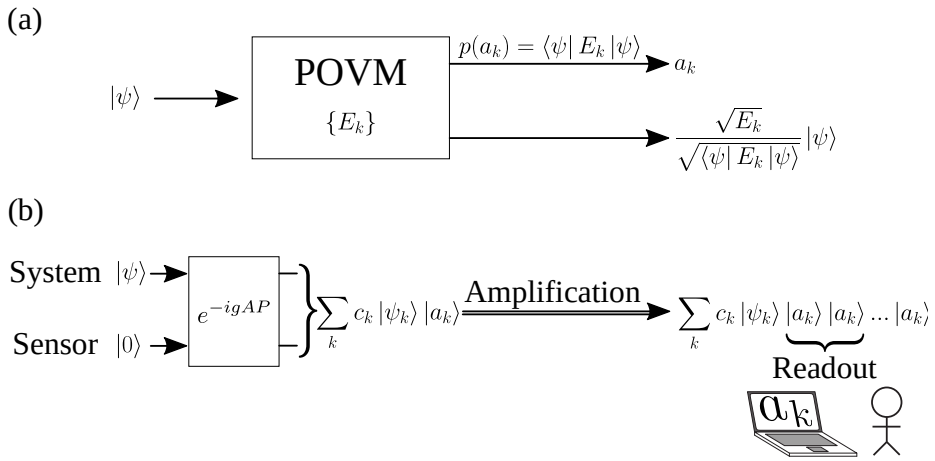

Figure 4.2: Quantum measurements with external agents. (a) The traditional approach to measurement characterised by the POVM elements $\{E_k\}$. The probability for an outcome a_k is $p(a_j) = \mathrm{Tr}(E_k\rho)$ and the corresponding minimally disturbing [147] state transformation is $|\psi\rangle \to \frac{\sqrt{E_k}|\psi\rangle}{\sqrt{\langle\psi|E_k|\psi\rangle}}$. (b) The von Neumann scheme for a measurement of a non-degenerate observable A provides a more detailed description than the textbook approach. It includes a quantum measurement device $\mathcal{M}$ and an amplification process whereby the information is copied onto multiple registers. The external observer reads out the state of some of these registers and records a classical result a_k. The cut between the external agent and the other subsystems has no observable consequences.

derivation, von Neumann (invoking Bohr [102, footnote 207]) argues that the agent being external is not unique to the quantum regime, and that the precise cut between the agent and the sensor is arbitrary even in the classical case. The aim of the derivation, which would later be called the von Neumann measurement scheme, was to regain the classical intuition that measurements are independent of the specific choice of the cut between the sensor and the agent. This *motility of the cut* is demonstrated by showing that the agent and the sensor can be treated as a single composite system which can be cut into subsystems arbitrarily without modifying the outcome probabilities or the state update rules.

To make a comparison between sensations and traditional measurements, we list a number of features that arise from the von Neumann scheme:

- Result - After the interaction, the sensor's memory is in a state that generally depends on the initial system.
- Broadcastability - The result can be copied and broadcast to others.
- Constrained back-action - A second sensor interacting identically with the same system yields the same result up to statistical uncertainty.
- Motility of the cut - There is no accepted scientific theory that separates the sensor from the external observer.

The first feature is essential in the definition of a measurement [154]. The next two points play a key role in communication since they allow multiple agents to communicate the results of their measurements by making copies and broadcasting them. Such communication engenders objectivity in the sense that different agents can agree on some specific property by making individual

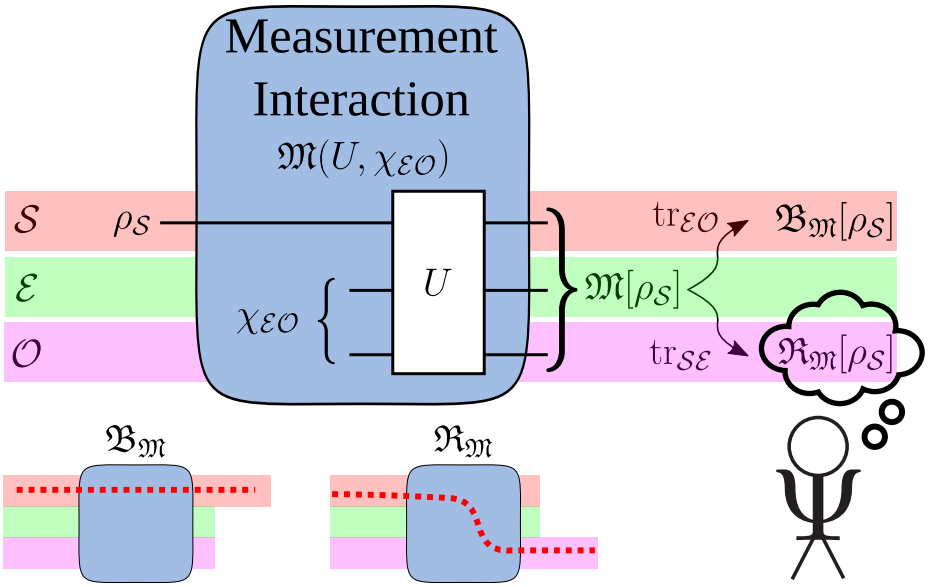

Figure 4.3: Quantum measurements with a quantum agent: A measurement interaction $\mathfrak{M}$ (blue box) fills an observer's memory $\mathcal{O}$ with information about a system $\mathcal{S}$ in the presence of an environment $\mathcal{E}$. The interaction is defined in terms of two objects: a unitary U (which couples the system $\mathcal{S}$, environment $\mathcal{E}$ and the observer's memory $\mathcal{O}$), and the initial $\mathcal{EO}$ state $\chi_{\mathcal{EO}}$. The interaction takes an initial system state $\rho_{\mathcal{S}}$ to a final $\mathcal{SO}$ state $\mathfrak{M}[\rho_{\mathcal{S}}]$. The result $\mathcal{A}_{\mathfrak{M}}[\rho_{\mathcal{S}}]$ is the reduced state encoded in the observer's memory. The interaction induces the result channel $\mathcal{A}_{\mathfrak{M}}$ (dashed red on bottom right) from system states to observer memory states and the back-action $\mathfrak{B}_{\mathfrak{M}}$ (dashed red on bottom left), a channel from system states to disturbed system states. The entire process is deterministic. The interaction is considered a sensation (according to Def. 1) as long as $\mathcal{A}_{\mathfrak{M}}[\rho_{\mathcal{S}}]$ is not a constant function of $\rho_{\mathcal{S}}$, i.e., $\mathfrak{M}$ is a sensation of $\mathcal{S}$ whenever the result depends on the state of $\mathcal{S}$.

measurements of the same system and comparing their results [154, 158–160]. Historically, these or some subset of these features are taken as the defining properties of measurements (e.g. [161]). Our aim in this work is to explore the consequences of keeping only the requirement that measurements have results that depend on the initial system.

4.3 The quantum observer

The features of von Neumann measurements match our classical experience, but do they also capture everything a quantum observer can experience? To start answering this question, we define sensations, the more general class of interactions enabled by access to a quantum sensor.

4.3.1 Defining sensation

As before, the system $\mathcal{S}$ to be observed is associated with the Hilbert space $\mathcal{H}_{\mathcal{S}}$. The sensor is a part of an observer $\mathcal{O}$ and interacts with the system. In contrast to traditional measurement, we consider the observer itself a quantum system. We associate the memory in the observer's sensor with the Hilbert space $\mathcal{H}_{\mathcal{O}}$. The sensation is a procedure which includes a unitary operation U on $\mathcal{S}$, $\mathcal{O}$, and possibly other subsystems. We call these other subsystems the environment $\mathcal{E}$, with Hilbert space $\mathcal{H}_{\mathcal{E}}$, because it is conceptually separate from the measured system and the observer. Despite the terminology, the environment need not be noisy and could simply represent an additional sensor

(see section 4.3.1).

For simplicity, we assume that free evolution can be ignored on the time scales of the sensation[1]. To keep the notation simple, we will also use no subscripts when describing an operator on the joint $\mathcal{SEO}$ Hilbert space $\mathcal{H}_\mathcal{S} \otimes \mathcal{H}_\mathcal{E} \otimes \mathcal{H}_\mathcal{O}$. Furthermore, we will use the term channel to refer to completely-positive trace-preserving maps. We denote such channels $\mathfrak{C} : \mathcal{X} \to \mathcal{Y}$ when they take states on $\mathcal{H}_\mathcal{X}$ to states on $\mathcal{H}_\mathcal{Y}$.

A sensation is driven by an interaction between the system, observer, and environment. The interaction is defined by a unitary U and the initial composite state $\chi_{\mathcal{EO}}$ of the environment $\mathcal{E}$ and the observer $\mathcal{O}$. Mathematically, the interaction is a quantum channel $\mathfrak{M}(U, \chi_{\mathcal{EO}}) : \mathcal{S} \to \mathcal{SO}$ acting on an arbitrary system state $\rho_\mathcal{S}$

$$\mathfrak{M}(U, \chi_{\mathcal{EO}})[\rho_\mathcal{S}] = \mathrm{Tr}_\mathcal{E}\left[U\rho_\mathcal{S} \otimes \chi_{\mathcal{EO}} U^\dagger\right] \tag{4.2}$$

(See Fig. 4.3 a). To simplify our notation we will henceforth drop the arguments in $\mathfrak{M}(U, \chi_{\mathcal{EO}})$.

For any interaction $\mathfrak{M} : \mathcal{S} \to \mathcal{SO}$, we also define a *result channel* $\mathcal{A}_\mathfrak{M} : \mathcal{S} \to \mathcal{O}$ that maps the state $\rho_\mathcal{S}$ onto a state in $\mathcal{H}_\mathcal{O}$ called the result,

$$\mathcal{A}_\mathfrak{M}[\rho_\mathcal{S}] = \mathrm{Tr}_\mathcal{S}\left[\mathfrak{M}[\rho_\mathcal{S}]\right]. \tag{4.3}$$

This result channel can be seen as the analogue of the POVM, but whereas the POVM maps system states to probabilities, the result channel $\mathcal{A}_\mathfrak{M}$ maps system states to observer states. Similarly, we introduce the *back-action*

$$\mathfrak{B}_\mathfrak{M}[\rho_\mathcal{S}] = \mathrm{Tr}_\mathcal{O}\left[\mathfrak{M}[\rho_\mathcal{S}]\right] \tag{4.4}$$

which is a channel that describes how the interaction modifies $\mathcal{S}$. This channel is the standard channel associated with measurement back-action (as defined in [147] for example). In a theory with external agents we would say that a channel is a measurement if the associated POVM elements are not all proportional to the identity, similarly the result channel plays the central role in the following definition of a measurement.

Definition 1 (Sensation, result)**.** *An interaction $\mathfrak{M} : \mathcal{S} \to \mathcal{SO}$ with an associated result channel $\mathcal{A}_\mathfrak{M} : \mathcal{S} \to \mathcal{O}$ is a* sensation *(of $\mathcal{S}$ by $\mathcal{O}$) if and only if there are two system states $\rho_\mathcal{S}, \sigma_\mathcal{S}$ such that $\mathcal{A}_\mathfrak{M}[\rho_\mathcal{S}] \neq \mathcal{A}_\mathfrak{M}[\sigma_\mathcal{S}]$. The* result *is the quantum state $\mathcal{A}_\mathfrak{M}[\rho_\mathcal{S}]$.*

Note that since the channel is linear, it is sufficient to consider pure states. That is, a channel $\mathfrak{M} : \mathcal{S} \to \mathcal{SO}$ with an associated result channel $\mathcal{A}_\mathfrak{M} : \mathcal{S} \to \mathcal{O}$ is a sensation when there are two pure states $\rho_\mathcal{S}, \sigma_\mathcal{S}$ such that $\mathcal{A}_\mathfrak{M}[\rho_\mathcal{S}] \neq \mathcal{A}_\mathfrak{M}[\sigma_\mathcal{S}]$.

The asymmetry in our definition of sensations as channels from $\mathcal{S}$ to $\mathcal{SO}$ (as opposed to $\mathcal{SO}$ to $\mathcal{SO}$) may seem like a "bug", but it is actually a crucial feature. It provides a formal lever to distinguish the observer from the observed. If two quantum agents interact, they will each experience a different sensation because the two agents will define themselves as the observer and the other as the system. A coupling between two agents $\mathcal{A}$ and $\mathcal{B}$ establishes an *objective* channel from $\mathcal{AB}$ to $\mathcal{AB}$, but the resulting sensation is *subjective* in that it depends on whether $\mathcal{A}$ is seen as the observer or the system.

[1] Note that in practice the free evolution can lead to significant corrections, see for example Sec. 4.3.2 below.

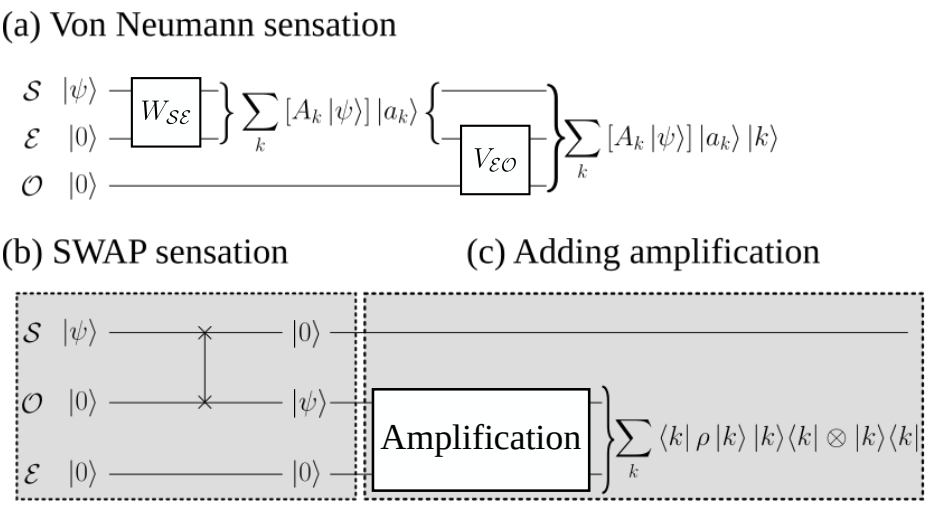

Figure 4.4: Examples of measurements with a quantum agent: (a) The circuit diagram for a von Neumann measurement performed in two steps (Eq. 4.5). The first, step $W_{\mathcal{SE}}$ couples between the environment (or measuring device) and the system. The second, $V_{\mathcal{EO}}$, couples between the environment and the observer. The result is a quantum state encoded in a preferred basis $\{|k\rangle\}_k$ which can be copied (amplified) and broadcast. Compare this to von Neumann's original approach (Fig. 4.2), where the observer is external to quantum dynamics and the result is a classical label. (b) The circuit diagram for a swap measurement. The observer learns everything about the system ($|\psi\rangle$ is now encoded in the memory), but the disturbance is maximal (the system retains no trace of its original state). There is no preferred basis and so the state cannot be copied and broadcast. (c) Amplifying in a specific basis $\{|k\rangle\}_k$ causes decoherence. The result can be copied and broadcast but phase information is lost.

We will soon explore concrete examples of specific sensations, but first we will give two examples of interactions that are not sensations. An interaction driven by any unitary of the form $U_{\mathcal{SEO}} = U_{\mathcal{SE}} \otimes U_{\mathcal{O}}$, is not a sensation. Second, consider an interaction of the form $U_{\mathcal{SEO}} = e^{iX_{\mathcal{S}} \otimes Y_{\mathcal{EO}}} \neq \mathbb{1}$. The interaction is not a sensation in the special case where $\chi_{\mathcal{EO}}$ happens to commute with $Y_{\mathcal{EO}}$, although it is a sensation otherwise.

Example 1: the von Neumann measurement

In the von Neumann measurement, the environment is a classical sensor. To measure an observable $A = \sum_k a_k A_k$ with eigenspace projectors A_k, we start with an initial product state written as $|\psi\rangle|0\rangle|0\rangle$, where $|\psi\rangle$ is an arbitrary $\mathcal{S}$ state and $|0\rangle|0\rangle$ is a fixed initial $\mathcal{EO}$ state. We then generate an interaction $W_{\mathcal{SE}}$ between the environment and the system and follow with an interaction $V_{\mathcal{EO}}$ between the system and the observer, so $U = V_{\mathcal{EO}} W_{\mathcal{SE}}$. These interactions and the initial $\mathcal{EO}$ states are chosen so that

$$|\psi\rangle|0\rangle|0\rangle \xrightarrow{W_{\mathcal{SE}}} \sum_k [A_k|\psi\rangle]|a_k\rangle|0\rangle \xrightarrow{V_{\mathcal{EO}}} \sum_k [A_k|\psi\rangle]|a_k\rangle|k\rangle\,. \tag{4.5}$$

where the environment states $|a_k\rangle$ are orthogonal to each other, as are the memory states $|k\rangle$ (we assume that the dimensions of $\mathcal{H}_{\mathcal{E}}$ and $\mathcal{H}_{\mathcal{O}}$ are large enough). Each of these interactions can be generated by a Hamiltonian in the form of Eq. (4.1).

The result of the interaction is the final memory state $\sum_k \langle\psi|A_k|\psi\rangle|k\rangle\langle k|$. The observer's information about the system is captured by the correlations between $\mathcal{S}$ and $\mathcal{O}$. The result depends

on the initial system state in the sense that each of the orthogonal sensor states 'points' at a corresponding system state with weights determined by the initial system state.

Example 2: The swap sensation

We now go to the extreme situation where the agent learns everything about the quantum state of the system by "swapping" the latter, lock, stock, and barrel with her quantum sensor's memory register. We refer to this operation as the *swap sensation*. For simplicity, we choose $\mathcal{O}$ to be the same dimension as $\mathcal{S}$ so U can be the standard SWAP gate [148] between $\mathcal{S}$ and $\mathcal{O}$. For an initial $\mathcal{SEO}$ state $|\psi\rangle|0\rangle|0\rangle$, the SWAP induces the transformation $|\psi\rangle|0\rangle|0\rangle \rightarrow |0\rangle|0\rangle|\psi\rangle$ (see Fig. 4.4 b) which puts the state $|\psi\rangle$ in the observer's sensor. Following this measurement, the observer' sensor contains everything about the state of $\mathcal{S}$ before the interaction, at the cost of a very strong back-action. The sensation's result cannot be shared across multiple sensors and there is no system observable associated with it. The agent senses *the state* $|\psi\rangle$, rather than a specific property of $|\psi\rangle$.

The back-action of a swap sensation is so strong, one may wonder whether it is even appropriate to call $\mathcal{S}$ the system once its contents have been entirely swapped with a part of the observer. In practice, $\mathcal{S}$ is often a small piece of a much larger system. For example, if an observer uses a swap sensation to store a photon in a quantum memory (explored further in Sec. 4.3.2), she only senses one small portion of the entire electromagnetic field. Whatever state was swapped out from her sensor's memory would start to participate in the dynamics of electromagnetism, so there is a physical sense in which $\mathcal{S}$ is still the system, even afters its contents have been completely disturbed.

Example 3: The decohered swap

A more realistic scenario involves a memory which is open to the environment. Analysis in this case depends on the precise dynamics of the coupling to the environment. One possibility that allows us to recapture the classically intuitive broadcasting feature is dephasing of $\mathcal{O}$ in some preferred basis $\{|k\rangle\}_k$ through interaction with the environment (see Fig 4.4 c). The full transformation for the $\mathcal{SO}$ subsystems would then be

$$\rho_{\mathcal{S}} \otimes \tau_{\mathcal{O}} \rightarrow \tau_{\mathcal{S}} \otimes \rho_{\mathcal{O}} \rightarrow \tau_{\mathcal{S}} \otimes \sum_k \langle k|\rho|k\rangle |k\rangle\langle k|_{\mathcal{O}} \tag{4.6}$$

The observer's state is then similar to the one in the von Neumann scheme above (Eq. 4.5) with equivalence in the case $A_k = |k\rangle\langle k|$, however there are no longer any correlations with $\mathcal{S}$. Correlations with $\mathcal{E}$ would be similar to those of Eq. (4.5) and in principle $\mathcal{E}$ could include many copies of the result. As we will show below, the swap-and-decohere process is similar to the behaviour of a photon detector. The main feature we want to highlight for now is that once decoherence kicks in, the sensation can be associated with an observable like a traditional measurement. The main features of all three sensations discussed above are presented in Table 4.1 using terminology which we develop further in section 4.4.

4.3.2 Physical models for a swap sensation

The swap sensation is an extreme example of a new capability granted by quantum sensors with ideal quantum memories. We now show that this sensation is not only physically feasible, but that

the dephased swap is also fairly commonplace.

Photon detectors

Photoelectric devices that measure light intensity are among the most common ways to sense the world. These devices typically work by swapping the state of the incoming light field with the state of photoelectrons, which then interact with each other and rapidly decohere (see Appendix. 4.7.2). This detection process is essentially the decohered swap measurement described above in Sec. 4.3.1. The fact that one of the most ubiquitous ways of observing the world does not follow the von Neumann scheme and moreover acts like a decohered SWAP operation (with all information in the field being lost) is significant. In particular any assertion (see [154] for example) that good observations should be repeatable by multiple observers must be assessed with this in mind. While photodetection with rapid decoherence does not fit within the narrow model of von Neumann measurements, it is nevertheless a classical measurement in the sense that its outcomes can be modelled as classical labels rather than coherent quantum states. Only the number (as opposed to the relative phase) of photoelectrons detected is meaningful because the environment washes out any definite phase relation between photoelectron number states.

Optical quantum memories

If the environment's action on a photodetector can be sufficiently tamed, it becomes more than a mere measurement. It becomes a quantum memory for an optical mode. Such a memory is not beholden to any particular optical observable. Its dynamics are described by sensations where the optical mode is the system to be measured, and the memory mode represents the sensor. It has been demonstrated that photon storage in an off-resonant Raman quantum memory is equivalent to a beamsplitter interaction between a flying photon mode ($a^\dagger$) and a stationary spin-wave excitation ($b^\dagger$) [162, 163] (see Fig. 4.5). The 'reflectivity' in this beamsplitter interaction is given by the storage efficiency of the memory which can, in theory, approach unity [164]. This storage process acts like a SWAP between the bosonic optical and spin-wave memory modes. Any superposition of photon number states in the optical mode becomes the same superposition of spin-wave excitations in the spin-wave mode and vice versa.

Perfect or near-perfect quantum memories are yet to be demonstrated, but it is reasonable to expect that such devices will exist in the not-too-distant future, most likely with some type of error correction mechanisms to increase coherence times. Some of these memories, in particular those directly connected to communication channels and sensors, will likely be optical memories with a mechanism that resembles a SWAP operation with an incoming light mode. A sufficiently advanced quantum computer might interact with the world mostly through swap sensations (see Sec. 4.5.2).

4.4 Information theory for quantum observers

The information gained from a measurement is usually quantified through some function of the probability distribution associated with the possible measurement results, viewed as classical labels. This approach cannot be applied as is to our deterministic framework that defines results as quantum states. In this section we present an intuitive way to think about information gain and disturbance

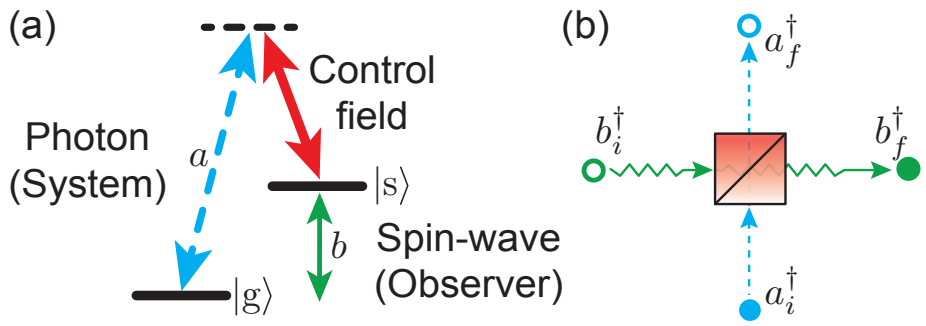

Figure 4.5: (a) The 3-level system for an off-resonant Raman quantum memory. A flying photon mode a is mapped, via a strong control field, to a stationary spin-wave excitation. The spin-wave mode b is an excitation from the ground state ($|g\rangle$) to the storage state ($|s\rangle$) of the medium. (b) The storage process can be represented as a beamsplitter interaction between the optical and spin-wave states. With unit reflectivity, i.e., storage efficiency, number information is swapped between modes a and b: $b_i^\dagger \to a_f^\dagger$ and $a_i^\dagger \to b_f^\dagger$.

that can be applied in the quantum-agent scenario. We start by introducing *maximally informative* and *maximally disturbing* sensations in Sec. 4.4.1 and point out that their non-informative and non-disturbing counterparts are not sensations. We then (Sec 4.4.2) introduce an additional agent $\mathcal{A}$ who is initially entangled with $\mathcal{S}$ (see Fig 4.4) and show that correlations with this agent can be used to quantify information gain and disturbance. We calculate the information gain and disturbance for the von Neumann, swap, and decohered swap sensations (Sec. 4.4.3). We discover, and subsequently prove, that even the most exotic sensation can never inform more than it disturbs.

4.4.1 Maximal information gain and disturbance

A sensation $\mathfrak{M}$ is *maximally informative* whenever the observer's final memory state and the details of $\mathfrak{M}$ are sufficient to produce at least one state identical to any arbitrary initial system state.

Definition 2 (Maximally informative sensation)**.** *A sensation $\mathfrak{M} : \mathcal{S} \to \mathcal{SO}$ with an associated result channel $\mathcal{A}_\mathfrak{M} : \mathcal{S} \to \mathcal{O}$ is called maximally informative when there exists a quantum channel $\mathcal{A}_\mathfrak{M}^{-1} : \mathcal{O} \to \mathcal{S}$ such that the composition of channels $\mathcal{A}_\mathfrak{M}^{-1} \circ \mathcal{A}_\mathfrak{M} = \mathtt{1}$ where $\mathtt{1}$ is the identity channel.*

It is tempting to demand that a maximally informative sensation enables the observer to produce not just one, but any number of states identical to a given input. While that requirement might be appropriate for a classical observer, quantum observers must abide by the no-cloning theorem [165, 166]. A related, but distinct notion in standard quantum mechanics is an informationally complete measurement [167]. These measurements eventually allow an observer to produce many copies of a measured state, but only after measuring many identical instances of that state.

The opposite limit of a maximally informative sensation is an interaction in which the observer's final state is independent of the initial system state. Such a *non-informative interaction* is in fact not a sensation under Def. 1.

Definition 3 (Non-informative interaction)**.** *An interaction $\mathfrak{M} : \mathcal{S} \to \mathcal{SO}$ with an associated result channel $\mathcal{A}_\mathfrak{M} : \mathcal{S} \to \mathcal{O}$ is called non-informative when $\mathcal{A}_\mathfrak{M}[\rho_\mathcal{S}] = \mathcal{A}_\mathfrak{M}[\sigma_\mathcal{S}]$ for any pair of states $\rho_\mathcal{S}, \sigma_\mathcal{S}$ in $\mathcal{S}$.*

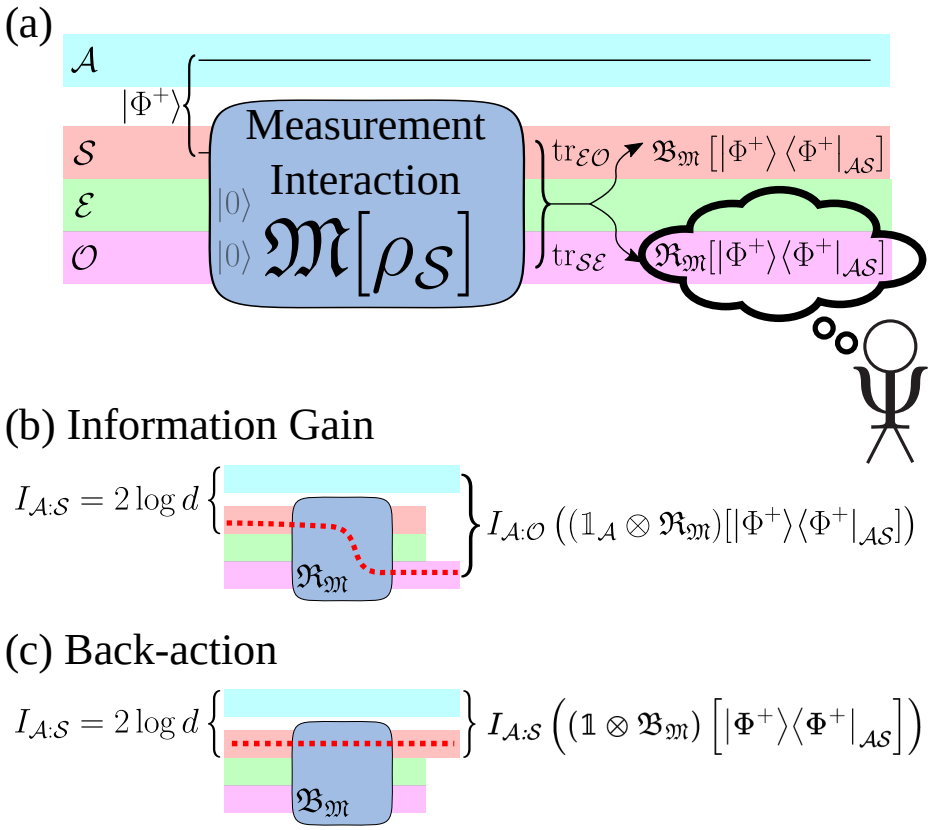

Figure 4.6: Information gain and disturbance: (a) A second agent $\mathcal{A}$ is initially entangled with $\mathcal{S}$ so that they are maximally correlated, $I_{\mathcal{A}:\mathcal{S}} = 2\log d$. The observer $\mathcal{O}$ is initially uncorrelated with $\mathcal{A}$. (b) The information gain is defined as the change in mutual information between $\mathcal{A}$ and $\mathcal{O}$ after the sensation (Eq. 4.8). (c) The disturbance is the change in mutual information between $\mathcal{A}$ and $\mathcal{S}$ (Eq. 4.9).

	von Neumann	SWAP	SWAP with decoherence
Motility of the cut	Yes	No	Yes
Broadcastable	Yes	No	Yes
Repeatable	Yes	No	No
Reversibility	Requires environment	Yes	Requires environment
Information gain $G(\mathfrak{M})$	Heisenberg	Maximal	Heisenberg
Disturbance $D(\mathfrak{M})$	Heisenberg	Maximal	Maximal

Table 4.1: Comparing three types of sensations: the von Neumann scheme, the swap, and the swap with decoherence (see Sec. 4.3.1,4.3.1 for details). Motility of the cut refers to the possibility of identifying different cuts between the observer and the environment. The result is broadcastable when it can be copied and shared with other observers, and the measurement is repeatable if a second measurement of the same type will produce the same outcome. Reversibility refers to the resources required for reversing the operation so that the system will be restored to its original state (the resources are either access to $\mathcal{SO}$ or access the entire $\mathcal{SEO}$). Information gain and disturbance (Defined in Sec. 4.4.2) are given in terms of two reference points defined in Sec. 4.4.1. For a system of dimension d, the Heisenberg limit is $\log d$ and maximal is $2\log d$. The swap sensation obtains maximal information at the cost of maximal disturbance. The decohered swap performs as well or worse than the von Neumann scheme on all accounts and is essentially equivalent to a destructive von Neumann measurements like photodetection.

A sensation is *maximally disturbing* if the final system state is independent of the initial system state.

Definition 4 (Maximally disturbing sensation)**.** *A sensation $\mathfrak{M}:\mathcal{S}\to\mathcal{SO}$ with an associated back-action $\mathfrak{B}_{\mathfrak{M}}:\mathcal{S}\to\mathcal{S}$ is called maximally disturbing when $\mathfrak{B}_{\mathfrak{M}}[\rho_{\mathcal{S}}]=\mathfrak{B}_{\mathfrak{M}}[\sigma_{\mathcal{S}}]$ for any pair of states $\rho_{\mathcal{S}},\sigma_{\mathcal{S}}$ in $\mathcal{S}$.*

By contrast, a *non-disturbing interaction* is one that allows the system to perfectly recover its initial state from its final state.

Definition 5 (Non-disturbing interaction)**.** *An interaction $\mathfrak{M}:\mathcal{S}\to\mathcal{SO}$ with an associated back-action $\mathfrak{B}_{\mathfrak{M}}:\mathcal{S}\to\mathcal{S}$ is called non-disturbing when there exists a quantum channel $\mathfrak{B}_{\mathfrak{M}}^{-1}:\mathcal{S}\to\mathcal{S}$ such that the composition of channels $\mathfrak{B}_{\mathfrak{M}}^{-1}\circ\mathfrak{B}_{\mathfrak{M}}=\mathfrak{1}$ where $\mathfrak{1}$ is the identity channel.*

4.4.2 Quantifying information gain and disturbance

We seek an information gain function $G(\mathcal{A}_{\mathfrak{M}})$ and a disturbance function $D(\mathfrak{B}_{\mathfrak{M}})$ to quantitatively describe the results and back-action of an interaction $\mathfrak{M}$. These functions must be compatible with the definitions given above for maximally informative, non-informative, maximally disturbing, and non-disturbing. Furthermore, we demand that no local operation on $\mathcal{O}$ after the interaction increases $G(\mathcal{A}_{\mathfrak{M}})$. Similarly, no local operation on $\mathcal{S}$ after the interaction may decrease $D(\mathfrak{B}_{\mathfrak{M}})$. These requirements are summarized below.

- $G(\mathcal{A}_{\mathfrak{M}})=0$ when $\mathfrak{M}$ is non-informative and strictly positive otherwise.
- $G(\mathcal{A}_{\mathfrak{M}})$ maximizes for a given system $\mathcal{S}$ when $\mathfrak{M}$ is maximally informative.
- $G(\mathcal{A}_{\mathfrak{M}})$ is non-increasing under local operations on $\mathcal{O}$: if $\mathfrak{M}'=\mathfrak{C}_{\mathcal{O}}\circ\mathfrak{M}$ and $\mathfrak{C}_{\mathcal{O}}$ is a local channel on $\mathcal{O}$, then $G(\mathfrak{M}')\leq G(\mathfrak{M})$.

- $D(\mathfrak{B}_{\mathfrak{M}}) = 0$ when $\mathfrak{M}$ is non-disturbing and strictly positive otherwise.
- $D(\mathfrak{B}_{\mathfrak{M}})$ maximizes for a given system $\mathcal{S}$ when $\mathfrak{M}$ is maximally disturbing.
- $D(\mathfrak{B}_{\mathfrak{M}})$ is non-decreasing under local operations on $\mathcal{S}$: if $\mathfrak{M}' = \mathfrak{C}_{\mathcal{O}} \circ \mathfrak{M}$ and $\mathfrak{C}_{\mathcal{O}}$ is a local channel on $\mathcal{O}$, then $D(\mathfrak{M}') \geq D(\mathfrak{M})$.

To construct functions $G(\mathcal{A}_{\mathfrak{M}})$ and $D(\mathfrak{B}_{\mathfrak{M}})$ that respect the above properties, we will consider a second agent $\mathcal{A}$ who is maximally entangled with $\mathcal{S}$ before the measurement interaction. Maximally entangling $\mathcal{S}$ with $\mathcal{A}$ reflects the assumption that the observer has no prior knowledge about the system state $\rho_{\mathcal{S}}$. [2] For concreteness, we choose the entangled state to be $|\Phi^+\rangle_{\mathcal{AS}} = \frac{1}{\sqrt{d}} \sum_{k=1}^{d} |k\rangle_{\mathcal{A}} |k\rangle_{\mathcal{S}}$ where $d = \dim(H_{\mathcal{S}}) = \dim(H_{\mathcal{A}})$ and $\{|k\rangle\}_{k=1}^{d}$ is a complete, orthonormal basis. [3] We will quantify the correlations between two subsystems $\mathcal{X}$ and $\mathcal{Y}$ via mutual information, defined as

$$I_{\mathcal{X}:\mathcal{Y}}(\tau_{\mathcal{XY}}) = S(\tau_{\mathcal{X}}) + S(\tau_{\mathcal{Y}}) - S(\tau_{\mathcal{XY}}) \tag{4.7}$$

where $S(\tau) = -\mathrm{Tr}\left[\tau \log \tau\right]$ is the von Neumann entropy of a state τ. Mutual information enjoys some properties [148, 168, 169] which are specifically useful for our purposes:

- $I_{\mathcal{X}:\mathcal{Y}}(\tau_{\mathcal{XY}}) \geq 0$ with equality if and only if $\tau_{\mathcal{XY}}$ is a product state, i.e. $\tau_{\mathcal{XY}} = \tau_{\mathcal{X}} \otimes \tau_{\mathcal{Y}}$.
- The mutual information reaches its maximal value $2 \log d$ when $\tau_{\mathcal{XY}}$ is a maximally entangled state.
- Mutual information is non-increasing under local operations.

We can now quantify both the information gain and back-action by looking at the change in mutual information after the measurement interaction. We define information gain $G(\mathcal{A}_{\mathfrak{M}})$ as $I_{\mathcal{A}:\mathcal{O}}$ after the interaction $\mathfrak{M}$

$$G(\mathcal{A}_{\mathfrak{M}}) \equiv I_{\mathcal{A}:\mathcal{O}}\left((\mathfrak{1}_{\mathcal{A}} \otimes \mathcal{A}_{\mathfrak{M}})\left[|\Phi^+\rangle\langle\Phi^+|_{\mathcal{AS}}\right]\right). \tag{4.8}$$

and the disturbance $D(\mathfrak{B}_{\mathfrak{M}})$ as the drop in $I_{\mathcal{A}:\mathcal{S}}$ after $\mathfrak{M}$ (see Fig. 4.6)

$$D(\mathfrak{B}_{\mathfrak{M}}) \equiv I_{\mathcal{A}:\mathcal{S}}\left(|\Phi^+\rangle\langle\Phi^+|_{\mathcal{AS}}\right) - I_{\mathcal{A}:\mathcal{S}}\left((\mathfrak{1}_{\mathcal{A}} \otimes \mathfrak{B}_{\mathfrak{M}})\left[|\Phi^+\rangle\langle\Phi^+|_{\mathcal{AS}}\right]\right). \tag{4.9}$$

To see that these quantities make sense, we examine the qualitative behaviour of $I_{\mathcal{A}:\mathcal{O}}$ and $I_{\mathcal{A}:\mathcal{S}}$. First we note that once we fix $\dim(\mathcal{H}_{\mathcal{S}}) = \dim(\mathcal{H}_{\mathcal{A}}) = d$, the initial correlations are $I_{\mathcal{A}:\mathcal{S}}(|\Phi^+\rangle\langle\Phi^+|_{\mathcal{AS}}) = 2\log d$. Since $\mathcal{O}$ is initially uncorrelated with $\mathcal{A}$ and $\mathcal{S}$, we also have $I_{\mathcal{A}:\mathcal{SO}}(|\Phi^+\rangle\langle\Phi^+|_{\mathcal{AS}} \otimes \chi_{\mathcal{O}}) = 2\log d$. The measurement interaction $\mathfrak{M}$ is a local operation on $\mathcal{SO}$, so $I_{\mathcal{A}:\mathcal{SO}}(\mathfrak{M}[|\Phi^+\rangle\langle\Phi^+|_{\mathcal{AS}}]) \leq 2\log d$. Ignoring $\mathcal{O}$ to obtain the back-action $\mathfrak{B}_{\mathfrak{M}}$ is a local operation, so $I_{\mathcal{A}:\mathcal{S}}(\mathfrak{B}_{\mathfrak{M}}[|\Phi^+\rangle\langle\Phi^+|_{\mathcal{AS}}]) \leq 2\log d$. Ignoring $\mathcal{S}$ to obtain the result channel $\mathcal{A}_{\mathfrak{M}}$ is also local, so $I_{\mathcal{A}:\mathcal{O}}(\mathcal{A}_{\mathfrak{M}}[|\Phi^+\rangle\langle\Phi^+|_{\mathcal{AS}}]) \leq 2\log d$. As a result,

$$0 \leq G(\mathcal{A}_{\mathfrak{M}}),\ D(\mathfrak{B}_{\mathfrak{M}}) \leq 2\log d. \tag{4.10}$$

[2] It is possible to modify the approach by encoding any prior knowledge the observer has in the initial $\mathcal{AS}$ state so that $\mathcal{ASEO}$ would be the purification of the ensemble of initial states, but the details of such modifications are beyond the scope of this work.

[3] For the sake of simplicity, we consider only finite dimensional Hilbert spaces.

4.4.3 Examples

Let us consider the simple case where each subsystem is a qubit. Both $\mathcal{E}$ and $\mathcal{O}$ are initially in the state $|0\rangle$ and the maximally entangled $\mathcal{AS}$ state is $|\Phi^+\rangle = \frac{1}{\sqrt{2}}[|00\rangle + |11\rangle]$. In the von Neumann scheme, the final $\mathcal{ASEO}$ state is $\frac{1}{\sqrt{2}}[|0000\rangle + |1111\rangle]$, which gives $G(\mathcal{A}_\mathfrak{M}) = D(\mathfrak{B}_\mathfrak{M}) = \log 2$.

For a swap sensation, the final $\mathcal{ASO}$ state is $\frac{1}{\sqrt{2}}[|000\rangle + |101\rangle]$, so the reduced $\mathcal{AO}$ state is maximally entangled and $G(\mathcal{A}_\mathfrak{M}) = 2\log 2$ (this can also be seen by noting that $\mathcal{A}_\mathfrak{M}$ is the $\mathcal{S} \to \mathcal{O}$ identity). The channel $\mathfrak{B}_\mathfrak{M}$ takes all system states to $|0\rangle_\mathcal{S}$ so recovery is impossible and the disturbance is maximal: $D(\mathfrak{B}_\mathfrak{M}) = 2\log 2$.

The decohered swap sensation yields $\frac{1}{2}[|000\rangle\langle 000| + |101\rangle\langle 101|]$ as the final $\mathcal{ASO}$ state. The final $\mathcal{AO}$ state is the classically correlated state $\frac{1}{2}[|00\rangle\langle 00| + |11\rangle\langle 11|]$, which has $G(\mathcal{A}_\mathfrak{M}) = \log 2$. The final $\mathcal{AS}$ state is uncorrelated $\frac{1}{2}[|0\rangle\langle 0| + |1\rangle\langle 1|] \otimes |0\rangle\langle 0|$ and has $D(\mathfrak{B}_\mathfrak{M}) = 2\log 2$.

These results generalize naturally to d dimensional systems. The von Neumann scheme has $G(\mathcal{A}_\mathfrak{M}) = D(\mathfrak{B}_\mathfrak{M}) = \log d$, which we call the *Heisenberg limit*. The swap sensation has $G(\mathcal{A}_\mathfrak{M}) = D(\mathfrak{B}_\mathfrak{M}) = 2\log d$ and the decohered swap sensation has $G(\mathcal{A}_\mathfrak{M}) = \log d$ and $D(\mathfrak{B}_\mathfrak{M}) = 2\log d$. These results are summarised in Table 4.1.

The fact that the information gain of a swap sensation is $2\log d$ warrants an explanation. Intuitively, a swap should provide at least *some* information, even if it is not obvious how much. It should provide at least as much information as any von Neumann sensation, because once the system state falls into the memory of the agent's sensor, she is free to post-process it with any von Neumann sensation she sees fit. Yet a naive analysis of the swap sensation suggests it provides no information. To wit, the swap sensation maps any system state $|\psi\rangle$ to a separable state $|0\psi\rangle$. The system and observer are completely uncorrelated, no matter the initial system state. Any attempt to quantify information gain based on correlations of observer and system observables will fail to match the intuition that a swap offers non-zero information. It is a triumph of the sensation formalism that it succeeds in assigning the swap non-zero information. In fact, it assigns the swap the highest possible value of $2\log d$ for a given system dimension d.

4.4.4 Information-disturbance relation

The examples above suggest a relationship between the information gain $G(\mathcal{A}_\mathfrak{M})$ and disturbance $D(\mathfrak{B}_\mathfrak{M})$ of a measurement interaction $\mathfrak{M}$. In the first two examples (von Neumann and swap) we had $G(\mathcal{A}_\mathfrak{M}) = D(\mathfrak{B}_\mathfrak{M})$ and in the last example (decohered swap) we had $D(\mathfrak{B}_\mathfrak{M}) > G(\mathcal{A}_\mathfrak{M})$. In all three examples, the observer disturbed at least as much information as she gained. In the following theorem, we prove that $0 \leq D(\mathfrak{B}_\mathfrak{M}) - G(\mathcal{A}_\mathfrak{M})$. Furthermore, the examples suggest that when the sensation yields a pure state, the disturbance equals the information gain. We show that this is true in general by proving that the difference between the disturbance and information gain is bounded from above by twice the joint entropy of the $\mathcal{ASO}$ system.

Theorem 1. *Consider a measurement interaction $\mathfrak{M} : \mathcal{S} \to \mathcal{SO}$ of a system $\mathcal{S}$ with a Hilbert space of finite dimension d. Let $|\Phi^+\rangle_{\mathcal{AS}}$ be the state of that system maximally entangled with an ancilla $\mathcal{A}$. Let $\rho_{\mathcal{ASO}} = (\mathfrak{1}_\mathcal{A} \otimes \mathfrak{M})[|\Phi^+\rangle\langle\Phi^+|_{\mathcal{AS}}]$ be the state after the interaction. Then the information gain $G(\mathcal{A}_\mathfrak{M}) = I_{\mathcal{A}:\mathcal{O}}(\rho_{\mathcal{AO}})$ and disturbance $D(\mathfrak{B}_\mathfrak{M}) = 2\log d - I_{\mathcal{A}:\mathcal{S}}(\rho_{\mathcal{AS}})$ satisfy*

$$0 \leq D(\mathfrak{B}_\mathfrak{M}) - G(\mathcal{A}_\mathfrak{M}) \leq 2S(\rho_{\mathcal{ASO}}) \tag{4.11}$$

Proof. We start by proving $0 \leq D(\mathfrak{B}_{\mathfrak{M}}) - G(\mathcal{A}_{\mathfrak{M}})$. Our proof is based on the strong subadditivity of quantum information, which can be expressed as the following inequality valid for any tripartite state: $\tau_{\mathcal{X}\mathcal{Y}\mathcal{Z}}$: [148, Eq. 11.114]

$$I_{\mathcal{X}:\mathcal{Y}}(\tau_{\mathcal{X}\mathcal{Y}}) + I_{\mathcal{X}:\mathcal{Z}}(\tau_{\mathcal{X}\mathcal{Z}}) \leq 2S(\tau_{\mathcal{X}}). \tag{4.12}$$

Applying this inequality to $\rho_{\mathcal{A}\mathcal{S}\mathcal{O}}$ shows that

$$I_{\mathcal{A}:\mathcal{O}}(\rho_{\mathcal{A}\mathcal{O}}) \leq 2S_{\mathcal{A}}(\rho_{\mathcal{A}}) - I_{\mathcal{A}:\mathcal{S}}(\rho_{\mathcal{A}\mathcal{S}}). \tag{4.13}$$

The interaction $\mathfrak{M}$ does not act on the ancilla, so the $\mathcal{A}$ subsystem remains in its initial state, which was half of a maximally entangled state. Consequently, $S(\rho_{\mathcal{A}}) = \log d$. Substituting this value, along with the definitions for disturbance and information gain reveals $G(\mathcal{A}_{\mathfrak{M}}) \leq D(\mathfrak{B}_{\mathfrak{M}})$.

Next we prove $D(\mathfrak{B}_{\mathfrak{M}}) - G(\mathcal{A}_{\mathfrak{M}}) \leq 2S(\rho_{\mathcal{A}\mathcal{S}\mathcal{O}})$. The proof relies on a corollary of strong subadditivity known as the Araki-Lieb triangle inequality[170], which states that any bipartite state $\tau_{\mathcal{X}\mathcal{Y}}$ obeys the following inequality:

$$|S(\tau_{\mathcal{X}}) - S(\tau_{\mathcal{Y}})| \leq S(\tau_{\mathcal{X}\mathcal{Y}}). \tag{4.14}$$

We also reuse the fact that $S(\rho_{\mathcal{A}}) = \log d$.

$$\begin{aligned} D(\mathfrak{B}_{\mathfrak{M}}) - G(\mathcal{A}_{\mathfrak{M}}) &= 2\log d - I_{\mathcal{A}:\mathcal{S}}\left(\rho_{\mathcal{A}\mathcal{S}}\right) - I_{\mathcal{A}:\mathcal{O}}\left(\rho_{\mathcal{A}\mathcal{O}}\right) && (4.15)\\ &= 2S(\rho_{\mathcal{A}}) - [S(\rho_{\mathcal{A}}) + S(\rho_{\mathcal{S}}) - S(\rho_{\mathcal{A}\mathcal{S}})] - [S(\rho_{\mathcal{A}}) + S(\rho_{\mathcal{O}}) - S(\rho_{\mathcal{A}\mathcal{O}})] && (4.16)\\ &= [S(\rho_{\mathcal{A}\mathcal{S}}) - S(\rho_{\mathcal{O}})] + [S(\rho_{\mathcal{A}\mathcal{O}}) - S(\rho_{\mathcal{S}})] && (4.17)\\ &\leq 2S(\rho_{\mathcal{A}\mathcal{S}\mathcal{O}}) && (4.18) \end{aligned}$$

The last line follows from applying the triangle inequality to obtain $S(\rho_{\mathcal{A}\mathcal{S}}) - S(\rho_{\mathcal{O}}) \leq S(\rho_{\mathcal{A}\mathcal{S}\mathcal{O}})$ and $S(\rho_{\mathcal{A}\mathcal{O}}) - S(\rho_{\mathcal{S}}) \leq S(\rho_{\mathcal{A}\mathcal{S}\mathcal{O}})$.

□

The upper bound in Eq. 4.11 shows that a sufficient condition for a sensation to inform as much as it disturbs is for it to map pure state to pure states, and thus output an $\mathcal{A}\mathcal{S}\mathcal{O}$ state with zero entropy. However, this sufficient condition is not a necessary condition. The von Neumann measurement considered in Sec. 4.4.3 produced the $\mathcal{A}\mathcal{S}\mathcal{E}\mathcal{O}$ state $\frac{1}{\sqrt{2}}[|0000\rangle + |1111\rangle]$. Although the reduced $\mathcal{A}\mathcal{S}\mathcal{O}$ state is mixed, the sensation has equal disturbance and information gain. A complete classification of the necessary and sufficient conditions for a sensation to inform as much as it disturbs would essentially give a recipe for ideal, minimally disturbing measurements, but it is beyond the scope of this work.

4.5 Agency in the quantum world

In the previous sections we developed a framework to study measurements involving agents equipped with quantum sensors. Within this framework we extended the classically motivated concepts of observation and uncertainty into the quantum regime without trying to force a connection to our own experience. While our experience of the world seems to be classical at least in the sense

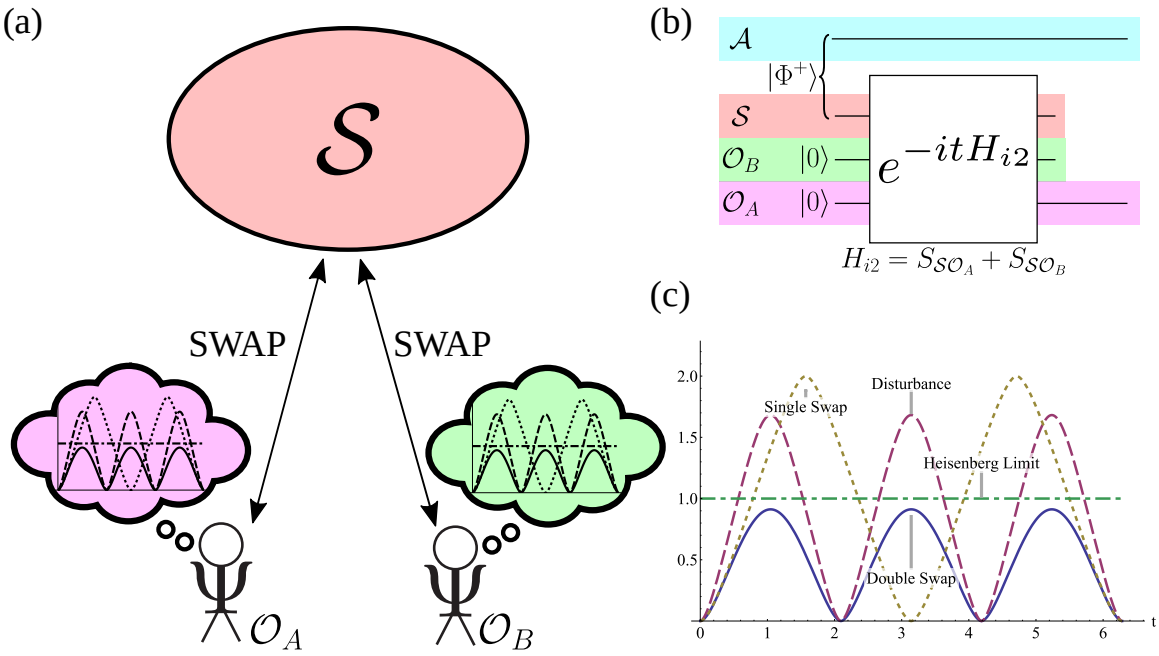

Figure 4.7: Simultaneous observations using a swap interaction (a) Two observers $\mathcal{O}_A$ and $\mathcal{O}_B$ simultaneously couple to the same system using the swap Hamiltonian. (b) A circuit diagram for the sensation with an ancilla $\mathcal{A}$ added to account for disturbance and information gain. (c) Informational quantities in bits as a function of time. The solid blue curve denotes the information gained by each observer individually during the double swap. Dashed purple shows the disturbance to the original system. It also equals the information gained by both observers when they cooperate and act as a single, joint observer. Olive dots denote the single swap information gain and disturbance, which describes what would have happened if only one observer attempted to sense the system. Green dashed dots show the Heisenberg limit for reference, which corresponds to the information gain and disturbance of an ideal von Neumann measurement. At the cost of extra disturbance compared to a von Neumann measurement, swap observers can nearly achieve the Heisenberg limit without cooperation and significantly exceed it with cooperation.

that our observations can be described using POVMs, there seems to be no law of nature that can rule out the more general type of observation described in Sec. 4.3 above (It should however be emphasised that a wide body of work has been devoted to finding such laws; e.g. the quantum Darwinism [158, 159, 171] and spontaneous collapse [172] programs). If we believe quantum theory applies at all levels, then quantum agents can exist in principle, for example in the form of sufficiently advanced fault tolerant quantum computers with peripheral quantum sensors (see Fig. 4.8). In this section we discuss quantum agency through well known results developed in the context of traditional measurements and explore possible directions for research in quantum computing.

4.5.1 Simultaneous observations

We now move to a scenario involving two observers $\mathcal{O}_A$ and $\mathcal{O}_B$ who try to sense the same system simultaneously (see Fig. 4.7). In the case of a von Neumann sensation of the same observable, this is a well studied scenario [171]. The two sensations commute and the outcomes are the same as those arising from the scenario where the observers perform the sensation one after the other, or a situation where the two observers monitor the same sensor. In all of these cases the observers do not influence each other's sensation and all can reach the Heisenberg limit and moreover have correlated results.

What happens if two observers attempt to sense the same system simultaneously, both using the same swap sensation? The SWAP operator $S_{\mathcal{SO}_A}$ that swaps system states with memory states in $\mathcal{O}_A$'s sensor does not commute with the otherwise identical SWAP operator $S_{\mathcal{SO}_B}$ for $\mathcal{O}_B$. As a result, the two observers' sensations will influence each other. We model the simultaneous swap using the interaction Hamiltonian $H_{i2} = S_{\mathcal{SO}_A} + S_{\mathcal{SO}_B}$. The system and observers are initially in the product state $|\psi\rangle_{\mathcal{S}} |0\rangle_{\mathcal{O}_A} |0\rangle_{\mathcal{O}_B}$. The Hamiltonian H_{i2} is applied for a time t, leading to the state $e^{-itH_{i2}} |\psi\rangle_{\mathcal{S}} |0\rangle_{\mathcal{O}_A} |0\rangle_{\mathcal{O}_B}$. At every moment in time, we associate a sensation with each observer, $\mathcal{O}_A$ and $\mathcal{O}_B$, denoted $\mathfrak{M}_A$ and $\mathfrak{M}_B$ respectively. Both of these sensations refer to the same dynamical process, save for an exchange in the notion of observer and environment. Since the situation is symmetric, we will only study it from observer $\mathcal{O}_A$'s perspective.

We explicitly calculate the time-evolved state in 4.24. From Eq. (4.24), we compute the information gain and disturbance and plot it for $d = 2$ in Fig. 4.7 c. For comparison with this "double swap" scenario, we plot the information gain and disturbance for a "single swap" sensation in which only $\mathcal{O}_A$ observes the system and the interaction Hamiltonian is $H_{i1} = S_{\mathcal{SO}_A}$. Initially, each observer gains nearly as much information from the double swap as the single swap. By the time each observer gains 0.5 bits of information (half the Heisenberg Limit), the presence of the other observer is felt and the double swap information begins to lag behind the single swap. While the single swap reaches the maximal information gain and disturbance of 2 bits at time $t = \pi/2$, the double swap caps out sooner at $t = \pi/3$ with an information gain of 0.91 bits and a disturbance of 1.68 bits. If each observer had instead performed the same von Neumann measurement on the system, they would have each gained 1 bit of information, slightly more than the double swap. They also would have only disturbed the system by 1 bit, significantly less than the double swap.

The double swap seems worse in terms of both information gain and disturbance than a von Neumann measurement, but there is more to the story. So far, we have only considered how much information $\mathcal{O}_A$ and $\mathcal{O}_B$ gain individually. However, if they cooperate we can treat them as a single joint observer and ask how much information $\mathcal{O} = \mathcal{O}_A\mathcal{O}_B$ gains. For this joint observer, the interaction with the system is unitary, so their information gain equals their disturbance and maximizes to 1.68 bits. This information gain significantly exceeds the 1 bit of information that one, two, or indeed any number of cooperative observers using the same von Neumann measurement can extract. Even though each von Neumann observer individually gains 1 bit from their measurement, it is all the *same*, redundant bit. At the cost of extra disturbance, two observers using a swap sensation can gain almost as much information individually as a von Neumann measurement while gaining significantly more information as a single, cooperative unit.

4.5.2 Quantum computers as agents

Work on mechanized observers who are part of the quantum system goes back at least as far as Everett [154] who imagined quantum automata observing the system in a generic way, but focused his attention on von Neumann type measurements and a classical experience where results are classical labels. Later, Albert [173, 174] showed that a quantum automaton with access to its own memory registers could perform measurements whose (classically interpreted) results seem paradoxical. These works inspired much of the early theoretical work on quantum computing, in particular Deutsch's pioneering work on universal quantum Turing machines [175]. Most subsequent research however,

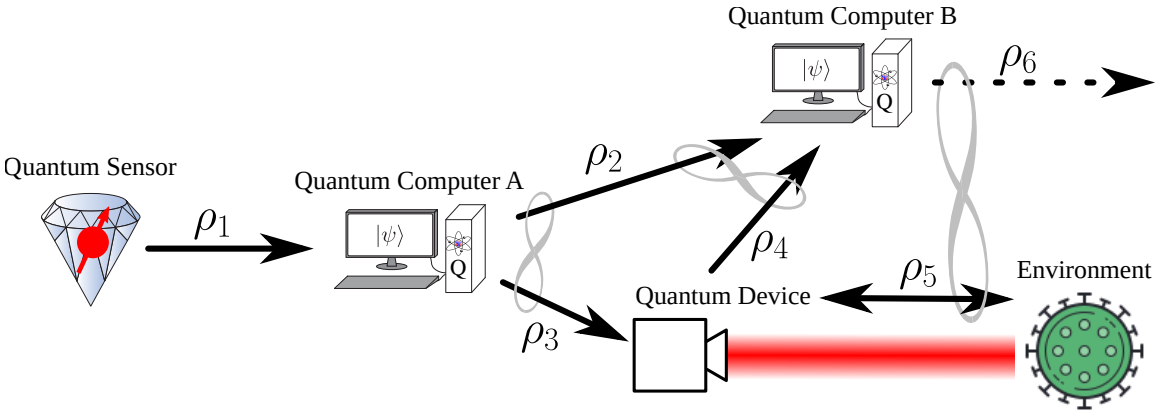

Figure 4.8: A quantum network where the different agents (the quantum computers) communicate via quantum communication channels and interact with the world via quantum peripherals. If we ascribe agency to sufficiently advanced quantum computers we expect that most of their interactions with each other and the rest of the world will be fully coherent.

regards quantum computers as devices to be used by classical agents. [4]

The usual quantum information processing paradigm involves classical inputs and outputs. In a sampling problem for example, the input is a classical description of some quantum circuit ending with a sequence of binary measurements, and the output is a string of bits that represents a sample from the probability distribution for the measurement outcomes. This picture is certainly realistic, but it can be modified in a quantum internet scenario where quantum computers are directly connected to quantum sensors that feed a quantum state as the input for a computation. These computers could interact with other quantum computers through quantum interconnects, so that they only share quantum information. If perfect quantum communication networks were available, we would expect most of the communication between quantum computers to involve no classical results (see Fig. 4.8). Quantum states generated by one computer could then be used to make decisions about which circuit to encode on other computers. While, most circuits are realized presently with classical control parameters, quantum controls have been used to run superpositions of circuits [177–179]. Quantum computers communicating in this way would have entangled circuits and classical results would only appear when these computers interact with us. [5] Such communication would allow many small quantum computing nodes to be joined together into a single distributed quantum computer.

Work on quantum computing theory tends to be based on the assumption that quantum theory can be applied as-is to arbitrarily large systems, yet the vast majority of work takes an anthropocentric view: classical input, classical output. Notably this approach even extends to problems in the QMA computational complexity class [180] which involve a proof encoded in a quantum state that is sent to a verifier who outputs a classical "accept" or "reject" with an appropriate probability. Exceptions include delegated quantum computing [181, 182] and compression protocols [183–185] which are usually framed as intermediate stages in a larger classical-in classical-out task. To the best of our knowledge, none of these have been studied as computational complexity classes. For example, one might study a type of decision problem where the language is defined in Hilbert space

[4] Note that the possibility of having quantum computers as observers is sometimes mentioned in the context of quantum foundations [176].

[5] and perhaps never if certain science fiction scenarios turn out to be correct.

and the verifier's output is a quantum state.

There are a number of difficulties in extending ideas in computational complexity to the fully quantum regime. One technical issue involves dealing with imperfections and handling non-orthogonal output states. Classically it is customary to expect that the right result would appear with a high probability (say 2/3) and that the results can be distinguished from each other. In the quantum case, one could try to deal with imperfections by asking that the real output state be close to some ideal output state. The metric used for the distance should make sense in the context of the problem. The usual distance measures used in quantum mechanics are interpreted in terms of probabilities for measurement outcomes, however as we showed here (Sec. 4.4.1), these can still make sense in a theory without probabilities. The same issue appears when dealing with non-orthogonal output states. There seems to be no inherent reason to claim that orthogonal states are more distinguishable to a quantum observer than non-orthogonal ones. More precisely: without the Born rule, there is no obvious notion of distinguishability which can be applied to orthogonal states. It might however be reasonable to expect that since unitary operators preserve the inner product, it has a special meaning. In fact this is probably unavoidable once we assign meaning to reduced density operators, or start thinking about broadcasting information to multiple observers [161].

4.6 Conclusions

The orthodox approach to measurement in quantum mechanics is based on an assumption that the observer is external to the quantum system and can observe the quantum world through *observables*. This approach works incredibly well to describe all known quantum phenomena and is unlikely to fail as long as observers (such as ourselves) have classical memories. Quantum memories do not seem to be a naturally occurring phenomenon, but much of the effort in quantum information processing is aimed at increasing coherence times and it is increasingly likely that engineered quantum memories will become commonplace in the not-too-distant future.

If we are to believe that the current technological trajectory will continue, we should entertain the idea of attributing agency to sufficiently advanced quantum computers. As we have shown in this work, such quantum agents would have access to a broader range of actions than those available to us. In particular, they would use sensations rather than conform to the narrow definition of measurement which has been adopted in quantum theory. We have explored these ideas and presented the swap sensation (Sec. 4.3.1 and Fig. 4.4 b) as an extreme case of quantum observation. Our ideas have already inspired an upcoming experiment [151] which empirically measures the information flow of several sensations.

We began with a generalized definition of measurement (Def. 1) whose deterministic result is a quantum state recorded in the quantum memory of an observer's sensor. To handle this more general formalism (which includes the von Neumann scheme as a special case) we modified the basic mathematical tools of quantum measurement theory and replaced the POVM with the result channel $\mathcal{A}_{\mathfrak{M}}$, which takes system states to states of the memory in the observer's sensor (see Fig. 4.3).

Using these tools, we suggested a method for quantifying information gain and disturbance (Sec. 4.4 and Fig. 4.6). These definitions led to expected results for von Neumann measurements while faithfully describing the swap sensation's exotic ability to provide complete information at the cost of maximal disturbance. We showed that the disturbance of a sensation always equals or exceeds

the information gained, which places a fundamental constraint on the information processing power of quantum agents. We provided a sufficient condition for a sensation to be ideal in the sense that it informs as much as it disturbs, but left open the task of identifying conditions that are both sufficient and necessary. We used these quantities to analyze a thought experiment in which two agents both attempt to use a swap sensation on the same system at the same time. The thought experiment revealed that cooperation amongst quantum agents is essential for making the most of certain sensations.

Our results are the first steps in studying fully quantum agents, but there is still much work to be done. We have only studied how quantum agents observe their surroundings, but the processes by which quantum agents might decide and act using those observations is still ripe for exploration. While much work is being done on studying new mechanisms for decoherence-free interactions, there is very little work on protocols, algorithms, and computational paradigms that involve purely quantum agents. While our framework formally separates the observer from the observed, the physical mechanism by which a quantum agent gains a sense of self is still a mystery.

We hope that our work encourages others to consider scenarios that involve multiple quantum agents who can interact with each other in a purely coherent, quantum mechanical way, for example a world-wide network of intelligent quantum computers (see Fig. 4.8). As we work towards building sophisticated quantum machines and a quantum internet, we should give careful consideration to how these machines would *think* and interact with the world around them. Learning from past oversights, we should not ignore the possibility of information being truly quantum mechanical.

4.7 Quantum agent supplementary materials

4.7.1 Traditional quantum measurements

Observables, outcomes and probabilities

Measurements in quantum mechanics have traditionally been associated with 'observables' which are mathematically represented as Hermitian operators. Each observable A has unique set of eigenstates (eigenspaces if it is degenerate) and eigenvalues so that it can be written as $A = \sum_k a_k A_k$ where $a_j \neq a_k$ unless $j = k$ and $\{A_k\}$ are projectors onto orthogonal subspaces. The (real) eigenvalues $\{a_k\}$ are usually used to label the possible measurement results, while the projectors $\{A_k\}$ are used for calculating the probabilities for each result. For a system initially in the state ρ, the probability that a measurement of A will yield the result a_k is given by the Born rule $p(a_k) = \mathrm{Tr}(A_k\rho)$

This formalism can be extended by noting that the set of orthogonal projectors $\{A_k\}$ can be replaced by a set of positive operators $\{E_k\}$ (not necessarily orthogonal) with $\sum_k E_k = \mathbb{1}$. Such a set of positive operators is called a positive operator valued measure (POVM) and its elements can be plugged into the Born rule to produce a probability distribution

$$p(a_k) = \mathrm{Tr}(E_k\rho) \tag{4.19}$$

for a set of possible measurement results labeled $\{a_k\}$. For simplicity we will refer to Eq. 4.19 as the Born rule.

In many cases we are also interested in the back-action of the measurement on the measured

system. The POVM does not provide sufficient information to predict a unique outgoing system state, although it can be used to identify a *minimally disturbing* measurement (as defined for example in [147]). For a minimally disturbing measurement, a result a_k with an associated POVM element E_k implies the transformation $\rho \to \frac{\sqrt{E_k}\rho\sqrt{E_k}}{\sqrt{\mathrm{Tr}(E_k\rho)}}$ on the measured system (see Fig. 4.2 a). In the special case of a measurement of an observable $A = \sum_k a_k A_k$, the minimally disturbing measurement is called a von Neumann measurement and the update rule is $\rho \to \frac{A_k \rho A_k}{\sqrt{\mathrm{Tr}(A_k\rho)}}$. When A_k is a rank-1 projector this rule has the simple form $\rho \to A_k$ i.e., the state projects onto the eigenstate associated with a_k. The disturbance is considered minimal since the update rule leaves eigenstates of A undisturbed.

The above description of a measurement (Born rule and state update rule) is in most cases sufficient for making predictions about the outcomes of experiments where the precise details of the measurement procedure and the observer can be ignored. It does however imply a hard cut between the observer and the measured system.

The von Neumann scheme

Von Neumann's approach can be used to model the measurement process associated with any POVM by treating a measurement apparatus as a quantum mechanical system initially in a state Υ. The measurement begins with some interaction $U_{\mathcal{SM}}$ so that $\rho \otimes \Upsilon \to U_{\mathcal{SM}}(\rho \otimes \Upsilon)U_{\mathcal{SM}}^\dagger$ after which the measurement result is encoded in the state of $\mathcal{M}$. To read out the result, an observer would need to measure an observable $\Pi_{\mathcal{M}} = \sum_k a_k \Pi_k$ on $\mathcal{M}$, where Π_k are orthogonal projectors and the labels a_k are distinct. The probability for a result a_k would then be $P(a_k|\rho_{\mathcal{S}}) = \mathrm{Tr}\left[(\mathbb{1}\otimes\Pi_k)U_{\mathcal{SM}}(\rho\otimes\Upsilon)U_{\mathcal{SM}}^\dagger\right]$. This equation can be written in the form of Born's rule (4.19) by identifying the POVM element $E_k = \mathrm{Tr}_{\mathcal{M}}\left[U_{\mathcal{SM}}^\dagger(\mathbb{1}\otimes\Pi_k)U_{\mathcal{SM}}(\mathbb{1}\otimes\Upsilon)\right]$ so that $P(a_k|\rho_{\mathcal{S}}) = \mathrm{Tr}\left[E_k\rho_{\mathcal{S}}\right]$. The procedure also gives the post-measurement state of the observed system given a result a_k as $\frac{\mathrm{Tr}_{\mathcal{M}}\left[(\mathbb{1}\otimes\Pi_k)U_{\mathcal{SM}}(\rho\otimes\Upsilon)U_{\mathcal{SM}}^\dagger\right]}{P(a_k|\rho_{\mathcal{S}})}$ [186]. The term *von Neumann scheme* is often used for the special case where this procedure is applied to the inner workings of a von Neumann measurement. For this measurement $U_{\mathcal{SM}}$ is generated by a Hamiltonian in the form of Eq. (4.1) (see Fig. 4.2 above and Sec. 4.3.1 below for more details).

The scheme above is more detailed than the Born and state update rules, but it is not complete since it invokes an observation of the measurement device (via $\Pi_{\mathcal{M}}$) with no details on how this measurement is constructed. It then begs the question *'how is the measurement device observed?'* to which we could give the same answer ad infinitum. At this point von Neumann invoked the external observer (which he previously justified). It is however possible to treat the result quantum mechanically - i.e. as a state $|a_k\rangle$ rather than a classical label 'a_k' - so that no external observers are required. This fully coherent approach comes with interpretational issues, but it can be argued that these are no more problematic than the alternative. As we will show in Sec. 4.3 the possibility of encoding the measurement result in a quantum state allows a more general definition of measurement where some observers can perceive the world in a way which cannot be modeled in the language of POVMs.

Side remark: Locality and the Born rule

Quantum mechanics with external (classical) observers is fairly well defined at least from an operational perspective where certain systems (e.g. humans, cameras, etc.) are postulated to be

classical and external. In such an approach one generally accepts the Born rule and a certain version of the collapse postulate as part of the quantum-to-classical transition. This in turn allows us to use some tools which we usually take for granted, especially those that have been adopted from statistical mechanics and information theory. One which is of particular significance here is the reduced state. Consider a system which is composed of two distinct subsystems: $\mathcal{S}$ and $\mathcal{M}$ such that its description is a state $|\psi\rangle_{\mathcal{SM}}$ in the tensor product Hilbert space $\mathcal{H}_{\mathcal{SM}} = \mathcal{H}_{\mathcal{S}} \otimes \mathcal{H}_{\mathcal{M}}$. The reduced state of the system is $\rho_{\mathcal{S}} = \mathrm{Tr}_{\mathcal{M}}[|\psi\rangle\langle\psi|]$, where $\mathrm{Tr}_{\mathcal{M}}$ is the partial trace over $\mathcal{H}_{\mathcal{M}}$. This reduced state contains all the information necessary for calculating probabilities for the outcomes of measurements via the Born rule (4.19). From the operational perspective of the external observer, this reduced state contains all there is to know about the system. The notion of a reduced state can also be extended to dynamics. Consider an initial product state $\rho_{\mathcal{S}} \otimes \tau_{\mathcal{M}}$ on $\mathcal{H}_{\mathcal{SM}} = \mathcal{H}_{\mathcal{S}} \otimes \mathcal{H}_{\mathcal{M}}$ and some Schrödinger evolution described by the unitary $U_{\mathcal{SM}}$. The local (reduced) dynamics is described by the completely positive trace preserving map $\mathfrak{C}(\rho_{\mathcal{S}}) = \mathrm{Tr}_{\mathcal{M}}[U_{\mathcal{SM}}\rho_{\mathcal{S}} \otimes \tau_{\mathcal{M}}U_{\mathcal{SM}}^{\dagger}]$ (also called the *quantum channel*).

Quantum theory with quantum observers provides a more difficult situation than a theory with external observers, and requires a more careful treatment of fundamental postulates and their interpretation. Our approach here is to take the 'standard' Schrödinger-picture quantum theory (without collapse) at face value, as is often done in many-worlds interpretations[6] [188, 189]. In particular, we assume that the reduced density operators are valid complete descriptions of the local states, and that reduced dynamics provide a complete description of the local dynamics. We note that this is not necessarily the situation in hidden variable theories such as those following de Broglie and Bohm's pilot wave [152], and that even in the many worlds interpretation the justification for assigning meaning to reduced density operators requires a complicated argument and non-trivial assumptions [190].

4.7.2 Photodetection

The usual treatment of photodetection [191, 192] begins with an atomic system interacting with an electric field through an interaction Hamiltonian of the form $H_i = \vec{d} \cdot \vec{E}$, where $\vec{d}$ is the dipole moment of the atom and $\vec{E}$ is the electric field. This Hamiltonian has the von Neumann form (4.1) with the atom acting as the measurement apparatus and the field $\vec{E}$ as the measured operator, and so we might be tempted to say that this is a von Neumann measurement of the field. However, free evolution cannot be neglected at optical frequencies, and the free evolution term in the Hamiltonian does not commute with the interaction term. The dynamics are usually treated by moving to a rotating frame and making the rotating wave approximation to get rid of terms that oscillate rapidly (see [192, Sec. 4.3]).

We treat the detector as a two-level atom and assume that the atoms are initially in the ground state and that the excited state is an ion and a free photoelectron. Each absorbed photon leads to the release of a photoelectron (see [192, Sec. 5.2] for a detailed derivation) which induces an irreversible amplification sequence whose details depend on the specifics of the detector. Ideally the detector would perform a perfect SWAP followed by dephasing so that the incoming photon number would be perfectly correlated with the amplified output signal; however, practical issues mean that photon number sensitivity is usually far from perfect.

[6] see Deutsch and Hayden [187] for a different (Heisenberg based) approach to many worlds.

4.7.3 Simultaneous swap

We calculate the state evolution and information exchange of the simultaneous swap sensation described in Sec. 4.5.1. There are two relevant (unnormalized) eigenstates of H_{i2}:

$$\begin{aligned} |e_2\rangle &= |\psi 00\rangle + |0\psi 0\rangle + |00\psi\rangle\,, \\ |e_{-1}\rangle &= 2\,|\psi 00\rangle - |0\psi 0\rangle - |00\psi\rangle\,. \end{aligned} \tag{4.20}$$

They have respective eigenvalues 2 and -1. These allow us to expand the initial state $|\psi 00\rangle$ in the eigenbasis of H_{i2}.

$$|\psi 00\rangle = \frac{|e_2\rangle + |e_{-1}\rangle}{3} \tag{4.21}$$

The evolved state is

$$\begin{aligned} e^{-itH_{i2}}\,|\psi 00\rangle &= \frac{e^{-2it}\,|e_2\rangle + e^{it}\,|e_{-1}\rangle}{3} \\ &= \frac{e^{-2it} + 2e^{it}}{3}\,|\psi 00\rangle + \frac{e^{-2it} - e^{it}}{3}\,[|0\psi 0\rangle + |00\psi\rangle]\,. \end{aligned} \tag{4.22}$$

When t is an integer multiple of $\frac{2}{3}\pi$, the state evolves back to its original uncorrelated state times a phase factor. For these t values, the interaction is not a sensation by Def. 1.

To calculate information gain and disturbance for the $d = 2$ case, we add a third agent $\mathcal{A}$ initially entangled with $\mathcal{S}$, so that the initial $\mathcal{AS}\mathcal{O}_A\mathcal{O}_B$ state is

$$|\Psi\rangle = \frac{|0000\rangle + |1100\rangle}{\sqrt{2}}. \tag{4.23}$$

The state evolves to

$$e^{-itH_i}\,|\Psi\rangle = \frac{1}{\sqrt{2}}\left[e^{-2it}\,|0000\rangle + \frac{e^{-2it} + 2e^{it}}{3}\,|1100\rangle + \frac{e^{-2it} - e^{it}}{3}\,[|1010\rangle + |1001\rangle]\right]. \tag{4.24}$$

The information gain is the mutual information of the reduced $\mathcal{AO}_A$ state,

$$\rho_{\mathcal{AO}_A} = \frac{1}{2}\left[|00\rangle + \frac{1 - e^{3it}}{3}\,|11\rangle\right]\left[\langle 00| + \frac{1 - e^{-3it}}{3}\,\langle 11|\right] + \frac{7 + 2\cos(3t)}{18}\,|10\rangle\langle 10|\,. \tag{4.25}$$

The disturbance is 2 minus the mutual information of the reduced $\mathcal{AS}$ state,

$$\rho_{\mathcal{AS}} = \frac{1}{2}\left[|00\rangle + \frac{1 + 2e^{3it}}{3}\,|11\rangle\right]\left[\langle 00| + \frac{1 + 2e^{-3it}}{3}\,\langle 11|\right] + \frac{2 - 2\cos(3t)}{9}\,|10\rangle\langle 10|\,. \tag{4.26}$$

4.8 Quantum agents outro

4.8.1 Contributions

The paper in the previous section started as several animated conversations among Aephraim's group about quantum agency. Aharon Brodutch and Kent Bonsma-Fisher lead those conversations and came up with the idea to look past the standard von Neumann notion of quantum measurement. I, along with Hugo Ferretti, Edwin Tham, Arthur Pang, and occasionally Aephraim Steinberg

contributed to these initial conversations as well. Kent devised almost all the figures while Aharon wrote an initial draft of the manuscript. The first round of reviewers commented that the ideas in the manuscript were interesting, but it was unclear how much if any of them were new. I stepped up to lead revisions of the manuscript based on this feedback, and came up with almost all the quantitative results in the present version in the process. Specifically, I developed the definitions of information gain and disturbance and proved the inequalities between them. Aharon and I worked together to calculate the simultaneous swap scenario presented in the paper.

4.8.2 Follow up

The purpose of the entangled sheep paper was to create a conceptual and mathematical framework naturally suited for problems involving quantum agents. Broadly speaking, there are two avenues for furthering the research program the paper set out: applying the framework to concrete problems and continued development of the framework itself.

Our paper introduced a scenario (Sec. 4.5.1) in which two observers simultaneously use a swap sensation to observe the same system. While there is certainly potential to come up with and analyze more scenarios, I think we have only scratched the surface of the simultaneous swap. We computed that each observer individually gains up to 0.91 bits of information and that the observers jointly share up to 1.68 bits of information between them, but we did not delve into the nature of this information. How might this information be used operationally for various tasks like steering or cloning? The fact that the sum of the observers' individual gains is greater than their shared gain suggests some level of redundancy in the gained information and points to genuine tri-partite correlations. Do these tri-partite correlations enable protocols that would not be possible with only two-party correlations? How do different continuous-time models of the swap sensation impact the information exchange? How well does our simultaneous swap thought experiment map onto a real scenario in which photons trapped in a cavity leak symmetrically through one end of the cavity or the other?

The framework we developed defines tools for calculating the flow of information between quantum agents with finite-dimensional sensors and no prior knowledge of the systems they sense. The growing interest in continuous-variable quantum computing motivates extending our framework to describe infinite-dimensional sensors, but finding the appropriate extension is mathematically daunting. Our definitions of information gain and disturbance rely on maximally entangled states, which are straightforward to define in finite dimensions, but notoriously difficult to describe rigorously in infinite dimensions. For example, a naive attempt to define a maximally entangled state of two photonic modes produces a non-normalizable state with infinite energy. The continuous-variable quantum computing community surely has rigorous ways of dealing with these issues, so mining their literature for ideas should be a good starting point.

Accounting for prior information is crucial at both a conceptual and practical level. A good framework for information flow should assign zero information gain to an agent that senses a state they already know everything about. However, the current definitions of information gain and disturbance stipulate the system starts maximally entangled with some ancilla, leaving no room to account for any prior knowledge the observer might have. A natural way to include such knowledge in our framework would be to allow the initial system state to be only partially entangled with an ancilla, or even not entangled at all. The amount of entanglement and the reduced state of the

system would model the observer's prior knowledge. Applying our current formulas for information flow based on mutual information to such a non-maximally entangled state would give sensible results in situations where the observer's prior knowledge is accurate. What if an observer believes with all their heart that a system is in a particular pure state, but upon sensing it, realizes it was in an orthogonal state? Our framework ought to assign some non-zero information to the observer's sensation, but exactly how much is unclear. I expect that properly extending our framework to handle prior knowledge will involve generalizing our usage of mutual information to relative entropy, which is the tool of choice in classical statistics to measure the communication cost of sending information to a receiver with a mismatched prior.

4.8.3 Relation to interpretations of quantum mechanics

After reading the paper in this chapter, one may wonder where the work sits amongst the zoo of interpretations of quantum mechanics. However, the ideas presented in the entangled sheep paper are *not* an interpretation of quantum mechanics. The work does not take a position on what the elements of reality are. At the same time, it is not a new theory of nature. Our framework does not suggest any changes to the usual calculations of quantum mechanics nor predict any new phenomenon. So if the ideas are not an interpretation or a theory, what exactly are they?

At its core, the quantum sheep paper is a plea to the quantum mechanics community to expand the definition of measurement. Quantum agents with coherent quantum memories will interact with and sense their surroundings. If we refuse to see these actions as measurements, we will be at a loss for words to describe the information flow among these agents. By defining a set of terminology and associated mathematical definitions, we hope to endow researchers with a common language for conceptualizing, analyzing, and discussing a future where quantum agents thrive.

Bibliography

[1] E. Knill, R. Laflamme, and G. J. Milburn. "A scheme for efficient quantum computation with linear optics". In: *Nature* 409.6816 (Jan. 2001), pp. 46–52. ISSN: 1476-4687. DOI: 10.1038/35051009. URL: https://doi.org/10.1038/35051009.

[2] Charles H. Bennett and Gilles Brassard. "Quantum cryptography: Public key distribution and coin tossing." In: vol. 175. 1984, pp. 175–179.

[3] P. Ben Dixon et al. "Ultrasensitive Beam Deflection Measurement via Interferometric Weak Value Amplification". In: *Phys. Rev. Lett.* 102 (17 Apr. 2009), p. 173601. DOI: 10.1103/PhysRevLett.102.173601. URL: https://link.aps.org/doi/10.1103/PhysRevLett.102.173601.

[4] Andrew N Jordan, Julián Martínez-Rincón, and John C Howell. "Technical advantages for weak-value amplification: when less is more". In: *Physical Review X* 4.1 (2014), p. 011031.

[5] Charles H. Bennett et al. "Teleporting an unknown quantum state via dual classical and Einstein-Podolsky-Rosen channels". In: *Phys. Rev. Lett.* 70 (13 Mar. 1993), pp. 1895–1899. DOI: 10.1103/PhysRevLett.70.1895. URL: https://link.aps.org/doi/10.1103/PhysRevLett.70.1895.

[6] David Deutsch. "Quantum mechanics near closed timelike lines". In: *Physical Review D* 44.10 (1991), p. 3197.

[7] Seth Lloyd et al. "Closed timelike curves via postselection: theory and experimental test of consistency". In: *Physical Review Letters* 106.4 (2011), p. 040403.

[8] Martin Ringbauer et al. "Experimental simulation of closed timelike curves". In: *Nature communications* 5 (2014), p. 4145.

[9] Noah Lupu-Gladstein et al. "Negative Quasiprobabilities Enhance Phase Estimation in Quantum-Optics Experiment". In: *Phys. Rev. Lett.* 128 (22 June 2022), p. 220504. DOI: 10.1103/PhysRevLett.128.220504. URL: https://link.aps.org/doi/10.1103/PhysRevLett.128.220504.

[10] Noah Lupu-Gladstein et al. "Quantum violations of classical counting principles via variable-strength non-local measurements". In preparation. 2024.

[11] Noah Lupu-Gladstein et al. "Do qubits dream of entangled sheep? Quantum measurement without classical output". In: *New Journal of Physics* 26.5 (May 2024), p. 053029. DOI: 10.1088/1367-2630/ad48ad. URL: https://dx.doi.org/10.1088/1367-2630/ad48ad.

[12] Samuel L. Braunstein and Carlton M. Caves. "Statistical distance and the geometry of quantum states". In: *Phys. Rev. Lett.* 72 (22 May 1994), pp. 3439–3443. DOI: 10.1103/PhysRevLett.72.3439. URL: https://link.aps.org/doi/10.1103/PhysRevLett.72.3439.

[13] Jing Liu et al. "Quantum Fisher information and symmetric logarithmic derivative via anti-commutators". In: *Journal of Physics A: Mathematical and Theoretical* 49.27 (May 2016), p. 275302. DOI: 10.1088/1751-8113/49/27/275302. URL: https://dx.doi.org/10.1088/1751-8113/49/27/275302.

[14] David R. M. Arvidsson-Shukur et al. "Quantum advantage in postselected metrology". In: *Nature Communications* 11.1 (July 2020), p. 3775. ISSN: 2041-1723. DOI: 10.1038/s41467-020-17559-w. URL: https://doi.org/10.1038/s41467-020-17559-w.

[15] Lee A. Rozema et al. "Violation of Heisenberg's Measurement-Disturbance Relationship by Weak Measurements". In: *Phys. Rev. Lett.* 109 (10 Sept. 2012), p. 100404. DOI: 10.1103/PhysRevLett.109.100404. URL: https://link.aps.org/doi/10.1103/PhysRevLett.109.100404.

[16] Vittorio Giovannetti, Seth Lloyd, and Lorenzo Maccone. "Quantum-enhanced measurements: beating the standard quantum limit". In: *Science* 306.5700 (2004), pp. 1330–1336.

[17] Vittorio Giovannetti, Seth Lloyd, and Lorenzo Maccone. "Quantum metrology". In: *Physical review letters* 96.1 (2006), p. 010401.

[18] Vittorio Giovannetti, Seth Lloyd, and Lorenzo Maccone. "Advances in quantum metrology". In: *Nature photonics* 5.4 (2011), p. 222.

[19] Emanuele Polino et al. "Photonic quantum metrology". In: *AVS Quantum Science* 2.2 (2020), p. 024703. DOI: 10.1116/5.0007577. eprint: https://doi.org/10.1116/5.0007577. URL: https://doi.org/10.1116/5.0007577.

[20] Seung-Jin Yoon et al. "Experimental quantum polarimetry using heralded single photons". In: *Metrologia* 57.4 (2020), p. 045008.

[21] J. Abadie et al. "A gravitational wave observatory operating beyond the quantum shot-noise limit". In: *Nature Physics 2011 7:12* 7.12 (Sept. 2011), pp. 962–965. ISSN: 1745-2481. DOI: 10.1038/nphys2083. URL: https://www.nature.com/articles/nphys2083.

[22] B. P. Abbott et al. "Observation of Gravitational Waves from a Binary Black Hole Merger". In: *Phys. Rev. Lett.* 116 (6 Feb. 2016), p. 061102. DOI: 10.1103/PhysRevLett.116.061102. URL: http://link.aps.org/doi/10.1103/PhysRevLett.116.061102.

[23] Nirmalya Ghosh and Alex I Vitkin. "Tissue polarimetry: concepts, challenges, applications, and outlook". In: *Journal of biomedical optics* 16.11 (2011), p. 110801.

[24] Dmitry Budker and Michael Romalis. "Optical magnetometry". In: *Nature physics* 3.4 (2007), pp. 227–234.

[25] Emanuel Knill et al. "Randomized benchmarking of quantum gates". In: *Physical Review A* 77.1 (2008), p. 012307.

[26] Miroslav Dobšíček et al. "Arbitrary accuracy iterative quantum phase estimation algorithm using a single ancillary qubit: A two-qubit benchmark". In: *Phys. Rev. A* 76 (3 Sept. 2007), p. 030306. DOI: 10.1103/PhysRevA.76.030306. URL: https://link.aps.org/doi/10.1103/PhysRevA.76.030306.

[27] Harald Cramér. *Mathematical methods of statistics (PMS-9)*. Vol. 9. Princeton University Press, 2016.

[28] C Radhakrishna Rao. "Information and the accuracy attainable in the estimation of statistical parameters". In: *Breakthroughs in statistics*. Springer, 1992, pp. 235–247.

[29] Joshua Combes et al. "Quantum limits on postselected, probabilistic quantum metrology". In: *Phys. Rev. A* 89 (5 May 2014), p. 052117. DOI: 10.1103/PhysRevA.89.052117. URL: https://link.aps.org/doi/10.1103/PhysRevA.89.052117.

[30] Christopher Ferrie and Joshua Combes. "Weak Value Amplification is Suboptimal for Estimation and Detection". In: *Phys. Rev. Lett.* 112 (4 Jan. 2014), p. 040406. DOI: 10.1103/PhysRevLett.112.040406. URL: https://link.aps.org/doi/10.1103/PhysRevLett.112.040406.

[31] Jérémie Harris, Robert W Boyd, and Jeff S Lundeen. "Weak value amplification can outperform conventional measurement in the presence of detector saturation". In: *Phys. Rev. Lett.* 118.7 (2017), p. 070802.

[32] Josiah Sinclair et al. "Weak-value amplification and optimal parameter estimation in the presence of correlated noise". In: *Phys. Rev. A* 96 (5 Nov. 2017), p. 052128. DOI: 10.1103/PhysRevA.96.052128. URL: https://link.aps.org/doi/10.1103/PhysRevA.96.052128.

[33] Matin Hallaji et al. "Weak-value amplification of the nonlinear effect of a single photon". In: *Nature Physics* 13.6 (June 2017), pp. 540–544. ISSN: 1745-2481. DOI: 10.1038/nphys4040. URL: https://doi.org/10.1038/nphys4040.

[34] Gerardo I. Viza et al. "Experimentally quantifying the advantages of weak-value-based metrology". In: *Phys. Rev. A* 92 (3 Sept. 2015), p. 032127. DOI: 10.1103/PhysRevA.92.032127. URL: https://link.aps.org/doi/10.1103/PhysRevA.92.032127.

[35] Xiaodong Qiu et al. "Precision phase estimation based on weak-value amplification". In: *Applied Physics Letters* 110.7, 071105 (Feb. 2017), p. 071105. DOI: 10.1063/1.4976312.

[36] Yakir Aharonov, David Z. Albert, and Lev Vaidman. "How the result of a measurement of a component of the spin of a spin- *1/2* particle can turn out to be 100". In: *Phys. Rev. Lett.* 60 (14 Apr. 1988), pp. 1351–1354. DOI: 10.1103/PhysRevLett.60.1351. URL: http://link.aps.org/doi/10.1103/PhysRevLett.60.1351.

[37] I. M. Duck, P. M. Stevenson, and E. C. G. Sudarshan. "The sense in which a "weak measurement" of a spin-1/2 particle's spin component yields a value 100". In: *Phys. Rev. D* 40 (6 Sept. 1989), pp. 2112–2117. DOI: 10.1103/PhysRevD.40.2112. URL: https://link.aps.org/doi/10.1103/PhysRevD.40.2112.

[38] Onur Hosten and Paul Kwiat. "Observation of the Spin Hall Effect of Light via Weak Measurements". In: *Science* 319.5864 (2008), pp. 787–790. ISSN: 0036-8075. DOI: 10.1126/science.1152697. URL: http://science.sciencemag.org/content/319/5864/787.

[39] Shengshi Pang, Justin Dressel, and Todd A. Brun. "Entanglement-Assisted Weak Value Amplification". In: *Phys. Rev. Lett.* 113 (3 July 2014), p. 030401. DOI: 10.1103/PhysRevLett.113.030401. URL: https://link.aps.org/doi/10.1103/PhysRevLett.113.030401.

[40] Shengshi Pang and Todd A. Brun. "Improving the Precision of Weak Measurements by Post-selection Measurement". In: *Phys. Rev. Lett.* 115 (12 Sept. 2015), p. 120401. DOI: 10.1103/PhysRevLett.115.120401. URL: https://link.aps.org/doi/10.1103/PhysRevLett.115.120401.

[41] David J. Starling et al. "Optimizing the signal-to-noise ratio of a beam-deflection measurement with interferometric weak values". In: *Phys. Rev. A* 80 (4 Oct. 2009), 041803(R). DOI: 10.1103/PhysRevA.80.041803. URL: https://link.aps.org/doi/10.1103/PhysRevA.80.041803.

[42] David J. Starling et al. "Precision frequency measurements with interferometric weak values". In: *Phys. Rev. A* 82 (6 Dec. 2010), p. 063822. DOI: 10.1103/PhysRevA.82.063822. URL: https://link.aps.org/doi/10.1103/PhysRevA.82.063822.

[43] Omar S. Magaña-Loaiza et al. "Amplification of Angular Rotations Using Weak Measurements". In: *Phys. Rev. Lett.* 112 (20 May 2014), p. 200401. DOI: 10.1103/PhysRevLett.112.200401. URL: https://link.aps.org/doi/10.1103/PhysRevLett.112.200401.

[44] Kevin Lyons et al. "Power-Recycled Weak-Value-Based Metrology". In: *Phys. Rev. Lett.* 114 (17 Apr. 2015), p. 170801. DOI: 10.1103/PhysRevLett.114.170801. URL: https://link.aps.org/doi/10.1103/PhysRevLett.114.170801.

[45] Julián Martínez-Rincón et al. "Ultrasensitive inverse weak-value tilt meter". In: *Opt. Lett.* 42.13 (July 2017), pp. 2479–2482. DOI: 10.1364/OL.42.002479. URL: https://opg.optica.org/ol/abstract.cfm?URI=ol-42-13-2479.

[46] Patrick Egan and Jack A Stone. "Weak-value thermostat with 0.2 mK precision". In: *Opt. Lett* 37.23 (2012), pp. 4991–4993.

[47] Holger F. Hofmann et al. "Estimation of a quantum interaction parameter using weak measurements: Theory and experiment". In: *Phys. Rev. A* 86 (4 Oct. 2012), 040102(R). DOI: 10.1103/PhysRevA.86.040102. URL: https://link.aps.org/doi/10.1103/PhysRevA.86.040102.

[48] Yosep Kim et al. "Direct quantum process tomography via measuring sequential weak values of incompatible observables". In: *Nature communications* 9.1 (2018), pp. 1–6.

[49] Matthias Pfender et al. "High-resolution spectroscopy of single nuclear spins via sequential weak measurements". In: *Nature communications* 10.1 (2019), pp. 1–8.

[50] F. Piacentini et al. "Measuring Incompatible Observables by Exploiting Sequential Weak Values". In: *Phys. Rev. Lett.* 117 (17 Oct. 2016), p. 170402. DOI: 10.1103/PhysRevLett.117.170402. URL: https://link.aps.org/doi/10.1103/PhysRevLett.117.170402.

[51] Lajos Diósi. "Structural features of sequential weak measurements". In: *Physical Review A* 94.1 (2016), 010103(R).

[52] Alessio Avella et al. "Anomalous weak values and the violation of a multiple-measurement Leggett-Garg inequality". In: *Physical Review A* 96.5 (2017), p. 052123.

[53] Danko Georgiev and Eliahu Cohen. "Probing finite coarse-grained virtual Feynman histories with sequential weak values". In: *Physical Review A* 97.5 (2018), p. 052102.

[54] Holger F Hofmann. "Contextuality of quantum fluctuations characterized by conditional weak values of entangled states". In: *Physical Review A* 102.6 (2020), p. 062215.

[55] Giulio Foletto et al. "Experimental test of sequential weak measurements for certified quantum randomness extraction". In: *Phys. Rev. A* 103 (6 June 2021), p. 062206. DOI: 10.1103/PhysRevA.103.062206. URL: https://link.aps.org/doi/10.1103/PhysRevA.103.062206.

[56] Jiang-Shan Chen et al. "Experimental realization of sequential weak measurements of non-commuting Pauli observables". In: *Opt. Express* 27.5 (Mar. 2019), pp. 6089–6097. DOI: 10.1364/OE.27.006089. URL: http://www.osapublishing.org/oe/abstract.cfm?URI=oe-27-5-6089.

[57] Valeria Cimini et al. "Anomalous values, Fisher information, and contextuality, in generalized quantum measurements". In: *Quantum Science and Technology* 5.2 (Mar. 2020), p. 025007. DOI: 10.1088/2058-9565/ab7988. URL: https://doi.org/10.1088/2058-9565/ab7988.

[58] Yeon-Ho Choi et al. "Demonstration of simultaneous quantum steering by multiple observers via sequential weak measurements". In: *Optica* 7.6 (June 2020), pp. 675–679. DOI: 10.1364/OPTICA.394667. URL: http://www.osapublishing.org/optica/abstract.cfm?URI=optica-7-6-675.

[59] MS Blok et al. "Manipulating a qubit through the backaction of sequential partial measurements and real-time feedback". In: *Nature Physics* 10.3 (2014), pp. 189–193.

[60] John G. Kirkwood. "Quantum Statistics of Almost Classical Assemblies". In: *Phys. Rev.* 44 (1 July 1933), pp. 31–37. DOI: 10.1103/PhysRev.44.31. URL: https://link.aps.org/doi/10.1103/PhysRev.44.31.

[61] P. A. M. Dirac. "On the Analogy Between Classical and Quantum Mechanics". In: *Rev. Mod. Phys.* 17 (2-3 Apr. 1945), pp. 195–199. DOI: 10.1103/RevModPhys.17.195. URL: https://link.aps.org/doi/10.1103/RevModPhys.17.195.

[62] Lars M. Johansen. "Quantum theory of successive projective measurements". In: *Phys. Rev. A* 76 (1 July 2007), p. 012119. DOI: 10.1103/PhysRevA.76.012119. URL: https://link.aps.org/doi/10.1103/PhysRevA.76.012119.

[63] Jeff S Lundeen et al. "Direct measurement of the quantum wavefunction". In: *Nature* 474.7350 (2011), p. 188. URL: https://doi.org/10.1038/nature10120.

[64] Jeff S. Lundeen and Charles Bamber. "Procedure for Direct Measurement of General Quantum States Using Weak Measurement". In: *Phys. Rev. Lett.* 108 (7 Feb. 2012), p. 070402. DOI: 10.1103/PhysRevLett.108.070402. URL: https://link.aps.org/doi/10.1103/PhysRevLett.108.070402.

[65] Charles Bamber and Jeff S. Lundeen. "Observing Dirac's Classical Phase Space Analog to the Quantum State". In: *Phys. Rev. Lett.* 112 (7 Feb. 2014), p. 070405. DOI: 10.1103/PhysRevLett.112.070405. URL: https://link.aps.org/doi/10.1103/PhysRevLett.112.070405.

[66] G. S. Thekkadath et al. "Direct Measurement of the Density Matrix of a Quantum System". In: *Phys. Rev. Lett.* 117 (12 Sept. 2016), p. 120401. DOI: 10.1103/PhysRevLett.117.120401. URL: https://link.aps.org/doi/10.1103/PhysRevLett.117.120401.

[67] Nicole Yunger Halpern. "Jarzynski-like equality for the out-of-time-ordered correlator". In: *Phys. Rev. A* 95 (1 Jan. 2017), p. 012120. DOI: 10.1103/PhysRevA.95.012120. URL: https://link.aps.org/doi/10.1103/PhysRevA.95.012120.

[68] Nicole Yunger Halpern, Brian Swingle, and Justin Dressel. "Quasiprobability behind the out-of-time-ordered correlator". In: *Phys. Rev. A* 97 (4 Apr. 2018), p. 042105. DOI: 10.1103/PhysRevA.97.042105. URL: https://link.aps.org/doi/10.1103/PhysRevA.97.042105.

[69] José Raúl González Alonso, Nicole Yunger Halpern, and Justin Dressel. "Out-of-Time-Ordered-Correlator Quasiprobabilities Robustly Witness Scrambling". In: *Phys. Rev. Lett.* 122 (4 Feb. 2019), p. 040404. DOI: 10.1103/PhysRevLett.122.040404. URL: https://link.aps.org/doi/10.1103/PhysRevLett.122.040404.

[70] Nicole Yunger Halpern, Anthony Bartolotta, and Jason Pollack. "Entropic uncertainty relations for quantum information scrambling". In: *Communications Physics* 2.1 (2019), pp. 1–12. DOI: 10.1038/s42005-019-0179-8. URL: https://doi.org/10.1038/s42005-019-0179-8.

[71] Razieh Mohseninia, José Raúl González Alonso, and Justin Dressel. "Optimizing measurement strengths for qubit quasiprobabilities behind out-of-time-ordered correlators". In: *Phys. Rev. A* 100 (6 Dec. 2019), p. 062336. DOI: 10.1103/PhysRevA.100.062336. URL: https://link.aps.org/doi/10.1103/PhysRevA.100.062336.

[72] Aephraim M. Steinberg. "Conditional probabilities in quantum theory and the tunneling-time controversy". In: *Phys. Rev. A* 52 (1 July 1995), pp. 32–42. DOI: 10.1103/PhysRevA.52.32. URL: https://link.aps.org/doi/10.1103/PhysRevA.52.32.

[73] Justin Dressel et al. "Colloquium: Understanding quantum weak values: Basics and applications". In: *Rev. Mod. Phys.* 86 (1 Mar. 2014), pp. 307–316. DOI: 10.1103/RevModPhys.86.307. URL: https://link.aps.org/doi/10.1103/RevModPhys.86.307.

[74] Matthew F. Pusey. "Anomalous Weak Values Are Proofs of Contextuality". In: *Phys. Rev. Lett.* 113 (20 Nov. 2014), p. 200401. DOI: 10.1103/PhysRevLett.113.200401. URL: https://link.aps.org/doi/10.1103/PhysRevLett.113.200401.

[75] D. R. M. Arvidsson-Shukur, A. N. O. Gottfries, and C. H. W. Barnes. "Evaluation of counterfactuality in counterfactual communication protocols". In: *Phys. Rev. A* 96 (6 Dec. 2017), p. 062316. DOI: 10.1103/PhysRevA.96.062316. URL: https://link.aps.org/doi/10.1103/PhysRevA.96.062316.

[76] David R. M. Arvidsson-Shukur and Crispin H. W. Barnes. "Postselection and counterfactual communication". In: *Phys. Rev. A* 99 (6 June 2019), 060102(R). DOI: 10.1103/PhysRevA.99.060102. URL: https://link.aps.org/doi/10.1103/PhysRevA.99.060102.

[77] Ravi Kunjwal, Matteo Lostaglio, and Matthew F. Pusey. "Anomalous weak values and contextuality: Robustness, tightness, and imaginary parts". In: *Phys. Rev. A* 100 (4 Oct. 2019), p. 042116. DOI: 10.1103/PhysRevA.100.042116. URL: https://link.aps.org/doi/10.1103/PhysRevA.100.042116.

[78] Joe H. Jenne and David R. M. Arvidsson-Shukur. "Quantum Learnability is Arbitrarily Distillable". In: *arXiv preprint arXiv:1909.11116* (2021). URL: https://arxiv.org/abs/2104.09520.

[79] Richard Jozsa. "Complex weak values in quantum measurement". In: *Phys. Rev. A* 76 (4 Oct. 2007), p. 044103. DOI: 10.1103/PhysRevA.76.044103. URL: https://link.aps.org/doi/10.1103/PhysRevA.76.044103.

[80] Holger F Hofmann. "On the role of complex phases in the quantum statistics of weak measurements". In: *New Journal of Physics* 13.10 (Oct. 2011), p. 103009. DOI: 10.1088/1367-2630/13/10/103009. URL: https://doi.org/10.1088%2F1367-2630%2F13%2F10%2F103009.

[81] J. Dressel and A. N. Jordan. "Significance of the imaginary part of the weak value". In: *Phys. Rev. A* 85 (1 Jan. 2012), p. 012107. DOI: 10.1103/PhysRevA.85.012107. URL: https://link.aps.org/doi/10.1103/PhysRevA.85.012107.

[82] Jonathan T. Monroe et al. "Weak Measurement of a Superconducting Qubit Reconciles Incompatible Operators". In: *Phys. Rev. Lett.* 126 (10 Mar. 2021), p. 100403. DOI: 10.1103/PhysRevLett.126.100403. URL: https://link.aps.org/doi/10.1103/PhysRevLett.126.100403.

[83] A. E. Allahverdyan. "Nonequilibrium quantum fluctuations of work". In: *Phys. Rev. E* 90 (3 Sept. 2014), p. 032137. DOI: 10.1103/PhysRevE.90.032137. URL: https://link.aps.org/doi/10.1103/PhysRevE.90.032137.

[84] Harry J D Miller and Janet Anders. "Time-reversal symmetric work distributions for closed quantum dynamics in the histories framework". In: *New Journal of Physics* 19.6 (June 2017), p. 062001. DOI: 10.1088/1367-2630/aa703f. URL: https://doi.org/10.1088/1367-2630/aa703f.

[85] Amikam Levy and Matteo Lostaglio. "A quasiprobability distribution for heat fluctuations in the quantum regime". In: *arXiv preprint arXiv:1909.11116* (2019). URL: https://arxiv.org/abs/1909.11116.

[86] Matteo Lostaglio. "Certifying Quantum Signatures in Thermodynamics and Metrology via Contextuality of Quantum Linear Response". In: *Phys. Rev. Lett.* 125 (23 Dec. 2020), p. 230603. DOI: 10.1103/PhysRevLett.125.230603. URL: https://link.aps.org/doi/10.1103/PhysRevLett.125.230603.

[87] Robert B Griffiths. "Consistent histories and the interpretation of quantum mechanics". In: *Journal of Statistical Physics* 36.1-2 (1984), pp. 219–272. DOI: https://doi.org/10.1007/BF01015734.

[88] Sheldon Goldstein and Don N. Page. "Linearly Positive Histories: Probabilities for a Robust Family of Sequences of Quantum Events". In: *Phys. Rev. Lett.* 74 (19 May 1995), pp. 3715–3719. DOI: 10.1103/PhysRevLett.74.3715. URL: https://link.aps.org/doi/10.1103/PhysRevLett.74.3715.

[89] James B. Hartle. "Linear positivity and virtual probability". In: *Phys. Rev. A* 70 (2 Aug. 2004), p. 022104. DOI: 10.1103/PhysRevA.70.022104. URL: https://link.aps.org/doi/10.1103/PhysRevA.70.022104.

[90] Holger F Hofmann. "Complex joint probabilities as expressions of reversible transformations in quantum mechanics". In: *New Journal of Physics* 14.4 (Apr. 2012), p. 043031. DOI: 10.1088/1367-2630/14/4/043031. URL: https://doi.org/10.1088%2F1367-2630%2F14%2F4%2F043031.

[91] Holger F. Hofmann. "Derivation of quantum mechanics from a single fundamental modification of the relations between physical properties". In: *Phys. Rev. A* 89 (4 Apr. 2014), p. 042115. DOI: 10.1103/PhysRevA.89.042115. URL: https://link.aps.org/doi/10.1103/PhysRevA.89.042115.

[92] Holger F. Hofmann. "Quantum paradoxes originating from the nonclassical statistics of physical properties related to each other by half-periodic transformations". In: *Phys. Rev. A* 91 (6 June 2015), p. 062123. DOI: 10.1103/PhysRevA.91.062123. URL: https://link.aps.org/doi/10.1103/PhysRevA.91.062123.

[93] Holger F Hofmann. "On the fundamental role of dynamics in quantum physics". In: *The European Physical Journal D* 70.5 (2016), p. 118. DOI: https://doi.org/10.1140/epjd/e2016-70086-8.

[94] J. J. Halliwell. "Leggett-Garg inequalities and no-signaling in time: A quasiprobability approach". In: *Phys. Rev. A* 93 (2 Feb. 2016), p. 022123. DOI: 10.1103/PhysRevA.93.022123. URL: https://link.aps.org/doi/10.1103/PhysRevA.93.022123.

[95] Blake C Stacey. "Quantum theory as symmetry broken by vitality". In: *arXiv preprint arXiv:1907.02432* (2019). URL: https://arxiv.org/pdf/1907.02432.

[96] David R. M. Arvidsson-Shukur, Jacob Chevalier Drori, and Nicole Yunger Halpern. "Conditions tighter than noncommutation needed for nonclassicality". In: *Journal of Physics A: Mathematical and Theoretical* 54.28 (June 2021), p. 284001. DOI: 10.1088/1751-8121/ac0289. URL: https://doi.org/10.1088/1751-8121/ac0289.

[97] Stephan De Bievre. "Kirkwood-Dirac nonclassicality, support uncertainty and complete incompatibility". In: *arXiv e-prints*, arXiv:2106.10017 (June 2021), arXiv:2106.10017. arXiv: 2106.10017 [quant-ph].

[98] Michał Oszmaniec, Daniel J. Brod, and Ernesto F. Galvão. "Measuring relational information between quantum states, and applications". In: *arXiv e-prints*, arXiv:2109.10006 (Sept. 2021), arXiv:2109.10006. arXiv: 2109.10006 [quant-ph].

[99] Michael A. Nielsen and Isaac L. Chuang. *Quantum Computation and Quantum Information: 10th Anniversary Edition*. 10th. New York, NY, USA: Cambridge University Press, 2011. ISBN: 9781107002173.

[100] H. M. Wiseman. "Weak values, quantum trajectories, and the cavity-QED experiment on wave-particle correlation". In: *Phys. Rev. A* 65 (3 Feb. 2002), p. 032111. DOI: 10.1103/PhysRevA.65.032111. URL: https://link.aps.org/doi/10.1103/PhysRevA.65.032111.

[101] Weng-Kian Tham. "Quantum Homomorphic Encryption: Implementation and Applications". PhD thesis. University of Toronto, 2020. URL: https://hdl.handle.net/1807/103257.

[102] John von. Neumann, Robert T. Beyer (Translator), and Nicholas A. Wheeler (Editor). *Mathematical foundations of quantum mechanics*. Princeton University Press, 2018. ISBN: 9780691178561.

[103] Yakir Aharonov, Peter G Bergmann, and Joel L Lebowitz. "Time symmetry in the quantum process of measurement". In: *Physical Review* 134.6B (1964), B1410. URL: http://prola.aps.org/abstract/PR/v134/i6B/pB1410%7B%5C_%7D1.

[104] A Einstein, B Podolsky, and N Rosen. "Can Quantum-Mechanical Description of Physical Reality Be Considered Complete?" In: *Phys. Rev.* 47.10 (May 1935), pp. 777–780. DOI: 10.1103/PhysRev.47.777.

[105] Daniela Frauchiger and Renato Renner. "Quantum theory cannot consistently describe the use of itself". In: *Nature Communications* 9.1 (Dec. 2018), p. 3711. ISSN: 2041-1723. DOI: 10.1038/s41467-018-05739-8. URL: http://www.nature.com/articles/s41467-018-05739-8.

[106] Matthew F. Pusey, Jonathan Barrett, and Terry Rudolph. "On the reality of the quantum state". In: *Nature Physics* 8 (2012), p. 475. DOI: 10.1038/nphys2309. arXiv: 1111.3328. URL: http://arxiv.org/abs/1111.3328%20https://www.nature.com/nphys/journal/v8/n6/full/nphys2309.html.

[107] Lucien Hardy. "Are Quantum States Real?" In: *International Journal of Modern Physics B* 27.01n03 (Jan. 2013), p. 1345012. ISSN: 0217-9792. DOI: 10.1142/S0217979213450124. URL: http://www.worldscientific.com/doi/abs/10.1142/S0217979213450124.

[108] N David Mermin. "Making better sense of quantum mechanics". In: *Reports on Progress in Physics* 82.1 (Nov. 2018), p. 012002. DOI: 10.1088/1361-6633/aae2c6. URL: https://dx.doi.org/10.1088/1361-6633/aae2c6.

[109] Yakir Aharonov and Daniel. Rohrlich. *Quantum paradoxes : quantum theory for the perplexed.* Wiley-VCH, 2005, p. 289. ISBN: 9783527403912. URL: https://www.wiley.com/en-ca/Quantum+Paradoxes:+Quantum+Theory+for+the+Perplexed-p-9783527403912.

[110] Yakir Aharonov et al. "Revisiting Hardy's paradox: counterfactual statements, real measurements, entanglement and weak values". In: *Physics Letters A* 301.3 (2002), pp. 130–138. URL: http://www.sciencedirect.com/science/article/pii/S0375960102009866.

[111] Yakir Aharonov et al. "Quantum Cheshire Cats". In: *New Journal of Physics* 15.11 (Nov. 2013), p. 113015. ISSN: 1367-2630. DOI: 10.1088/1367-2630/15/11/113015. URL: http://dx.doi.org/10.1088/1367-2630/15/11/113015.

[112] Kazuhiro Yokota et al. "Direct observation of Hardy's paradox by joint weak measurement with an entangled photon pair". In: *New Journal of Physics* 11.3 (2009), p. 33011. URL: http://iopscience.iop.org/1367-2630/11/3/033011.

[113] Lucien Hardy. "Quantum mechanics, local realistic theories, and Lorentz-invariant realistic theories". In: *Physical Review Letters* 68.20 (May 1992), pp. 2981–2984. ISSN: 0031-9007. DOI: 10.1103/physrevlett.68.2981. URL: http://dx.doi.org/10.1103/PhysRevLett.68.2981.

[114] Aharon Brodutch and Eliahu Cohen. "A scheme for performing strong and weak sequential measurements of non-commuting observables". In: *Quantum Studies: Mathematics and Foundations* (Aug. 2016), pp. 1–15. DOI: 10.1007/s40509-016-0084-8. URL: http://link.springer.com/10.1007/s40509-016-0084-8.

[115] J S Lundeen and A M Steinberg. "Experimental joint weak measurement on a photon pair as a probe of Hardy's paradox". In: *Physical Review Letters* 102.2 (2009), p. 20404. URL: http://prl.aps.org/abstract/PRL/v102/i2/e020404.

[116] M Leifer and Robert Spekkens. "Pre- and Post-Selection Paradoxes and Contextuality in Quantum Mechanics". In: *Physical Review Letters* 95.20 (Nov. 2005). ISSN: 1079-7114. DOI: 10.1103/physrevlett.95.200405. URL: http://dx.doi.org/10.1103/PhysRevLett.95.200405.

[117] Matthew F. Pusey and Matthew S. Leifer. "Logical pre- and post-selection paradoxes are proofs of contextuality". In: *arXiv:1506.07850* (June 2015). DOI: 10.4204/EPTCS.195.22. arXiv: 1506.07850. URL: http://arxiv.org/abs/1506.07850%20http://dx.doi.org/10.4204/EPTCS.195.22.

[118] Tamar Ravon and Lev Vaidman. "The three-box paradox revisited". In: *J. Phys. A: Math. Theor.* 40.11 (Feb. 2007), 2873???2882. ISSN: 1751-8121. DOI: 10.1088/1751-8113/40/11/021. URL: http://dx.doi.org/10.1088/1751-8113/40/11/021.

[119] Kevin J Resch, Jeff S Lundeen, and Aephraim M Steinberg. "Experimental realization of the quantum box problem". In: *Physics Letters A* 324.2 (2004), pp. 125–131. URL: http://www.sciencedirect.com/science/article/pii/S0375960104002506.

[120] Yakir Aharonov et al. "Quantum violation of the pigeonhole principle and the nature of quantum correlations." In: *Proceedings of the National Academy of Sciences of the United States of America* 113.3 (Jan. 2016), pp. 532–5. ISSN: 1091-6490. DOI: 10.1073/pnas.1522411112. URL: http://www.ncbi.nlm.nih.gov/pubmed/26729862%20http://www.pubmedcentral.nih.gov/articlerender.fcgi?artid=PMC4725468.

[121] Yakir Aharonov et al. "Peculiar features of entangled states with postselection". In: *Physical Review A - Atomic, Molecular, and Optical Physics* (2013). ISSN: 10502947. DOI: 10.1103/PhysRevA.87.014105.

[122] Gregory Reznik et al. "Footprints of quantum pigeons". In: *Phys. Rev. Res.* 2 (2 Apr. 2020), p. 023004. DOI: 10.1103/PhysRevResearch.2.023004. URL: https://link.aps.org/doi/10.1103/PhysRevResearch.2.023004.

[123] Mordecai Waegell et al. "Confined contextuality in neutron interferometry: Observing the quantum pigeonhole effect". In: *Physical Review A* 96.5 (Nov. 2017), p. 052131. ISSN: 2469-9926. DOI: 10.1103/PhysRevA.96.052131. URL: https://link.aps.org/doi/10.1103/PhysRevA.96.052131.

[124] Ming Cheng Chen et al. "Experimental demonstration of quantum pigeonhole paradox". In: *Proceedings of the National Academy of Sciences of the United States of America* (2019). ISSN: 10916490. DOI: 10.1073/pnas.1815462116.

[125] Yakir Aharonov, David Z Albert, and Lev Vaidman. "How the result of a measurement of a component of the spin of a spin-1/2 particle can turn out to be 100". In: *Physical Review Letters* 60.14 (1988), p. 1351. URL: http://prl.aps.org/abstract/PRL/v60/i14/p1351%7B%5C_%7D1.

[126] F. De Zela. "Role of weak values in strong measurements". In: *Phys. Rev. A* 105 (4 Apr. 2022), p. 042202. DOI: 10.1103/PhysRevA.105.042202. URL: https://link.aps.org/doi/10.1103/PhysRevA.105.042202.

[127] Bengt E. Y. Svensson. "What Is a Quantum-Mechanical "Weak Value" the Value of?" In: *Foundations of Physics* 43.10 (Oct. 2013), pp. 1193–1205. ISSN: 1572-9516. DOI: 10.1007/s10701-013-9740-6. URL: https://doi.org/10.1007/s10701-013-9740-6.

[128] B E Y Svensson. "On the interpretation of quantum mechanical weak values*". In: *Physica Scripta* 2014.T163 (Dec. 2014), p. 014025. DOI: 10.1088/0031-8949/2014/T163/014025. URL: https://dx.doi.org/10.1088/0031-8949/2014/T163/014025.

[129] R.E. Kastner. "Weak values and consistent histories in quantum theory". In: *Studies in History and Philosophy of Science Part B: Studies in History and Philosophy of Modern Physics* 35.1 (2004), pp. 57–71. ISSN: 1355-2198. DOI: https://doi.org/10.1016/j.shpsb.2003.02.001. URL: https://www.sciencedirect.com/science/article/pii/S1355219803000881.

[130] G. S. Paraoanu. "Non-local parity measurements and the quantum pigeonhole effect". In: *Entropy* (2018). ISSN: 10994300. DOI: 10.3390/e20080606.

[131] Aharon Brodutch and Eliahu Cohen. "Nonlocal Measurements via Quantum Erasure." In: *Physical Review Letters* 116.7 (Feb. 2016), p. 070404. ISSN: 1079-7114. DOI: 10.1103/PhysRevLett.116.070404. URL: http://journals.aps.org/prl/abstract/10.1103/PhysRevLett.116.070404.

[132] K Resch and A Steinberg. "Extracting Joint Weak Values with Local, Single-Particle Measurements". In: *Physical Review Letters* 92.13 (Mar. 2004). DOI: 10.1103/PhysRevLett.92.130402. URL: http://dx.doi.org/10.1103/PhysRevLett.92.130402.

[133] Aharon Brodutch and Lev Vaidman. "Measurements of non local weak values". In: vol. 174. 1. June 2009, p. 012004. DOI: 10.1088/1742-6596/174/1/012004. URL: https://dx.doi.org/10.1088/1742-6596/174/1/012004.

[134] Zhao-Qin Wu et al. "Experimental proposal for performing nonlocal measurement of a product observable". In: *Optics Express* (2016). DOI: 10.1364/oe.24.027331.

[135] Yaron Kedem and Lev Vaidman. "Modular values and weak values of quantum observables". In: *Physical Review Letters* 105.23 (2010), p. 230401. URL: http://prl.aps.org/abstract/PRL/v105/i23/e230401.

[136] Keiichi Edamatsu. *Complete and Deterministic Bell State Measurement Using Nonlocal Spin Products*. 2016. arXiv: 1612.08578 [quant-ph].

[137] Kazuhiro Yokota and Nobuyuki Imoto. *Linear optics for direct observation of quantum violation of pigeonhole principle by joint weak measurement*. 2018. arXiv: 1812.04887 [quant-ph].

[138] Xiao Ye Xu et al. "Measurements of Nonlocal Variables and Demonstration of the Failure of the Product Rule for a Pre- and Postselected Pair of Photons". In: *Physical Review Letters* (2019). ISSN: 10797114. DOI: 10.1103/PhysRevLett.122.100405.

[139] Yuan Li et al. "Experimental nonlocal measurement of a product observable". In: *Optica* (2019). DOI: 10.1364/optica.6.001199.

[140] Wei Wei Pan et al. "Photonic realization of erasure-based nonlocal measurements". In: *Nanophotonics* (2019). ISSN: 21928614. DOI: 10.1515/nanoph-2019-0089.

[141] Wei-Wei Pan et al. "Direct Measurement of a Nonlocal Entangled Quantum State". In: *Phys. Rev. Lett.* 123 (15 Oct. 2019), p. 150402. DOI: 10.1103/PhysRevLett.123.150402. URL: https://link.aps.org/doi/10.1103/PhysRevLett.123.150402.

[142] Arthur Ou Teen Pang. "Quantum Sensors and Actuators for Quantum Agents". PhD thesis. University of Toronto, 2023.

[143] Niels Bohr. "Discussions with Einstein on epistemological problems in atomic physics". In: *Quantum Theory and Measurement*. Ed. by John Archibald Wheeler and Wojciech Hubert Zurek. Princeton University Press, 1983.

[144] Léon van Hove. "Von Neumann's contributions to quantum theory". In: *Bull. Am. Math. Soc* (1958). ISSN: 0002-9904. DOI: 10.1090/s0002-9904-1958-10206-2.

[145] K A Kirkpatrick. "Translation of Lueders' "Uber die Zustandsanderung durch den Messprozess" G. Luders, Ann. Phys. (Leipzig) 8 322-328 (1951)." In: *Ann. Phys.* Ann.15 (2006), pp. 663–670. arXiv: 0403007 [arXiv:quant-ph].

[146] Edward Brian Davies. *Quantum theory of open systems*. Academic Press, 1976.

[147] Howard M Wiseman and Gerard J Milburn. *Quantum Measurement and Control*. Cambridge University Press, 2009. ISBN: http://id.crossref.org/isbn/9780511813948. DOI: 10.1017/cbo9780511813948. URL: http://dx.doi.org/10.1017/CBO9780511813948.

[148] M. Nielsen and I. Chuang. *Quantum Computation and Quantum Information*. Cambridge University Press, Oct. 2010. ISBN: 9781107002173.

[149] Vedran Dunjko, Jacob M. Taylor, and Hans J. Briegel. "Quantum-Enhanced Machine Learning". In: *Phys. Rev. Lett.* 117 (13 Sept. 2016), p. 130501. DOI: 10.1103/PhysRevLett.117.130501. URL: https://link.aps.org/doi/10.1103/PhysRevLett.117.130501.

[150] M. J. Kewming, S. Shrapnel, and G. J. Milburn. "Designing a physical quantum agent". In: *Phys. Rev. A* 103 (3 Mar. 2021), p. 032411. DOI: 10.1103/PhysRevA.103.032411. URL: https://link.aps.org/doi/10.1103/PhysRevA.103.032411.

[151] Arthur O.T. Pang et al. "Information gain and measurement disturbance for quantum agents". In preperation.

[152] David Bohm. "A Suggested Interpretation of the Quantum Theory in Terms of "Hidden" Variables. II". In: *Phys. Rev.* 85 (2 Jan. 1952), pp. 180–193. DOI: 10.1103/PhysRev.85.180. URL: https://link.aps.org/doi/10.1103/PhysRev.85.180.

[153] Sheldon Goldstein. "Bohmian Mechanics". In: *Stanford Encyclopedia of Philosophy Archive* (2017).

[154] Hugh Everett. ""Relative State" Formulation of Quantum Mechanics". In: *Rev. Mod. Phys.* 29 (3 July 1957), pp. 454–462. DOI: 10.1103/RevModPhys.29.454. URL: https://link.aps.org/doi/10.1103/RevModPhys.29.454.

[155] Paul Busch, Pekka J Lahti, and Peter Mittelstaedt. *The quantum theory of measurement*. Vol. 2. Springer Science & Business Media, 1996.

[156] Markus P. Müller. *Law without law: From observer states to physics via algorithmic information theory*. Dec. 2020. DOI: 10.22331/Q-2020-07-20-301. arXiv: 1712.01826. URL: https://arxiv.org/abs/1712.01826v5.

[157] Christopher A. Fuchs, N. David Mermin, and Rüdiger Schack. "An introduction to QBism with an application to the locality of quantum mechanics". In: *American Journal of Physics* 82.8 (Aug. 2014), pp. 749–754. ISSN: 0002-9505. DOI: 10.1119/1.4874855. arXiv: 1311.5253. URL: https://arxiv.org/abs/1311.5253v1.

[158] Fernando G. S. L. Brandão, Marco Piani, and Paweł Horodecki. "Generic emergence of classical features in quantum Darwinism". In: *Nat. Comm.* 6.1 (Aug. 2015). ISSN: 2041-1723. DOI: 10.1038/ncomms8908. URL: http://dx.doi.org/10.1038/ncomms8908.

[159] Harold Ollivier, David Poulin, and Wojciech H. Zurek. "Objective Properties from Subjective Quantum States: Environment as a Witness". In: *Phys. Rev. Lett.* 93.22 (Nov. 2004). ISSN: 1079-7114. DOI: 10.1103/physrevlett.93.220401. URL: http://dx.doi.org/10.1103/PhysRevLett.93.220401.

[160] Chris Fields. "On the Ollivier–Poulin–Zurek Definition of Objectivity". In: *Axiomathes* 24.1 (July 2013), pp. 137–156. ISSN: 1572-8390. DOI: 10.1007/s10516-013-9218-3. URL: http://dx.doi.org/10.1007/s10516-013-9218-3.

[161] David Deutsch and Chiara Marletto. "Constructor theory of information". In: *Proc. R. Soc. Lond. A* 471.2174 (Feb. 2015), p. 20140540. ISSN: 1471-2946. DOI: 10.1098/rspa.2014.0540. URL: http://dx.doi.org/10.1098/rspa.2014.0540.

[162] K. F. Reim et al. "Multipulse Addressing of a Raman Quantum Memory: Configurable Beam Splitting and Efficient Readout". In: *Phys. Rev. Lett.* 108 (26 June 2012), p. 263602. DOI: 10.1103/PhysRevLett.108.263602. URL: https://link.aps.org/doi/10.1103/PhysRevLett.108.263602.

[163] Duncan G. England et al. "Phonon-Mediated Nonclassical Interference in Diamond". In: *Phys. Rev. Lett.* 117 (7 Aug. 2016), p. 073603. DOI: 10.1103/PhysRevLett.117.073603. URL: https://link.aps.org/doi/10.1103/PhysRevLett.117.073603.

[164] J. Nunn et al. "Mapping broadband single-photon wave packets into an atomic memory". In: *Phys. Rev. A* 75 (1 Jan. 2007), p. 011401. DOI: 10.1103/PhysRevA.75.011401. URL: https://link.aps.org/doi/10.1103/PhysRevA.75.011401.

[165] William K Wootters and Wojciech H Zurek. "A single quantum cannot be cloned". In: *Nature* 299.5886 (1982), pp. 802–803.

[166] DGBJ Dieks. "Communication by EPR devices". In: *Physics Letters A* 92.6 (1982), pp. 271–272.

[167] GM d'Ariano, Paolo Perinotti, and MF Sacchi. "Informationally complete measurements and group representation". In: *Journal of Optics B: Quantum and Semiclassical Optics* 6.6 (2004), S487.

[168] V. Vedral. "The role of relative entropy in quantum information theory". In: *Rev. Mod. Phys* 74.1 (Mar. 2002), pp. 197–234. ISSN: 1539-0756. DOI: 10.1103/revmodphys.74.197. URL: http://dx.doi.org/10.1103/RevModPhys.74.197.

[169] A Brodutch and K Modi. "Criteria for measures of quantum correlations". In: *Quant. Inf. Comp* 12 (Aug. 2012), p. 721. arXiv: arXiv:1108.3649 [quant-ph].

[170] Huzihiro Araki and Elliott H Lieb. "Entropy inequalities". In: *Communications in Mathematical Physics* 18.2 (1970), pp. 160–170.

[171] Wojciech Hubert Zurek. "Quantum Darwinism". In: *Nat. Phys.* 5.3 (Mar. 2009), pp. 181–188. ISSN: 1745-2481. DOI: 10.1038/nphys1202. URL: http://dx.doi.org/10.1038/nphys1202.

[172] Angelo Bassi et al. "Models of wave-function collapse, underlying theories, and experimental tests". In: *Rev. Mod. Phys.* 85.2 (Apr. 2013), pp. 471–527. ISSN: 1539-0756. DOI: 10.1103/revmodphys.85.471. URL: http://dx.doi.org/10.1103/RevModPhys.85.471.

[173] David Z. Albert. "On quantum-mechanical automata". In: *Phys. Lett. A* 98.5-6 (Oct. 1983), pp. 249–252. ISSN: 03759601. DOI: 10.1016/0375-9601(83)90863-0.

[174] David Z. Albert. "A Quantum-Mechanical Automation". In: *Phil. Sci.* (1987). ISSN: 0031-8248. DOI: 10.1086/289406.

[175] David Deutsch. "Quantum theory , the Church-Turing principle and the universal quantum computer". In: *Proc. R. Soc. Lond. A* 400.1818 (1985), pp. 97–117.

[176] Kok-Wei Bong et al. "A strong no-go theorem on the Wigner's friend paradox". In: *Nat. Phys.* (Aug. 2020).

[177] Giulio Chiribella and Hler Kristjansson. "Quantum Shannon theory with superpositions of trajectories". In: *Proc. R. Soc. Lond. A* 475.2225 (May 2019), p. 20180903. ISSN: 1471-2946. DOI: 10.1098/rspa.2018.0903. URL: http://dx.doi.org/10.1098/rspa.2018.0903.

[178] Giulia Rubino et al. "Experimental quantum communication enhancement by superposing trajectories". In: *Phys. Rev. Res.* 3 (1 Jan. 2021), p. 013093. DOI: 10.1103/PhysRevResearch.3.013093. URL: https://link.aps.org/doi/10.1103/PhysRevResearch.3.013093.

[179] Arthur O. T. Pang et al. "Experimental Communication Through Superposition of Quantum Channels". In: *Quantum* 7 (Oct. 2023), p. 1125. ISSN: 2521-327X. DOI: 10.22331/q-2023-10-03-1125. URL: https://doi.org/10.22331/q-2023-10-03-1125.

[180] Dorit Aharonov and Tomer Naveh. "Quantum NP - A Survey". In: *quant-ph/0210077* (2002).

[181] Weng Kit Tham et al. "Experimental demonstration of quantum fully homomorphic encryption with application in a two-party secure protocol". In: *Phys. Rev. X* 10.1 (2020), p. 011038.

[182] Joseph F. Fitzsimons. "Private quantum computation: an introduction to blind quantum computing and related protocols". In: *npj Quant. Inf.* 3.1 (June 2017). ISSN: 2056-6387. DOI: 10.1038/s41534-017-0025-3. URL: http://dx.doi.org/10.1038/s41534-017-0025-3.

[183] Lee A Rozema et al. "Quantum data compression of a qubit ensemble". In: *Phys. Rev. Lett.* 113.16 (2014), p. 160504.

[184] Alex Pepper, Nora Tischler, and Geoff J. Pryde. "Experimental Realization of a Quantum Autoencoder: The Compression of Qutrits via Machine Learning". In: *Phys. Rev. Lett.* 122.6 (Feb. 2019). ISSN: 1079-7114. DOI: 10.1103/physrevlett.122.060501. URL: http://dx.doi.org/10.1103/PhysRevLett.122.060501.

[185] Yuxiang Yang, Giulio Chiribella, and Daniel Ebler. "Efficient Quantum Compression for Ensembles of Identically Prepared Mixed States". In: *Phys. Rev. Lett.* 116.8 (Feb. 2016). ISSN: 1079-7114. DOI: 10.1103/physrevlett.116.080501. URL: http://dx.doi.org/10.1103/PhysRevLett.116.080501.

[186] Masanao Ozawa. "Quantum measuring processes of continuous observables". In: *Journal of Mathematical Physics* 25.1 (1984), pp. 79–87. DOI: 10.1063/1.526000. eprint: https://doi.org/10.1063/1.526000. URL: https://doi.org/10.1063/1.526000.

[187] David Deutsch and Patrick Hayden. "Information flow in entangled quantum systems". In: *Proc. R. Soc. Lond. A* 456.1999 (July 2000), pp. 1759–1774. ISSN: 1471-2946. DOI: 10.1098/rspa.2000.0585. URL: http://dx.doi.org/10.1098/rspa.2000.0585.

[188] Lev Vaidman. "Many-Worlds Interpretation of Quantum Mechanics". In: *The Stanford Encyclopedia of Philosophy*. Ed. by Edward N. Zalta. Fall 2018. Metaphysics Research Lab, Stanford University, 2018.

[189] Kelvin J. McQueen and Lev Vaidman. "In defence of the self-location uncertainty account of probability in the many-worlds interpretation". In: *Stud. Hist. Philos. Sci. B* (2019). ISSN: 18792502. DOI: 10.1016/j.shpsb.2018.10.003.

[190] Charles T. Sebens and Sean M. Carroll. "Self-locating Uncertainty and the Origin of Probability in Everettian Quantum Mechanics". In: *Br. J. Philos. Sci* (2018). ISSN: 14643537. DOI: 10.1093/bjps/axw004.

[191] Roy. J. Glauber. In: *Quantum Optics and Electronics*. Ed. by C DeWitt, A Blandin, and C Cohen-Tannoudji. Gordon and Breach, 1965, pp. 63–185.

[192] Christopher Gerry and Peter Knight. *Introductory Quantum Optics*. Cambridge: Cambridge University Press, 2004. ISBN: 9780511791239. DOI: 10.1017/CBO9780511791239. URL: http://ebooks.cambridge.org/ref/id/CBO9780511791239.